MULTI-LEVEL REGULATION OF T HELPER CELLS BY RETINOIC ACID RECEPTOR ALPHA

by

Leon Ray Friesen

A Dissertation

Submitted to the Faculty of Purdue University

In Partial Fulfillment of the Requirements for the degree of

Doctor of Philosophy

Weldon School of Biomedical Engineering

West Lafayette, Indiana

August 2019

THE PURDUE UNIVERSITY GRADUATE SCHOOL
STATEMENT OF COMMITTEE APPROVAL

Dr. Chang Kim, Co-Chair

Department of Comparative Pathobiology

Dr. Harm HogenEsch, Co-Chair

Department of Comparative Pathobiology

Dr. Timothy Ratliff

Department of Comparative Pathobiology

Dr. Yoon Yeo

Department of Industrial and Physical Pharmacy

Approved by:

Dr. Harm HogenEsch

Head of the Graduate Program

ACKNOWLEDGMENTS

My gratitude to my advisor, Dr. Chang Kim, for his constant support and efforts to train me to be an excellent immunologist. Without his guidance, I would not have reached the goal of becoming a productive scientist.

I also wish to thank my committee members, Drs. HogenEsch, Ratliff, and Yeo, who advised me throughout my degree program and provided listening ears and sound advice on experimental design and career development.

Current and former lab members have provided helpful input and assistance in countless ways. Seika Hashimoto-Hill, Myunghoo Kim, Jeongho Park, Qingyang Liu, Bikash Rana, and Ali Sepahi helped to maintain a positive and productive lab environment; thanks to the numerous others who spent time in the lab as well.

Prior research experiences also set the stage for my current achievements. Dr. Ray Kuhn provided excellent mentorship during my MS degree, and Xiao-Wen Cheng was gracious enough to initiate my laboratory research training as an undergraduate.

My family has been essential in this process as well. Without the support of my loving wife, Jill, and my children, my sense of purpose and determination would have failed. I also thank my father and mother for their unselfishness in my educational preparation and in the demands that come with my pursuit of a scientific career.

TABLE OF CONTENTS

LIST OF TABLES

LIST OF FIGURES

LIST OF ABBREVIATIONS

ADH	Alcohol dehydrogenase
Akt	Protein kinase B
ANOVA	Analysis of variance
APC	Antigen presenting cell
At-RA	All-trans retinoic acid
CCR	Chemokine receptor
CD	Cluster of differentiation
ChIP	Chromatin immunoprecipitation
CYP	Cytochrome p450 family
DAVID	Database for annotation, visualization, and integrated discovery
DC	Dendritic cell
DEG	Differentially expressed gene
ECAR	Extracellular acidification rate
KEGG	Kyoto Encyclopedia of Genes and Genomes
GFI1	Growth factor independent 1
Erk	Extracellular signal-regulated kinase
Ezh2	Enhancer of zeste 2 polycomb repressive complex 2 subunit
FCCP	Trifluoromethoxy carbonylcyanide phenylhydrazone
FoxP3	Forkhead box P3
FPKM	Fragments per kilobase of transcript per million mapped reads
HDAC	Histone deacetylase
HSC	Hepatic stellate cells
ICOS	Inducible costimulator
IFN	Interferon
IGB	Integrated genome browser
IL	Interleukin
IRS	Insulin receptor substrate
LCK	Lymphocyte-specific protein tyrosine kinase
Itg	Integrin

LI	Large intestine
JAK	Janus kinase
KEGG	Kyoto encyclopedia of genes and genomes
MAPK	Mitogen-activated protein kinase
MHC	Major histocompatibility complex
MLN	Mesenteric lymph node
MSCV	Murine stem cell virus
mTOR	Mammalian target of rapamycin
OCR	Oxygen consumption rate
PBS	Phosphate buffered saline
PCA	Principle component analysis
PI3K	Phosphoinositide 3-kinase
PPAR	Peroxisome proliferator-activated receptor
PTEN	PI3K-repressive phosphatase and tensin homolog
Rag	Recombination activating gene
RALDH	Retinaldehyde dehydrogenase
RARα	Retinoic acid receptor alpha
RARE	Retinoic acid response element
RBP	Retinol binding protein
RPMI	Roswell Park Memorial Institute
RXR	Retinoid X receptor
SEM	Standard error of the mean
SI	Small intestine
SP	Spleen
TCR	T cell receptor
Tfh	T follicular helper cell
Th1	IFN-γ producing T helper cell
Th9	IL-9 producing T helper cell
Th17	IL-17 producing T helper cell
Th2	IL-4-producing T helper cell
Tnp	Non-polarized T helper cell

Treg	Regulatory T cell
TRITC	Tetramethylrhodamine
TSS	Transcription start site
VAD	Vitamin A deficient

ABSTRACT

Author: Friesen, Leon, R. PhD
Institution: Purdue University
Degree Received: August 2019
Title: Multi-level Regulation of T Helper Cells by Retinoic Acid Receptor Alpha
Committee Chair: Dr. Chang Kim and Dr. Harm HogenEsch

The active metabolite of vitamin A, retinoic acid, is a key mediator of balanced immune responses. The major nuclear receptor of retinoic acid, retinoic receptor alpha (RARα), functions as a transcriptional regulator, with both active and repressive effects on transcription depending on interactions with nuclear cofactors dictated by ligand-binding effects on protein confirmation. While significant advances have been made in understanding the combined effects of retinoic acid and RARα, the individual roles of each remain incompletely identified.

Epigenetic effects of all-trans retinoic acid (At-RA) and RARα on the transcriptome of T helper cells were assessed using a novel transgenic mouse strain designed to overexpress RARα in T cells and a conditional knock out strain in which RARα was specifically deleted from T cells. At-RA and RARα had divergent roles in promoting Th17 and Treg differentiation, with RARα expression favoring Th17 differentiation over Treg differentiation, and At-RA promoting Treg differentiation over Th17 differentiation. Transcriptome analysis identified groups of At-RA and RARα differentially regulated genes (DEGs). Comparison of these genes to the H3k27 acetylated and tri-methylated epigenetic modifications demonstrated that RARα expression increased the overall level of these epigenetic modifications in all DEG groups, with enhanced control of transcriptional regulation mediated by higher RARα expression. Additionally, expression of transcriptional repressors was strongly regulated by At-RA in a RARα-dependent manner and had repressive effects on the differentiation of T helper cells.

Immunometabolism was also enhanced by RARα expression, leading us to study potential non-genomic roles of RARα on signaling pathways. The major TCR signaling pathways were enhanced by RARα but suppressed by At-RA, suggesting a mechanism by which RARα regulates cellular metabolism upon T cell activation.

In summary, we identified distinct epigenetic and non-genomic effects of RARα as novel regulatory mechanisms by which vitamin A and retinoic acid influence immune responses. Further research into these findings, notably RARα involvement in signal transduction pathways of immune cells, will define how this research can be translated into clinically-relevant applications.

1. LITERATURE REVIEW: VITAMIN A AND THE IMMUNE SYSTEM

The early 20th century discovery of vitamin A as "fat-soluble factor" by McCollum and Davis, with demonstration of its positive effects on the health of agricultural livestock, promoted consumption of foods containing this factor and further research on the function of this necessary dietary component.[1] Since then, biologically relevant roles of vitamin A have been identified in areas of development, retinogenesis, immunity, and others.[2,3] Dietary vitamin A deficiency (VAD) leads to ocular defects, anemia, and increased susceptibility to infections, with an estimated 250 million preschool children suffering from VAD globally.[4] Dietary supplementation of vitamin A reduces mortality associated with measles and other infections.[5]

1.1 Vitamin A metabolism and active metabolites

Vitamin A is acquired exclusively through dietary intake of plant carotenoids, meat and dairy sources, or supplements. Intestinal absorption by intestinal epithelial cells in the small intestine is followed by esterification, compartmentalization into chylomicrons, and release into the circulation (Figure 1.1).[6–8] Upon capture in the liver, retinyl esters from chylomicrons are stored in lipid droplets in hepatic stellate cells (HSCs). Storage of retinol and retinyl esters in the liver allows for controlled levels of circulatory vitamin A metabolites in times of excess or deficient vitamin A. Upon release of retinol from the liver, retinol-binding proteins (RBPs) transport retinol through the circulation. The RBP receptor, STRA6, facilitates retinol transport across the cell membrane by removal of retinol from the extracellular RBP complex and transfer to intracellular retinol-binding proteins. Metabolism of retinol into retinal is performed by alcohol dehydrogenases (ADHs), followed by irreversible metabolism into retinoic acid by retinaldehyde dehydrogenases (RALDHs). Expression of RALDHs is limited to specific cell

types, including $CD103^+$ dendritic cells and intestinal epithelial cells, restricting production of retinoic acid largely to intestinal or liver tissues.[9] Degradation of retinoic acid is accomplished by enzymes of the CYP26 family, with end products being oxidized metabolites that are secreted in bile and urine.

The predominant isoform of retinoic acid is all-trans retinoic acid (At-RA), although 9-cis-retinoic acid and 13-cis-retinoic acid have also been identified in tissues at lower levels.[10–12] Tissue concentrations of At-RA range from 1 to 46 nM, with plasma levels between 1 and 3 nM in mice and between 3 and 13 nM in humans.[13] At-RA levels are elevated in intestinal tissues due to local production by IECs and DCs, with the microbiome affecting At-RA production by altered expression of IEC retinol dehydrogenase.[14,15] Small intestinal IECs localized in the intestinal crypt are more efficient at producing At-RA than IECs localized on the villi.[16] Inflammation in the colon decreases At-RA concentrations through downregulation of RALDHs and upregulation of CYP26.[17] In addition to intestinal tissues, At-RA concentrations are elevated above circulatory concentrations in mouse brain (2 to 20 nM), kidney (6 to 9 nM), testis (8 to 33 nM), and adipose tissue (24 to 46 nM) tissues.[18,19]

1.2 Retinoid binding proteins

Transport of retinoids in the circulation is mediated by the RBP family of proteins that bind retinol, retinal, and At-RA; upon cellular uptake mediated by STRA6, At-RA is bound by cellular retinoic acid binding proteins (CRABP1 and CRABP2) in the cytosol (Table 1.1).[20–22] Transport of At-RA into the nucleus is mediated by CRABP2, where it can be transferred to nuclear retinoic receptors (RARs).[23,24] Fatty acid binding protein 5 (FABP5), in addition to binding long-chain fatty acids, also has the capacity to bind At-RA and transport it to the nucleus, but FABP5 selectively delivers At-RA to PPARδ/β while CRABP2 selectively delivers

At-RA to RARs.[25,26] Because RARs and PPARδ/β have opposite roles on cell proliferation, the CRABP2/FABP5 ratio in cells impacts At-RA effects, notably decreased cell proliferation with high CRABP2 and increased cell proliferation with high FABP5.[27] CRABP2/FABP5 ratios are altered in breast cancers, with increased FABP5 and decreased CRABP2 correlating with poor prognosis.[27,28] CRABP1 is also associated with poor prognosis, because it sequesters At-RA in the cytosol to prevent cell growth arrest induced by nuclear At-RA effects through RARs.[29] At-RA induces PPARδ/β gene expression through the co-activator SRC-1.[26] The retinaldehyde binding protein (CRALBP) is involved in visual cycle development and cone development , through its function in accepting 11-cis retinol in the isomerization reaction.[30,31]

Expression of the family of proteins capable of binding retinoids varies between tissues. RBP2 expression is highly enriched in intestinal tissues, indicating it is the major carrier of dietary retinoids, while RBP1 expression has broader expression, with highest expression in the ovary and fallopian tube indicating a potential role in retinoid delivery for fetal development.[32] CRABP2 expression is detected in the esophagus, salivary glands, uterus, and vagina; while CRABP1 is highest in the retina and thyroid glands. FABP5 has broad expression across tissues. CRALBP is expressed almost exclusively in the retina.[33] Nuclear receptors RARα, RARβ, RARγ, RXRα, RXRβ are all widely distributed among tissues with the exception of RXRγ, which is mainly expressed in skeletal muscle and the pituitary gland. The broad distribution patterns of nuclear receptors and restricted pattern of RBPs, CRABPs, and FABP5 indicate that retinoid concentrations at the tissue level are most influenced by the extracellular carrier proteins.

While tissue localization of retinoids dictates the retinoids available in the local environment, control of the cellular response to active retinoids is determined by their subcellular

localization. Whether inactivated by sequestration in the cytoplasm bound to CRABP1 or shuttled to the nucleus by CRABP2 or FABP5, At-RA localization, and activity are influenced by protein binding. The primary nuclear receptors for At-RA are the RAR family of receptors containing α, β, and γ proteins, of which α is most highly expressed in immune cells.[33] RARα is located predominantly in the nucleus, with cytoplasmic and plasma membrane localization occurring to a lesser degree.[34,35] While RARα itself has no enzymatic activity, it mediates transcriptional regulation through recruitment and interaction with active co-factors; additional interactions with extranuclear proteins have also been documented (Table 1.2).

1.3 RARα epigenetic effects

The RARα protein is a 462 amino acid (55 kDa) protein containing a ligand-binding domain (LBD), a DNA-binding domain (DBD), and an interspaced hinge region containing a nuclear localization signal (Figure 1.2).[36] The protein sequence is 99% conserved between mouse and human species. The DBD contains two zinc fingers that bind to DNA, while the LBD is responsible for binding to At-RA and dimerizing with RXR family proteins. Dimerization of RARα with RXRs promotes DNA binding at retinoic acid response elements (RAREs) with a consensus sequence of [(A/G)G(G/T)TCA].[37] Binding at these sites often, but not always, requires direct or inverted repeats of the binding motif, commonly interspaced by 0, 2, 5, 7, or 8 nucleotides. Additional cofactors that bind to the RARα: RXR complex include nuclear receptor corepressor proteins (Ncor1 and Ncor2), nuclear receptor coactivator proteins (SRC-1, SRC-2 and SRC-3), histone deacetylases (HDAC1, HDAC2, HDAC3, and HDAC4) and members of the polycomb repressive complex 2 (PRC2) including EZH2 and SUZ12.[38–42] Association of RARα with Kruppel-like factor 5 (KLF5) in the absence of At-RA was effective at suppressing expression of p21.[43,44] Ligand binding of At-RA to the RARα:RXR complex influences cofactor

binding affinities, with ligand binding favoring binding of nuclear receptor coactivator proteins, while nuclear receptor corepressors are typically bound in the absence of At-RA. HDAC binding, specifically HDAC2, interacts with RARα in the absence of At-RA and dissociates upon ligand binding. Dissociation of HDAC2 allows for subsequent RARα interaction with coactivators.[45]

1.4 RARα non-genomic effects

In addition to transcriptional effects, non-genomic effects of RARα have also been demonstrated. RARα is present in the cell membrane in lipid rafts, where it complexes with Gαq proteins.[46] This interaction induces p38MAPK activation in response to At-RA, which subsequently activates mitogen- and stress-activated kinase 1 (MSK1). In neuronal cells, Sertoli cells, and embryonic stem cells, activation of Erk and MAPK pathways are regulated by At-RA and RARα.[47–51] In neuroblastoma cells, the association of RARα with both p85 and p110 subunits of PI3K was demonstrated, with differential binding regulated by At-RA and PI3K activity linked to extranuclear RARα localization.[52] Cellular localization of RARα, as affected by At-RA binding and interaction with other proteins, alters both epigenetic (through nuclear RARα) and non-genomic (extranuclear RARα) effects. Thus, RARα protein interactions in the cytoplasm or cell membrane contribute to global RARα regulation.

1.5 At-RA and RARα effects on immune cells

The effects of retinoic acids on immune cells are generally attributed to their interaction with nuclear receptors and subsequent changes in transcriptome. As such, individual effects of At-RA and RARα are often amalgamated in the interpretation of results with alterations in vitamin A nutritional status or retinoic acid availability. Additional considerations include

differences in tissue concentrations of At-RA. Intestinal tissues maintain higher At-RA concentrations and At-RA signaling, although intestinal inflammation was shown to decrease the concentrations of At-RA due to decreased RALDH expression and increased CYP26 expression, promoting the idea that At-RA concentrations regulate immune responses in tissue-dependent and context-dependent manners.[17]

1.5.1 Effects on T cells

T lymphocytes are a vital component of the immune system. They originate in the bone marrow and mature into $CD4^+$ T helper cells and $CD8^+$ T cytotoxic cells in the thymus, with T cell receptor (TCR) affinity to antigens guiding developmental fate.[53] Naïve T cells emigrate from the thymus into the circulation, where they maintain a quiescent state until presented with TCR stimulation, coreceptor stimulation, and cytokine signaling to mature into effector T cells. Environmental factors affect the process of T cell differentiation, including microbes (e.g. segmented filamentous bacteria) and microbial metabolites (e.g. short-chain and long-chain fatty acids).[54–58] Metabolites of dietary components also affect T cells, and vitamin A-derived At-RA actively shapes T cell populations.[59]

Suppression of Th17 cell differentiation is one of the most prominent and dynamic effects of At-RA on T cells.[60–65] The suppressive effect of At-RA is mediated partially by suppression of IL-6R, IL-23R, and IRF4 expression, which are necessary receptors and transcription factors for Th17 differentiation.[66,67] TGF-β signaling is required for both Th17 and Treg differentiation, and the suppression of Th17 cells results in a compensatory increase in Treg differentiation, uniquely enabling At-RA to regulate inflammatory and regulatory T cells. *In vivo,* At-RA produced by $CD103^+$ dendritic cells promoted Treg generation to maintain immune tolerance in the intestine.[68] Supplementation of At-RA in the EAE model of multiple sclerosis

suppressed Th17 differentiation and disease progression.[67] In human ulcerative colitis (UC) colonic biopsy cultures, administration of At-RA reduced the TNFα concentration, while increasing FoxP3$^+$ cells and decreasing IL-17$^+$ cells.[69] One contradictory effect of At-RA on Th17 and Treg cell populations occurs *in vivo* in VAD. Mice on VAD diets have increased numbers of Tregs and decreased numbers of Th17 cells, along with weakened immune responses.[61,70] Loss of RARα increased Treg populations in certain tissues and reduced Th17 cell populations and overall T cell activation and proliferation.[71] At-RA and RARα are thus both important in the effectiveness of T cell responses to infection and balanced immune homeostasis.

In addition to effects on Th17 and Tregs, stabilizing or inducing effects on Th1 and T follicular helper (Tfh) cells, as well as suppressive effects on Th2 and Th9 cells are also noted.[72–79] Transdifferentiation of Th1 cells into Th17 cells is suppressed by At-RA suppression of Th17-related genes.[71] Th9 cells are suppressed by At-RA and RARα epigenetic control of IL-9 expression.[79] Th2- and Th17-related cytokines are decreased by At-RA treatment of allergic airway inflammation in human patients.[80] At-RA also has a role in facilitating resolution of inflammation, by inducing expression of the purinergic receptor P2X7, which facilitates cellular apoptosis in effector T cell populations to reduce immune cell responses.

Homing of T cells to tissues is accomplished by unique patterns of chemokine receptor and integrin expression. At-RA induces intestinal homing of T cells by induction of CCR9 and integrin α4β7 expression through At-RA-dependent binding of RARα to RAREs to regulate expression.[60,61,70,81] Thus, At-RA and RARα affect intestinal immune function and inflammation by regulating both T helper cell differentiation and homing to the intestine.

1.5.2 Effects on antigen presenting cells

Antigen presenting cells (APCs), which include dendritic cells (DCs), macrophages, and Langerhans cells (LCs), process and present foreign and self antigens via MHCII to T helper cells. At-RA treatment of DCs induces expression of RALDHs to further increase At-RA concentrations and indirectly induce Treg cell differentiation and CCR9 and integrin α4β7 expression in T cells.[82,83] At-RA can also suppress the expression of pro-inflammatory cytokines, whereas antagonism of RARα signaling shifts cytokine production to favor an inflammatory milieu.[84–86] At-RA and RARα also promote expression of the lipid antigen presentation molecule, CD1d, on DCs through activity of the peroxisome proliferator-activated receptor (PPARγ).[87] LCs are skin-resident DCs, which are characterized by their expression of the Langerin protein on their surface, that can migrate to skin-draining LNs. In VAD mice, large increases of Langerin$^+$ DCs in intestinal lymphoid tissues were noted, with phenotypic differences compared to Langerin$^-$ DCs in their inflammatory potential.[88] A complex and bidirectional regulation of skin LCs was identified using VAD diets and conditional RARα knockout mice, with At-RA inhibiting LC development, but RARα supporting LC development.[89] The effects of At-RA and RARα on immune responses reflect combined and synergistic effects on APCs, T helper cells, and other immune cells.

Table 1.1. Retinoid binding proteins, their ligands, and cellular localizations.

Retinoid-binding protein	**Ligand(s)**	**Cellular location**
Retinoic acid receptor alpha (RARα)	All-trans retinoic acid	Nucleus, cytosol
Retinoic acid receptor beta (RARβ)	All-trans retinoic acid	Nucleus
Retinoic acid receptor gamma (RARγ)	All-trans retinoic acid, 9-cis retinoic acid	Nucleus
Retinoid X receptor alpha (RXRα)	9-cis retinoic acid	Nucleus, Golgi
Retinoid X receptor beta (RXRβ)	9-cis retinoic acid	Nucleus
Retinoid X receptor gamma (RARγ)	9-cis retinoic acid	Nucleus
Cellular retinoic acid binding protein 1 (CRABP1)	All-trans retinoic acid	Cytosol
Cellular retinoic acid binding protein 2 (CRABP2)	All-trans retinoic acid	Cytosol, nucleus
Fatty acid binding protein 5 (FABP5)	All-trans retinoic acid, Long-chain fatty acids	Extracellular, cytosol, plasma membrane
Retinol binding protein 1 (RBP1)	Retinol, retinal	Cytosol, extracellular
Retinol binding protein 2 (RBP2)	Retinol, retinal	Golgi, cytosol, extracellular
Cellular retinaldehyde binding protein (CRALBP)	Retinal	Cytosol, nucleus

Table 1.2. RARα-interacting proteins, their roles, and cellular localization.

RARα-interacting protein	Role	Cellular location
RXRα	Transcriptional activator/repressor	Nucleus, Golgi
RXRβ	Transcriptional activator/repressor	Nucleus
RARγ	Transcriptional activator/repressor	Nucleus
KLF5	Transcriptional activator/repressor	Nucleus
p300	Transcriptional activator: histone acetyltransferase	Nucleus
MED1	RNA polymerase II transcription	Nucleus
MED25	RNA polymerase II transcription	Nucleus
HDAC1	Transcriptional repressor: histone deacetylase	Nucleus
HDAC2	Transcriptional repressor: histone deacetylase	Nucleus
HDAC3	Transcriptional repressor: histone deacetylase	Nucleus, Golgi
HDAC4	Transcriptional repressor: histone deacetylase	Nucleus, cytosol
EZH2	PRC2 complex member: methyltransferase	Nucleus
SUZ12	PRC2 complex member: methyltransferase	Nucleus
NCOR1	Transcriptional repressor	Nucleus, cytosol
NCOR2	Transcriptional repressor	Nucleus
SRC1	Transcriptional activator: histone acetyltransferase	Nucleus, cytosol, plasma membrane
SRC2	Transcriptional activator: histone acetyltransferase	Nucleus
SRC3	Transcriptional activator: histone acetyltransferase	Nucleus, cytosol
GαQ	Phospholipase C activator	Plasma membrane, cytosol, nucleus
p85	PI3K signaling	Plasma membrane, cytosol
Akt1	Serine/threonine protein kinase	Nucleus, cytosol, plasma membrane, mitochondria

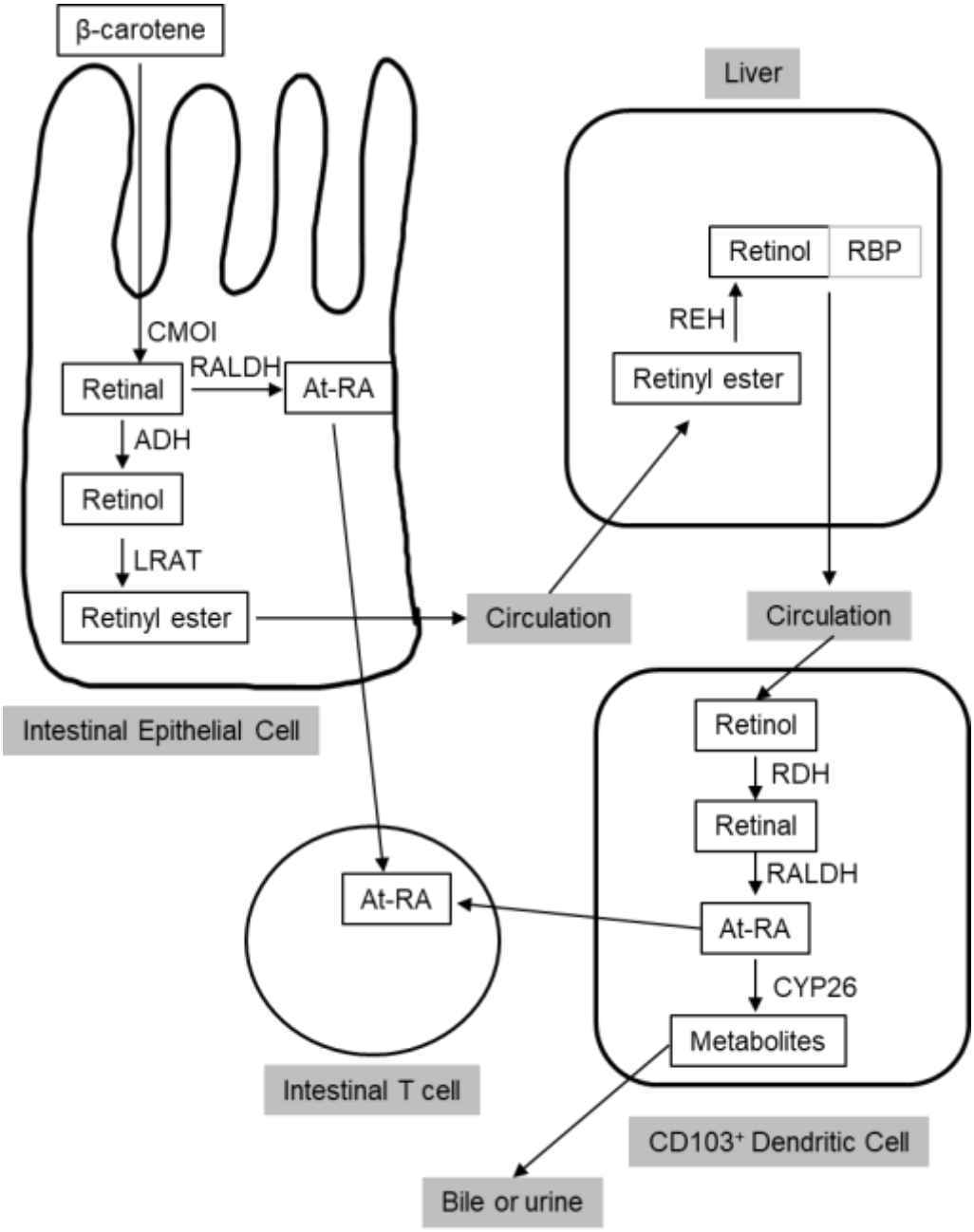

Figure 1.1. Vitamin A metabolism and At-RA delivery. Dietary β-carotene is absorbed by intestinal epithelial cells and metabolized to retinal by β-carotene-15,15′-oxygenase (CMOI). It is further metabolized to retinol by alcohol dehydrogenase (ADH) in a reversible reaction, followed by metabolism to retinyl esters by the lecithin:retinol acyltransferase (LRAT) enzyme. The retinyl esters are transported through the circulation bound within chylomicron droplets, and they are taken up by liver cells, where the retinyl esters are stored. In the liver, retinyl esters can be metabolized to retinol by retinyl ester hydrolase (REH), and retinol can be bound by retinol-binding protein (RBP) for transport through the circulation. CD103+ dendritic cells are able to metabolize retinol to retinal with retinol dehydrogenase (RDH), which allows further metabolism to the active form, all-trans retinoic acid (At-RA) by retinaldehyde dehydrogenase (RALDH). Degradation of At-RA by CYP26 controls concentrations.

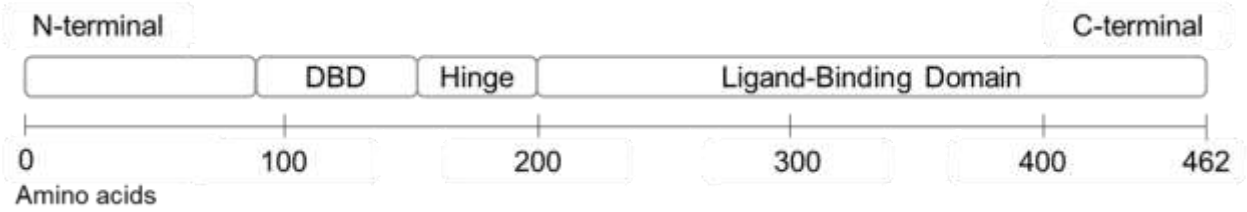

Figure 1.2. RARα protein structure.DBD: DNA-binding domain.

2. RETINOIC ACID AND RETINOIC RECEPTOR ALPHA REGULATE T CELL DIFFERENTIATION THROUGH EPIGENETIC CONTROL OF GFI1 EXPRESSION

2.1 Introduction

Dietary Vitamin A and its metabolites, retinoic acids, are necessary for maintaining immune homeostasis, with known effects on T lymphocytes, dendritic cells, Langerhans cells, and innate lymphoid cells.[89–94] T helper cells, as effector and regulatory cells responsible for coordinating immune responses, are notably affected by retinoic acid. These effects include retinoic acid suppression of Th17 cell differentiation and induction of Treg differentiation.[61,63,64,95,96] Other effects of retinoic acid include promotion of Th1 and Th2 differentiation and suppression of Th9 differentiation, as well as control of immune cell homing to intestinal tissues through induction of chemokine receptors CCR9 and Itgα4β7.[71,79,97–100]

Retinoic acid in its predominant form, all-trans retinoic acid (At-RA), mediates its effects through binding to nuclear receptors to modulate transcription. The predominant binding partner of At-RA in T helper cells is retinoic acid receptor α (RARα), which dimerizes with retinoid x receptor alpha (RXRα) to bind to retinoic acid response elements (RAREs) within genomic DNA.[101–103] Recruitment of various cofactors, selectively affected by the absence or presence of bound At-RA, promotes activation or repression of transcription. Histone modifications, such as acetylation and methylation, are mechanisms of epigenetic transcriptional regulation. Epigenetic-modulating cofactors that bind to RARα/RXRα include NCOR1, SRC1, SRC3, EZH2, and HDACs (1, 2, 3, and 4).[104–107] The effects of At-RA and RARα on epigenetic modifications have been identified as mechanisms for controlling T helper cell differentiation and effector function, but the independent roles of At-RA and RARα have not been fully characterized.

The effects of At-RA and RARα on Th17 cells are controversial, with reports of mostly suppressive effects, but also some stimulating effects, notably *in vivo*.[60,61,71,108] Possible antagonistic roles of At-RA and RARα in controlling Th17 differentiation could provide an explanation for discrepancies in vitamin A regulation of Th17 and other effector cells. Th9 cells were also recently identified as being suppressed by At-RA in a RARα-dependent manner.[79] These cells are implicated in allergic and autoimmune diseases, and a complete understanding of their regulation by At-RA and RARα will help to understand their role in diseases and provide potentially new therapeutic strategies.

In this study, we demonstrate divergent roles of At-RA and RARα on the epigenetic modifications and corresponding transcriptome of Th17 cells, which underlie alterations in Th17 differentiation *in vitro* and in a T-cell transfer model of colitis. We show regulation of Kyoto Encyclopedia of Genes and Genomes (KEGG) pathways by At-RA and/or RARα in these cells and noted strong regulatory control of the transcriptional repressor, GFI1. We further identified that upregulation of GFI1 by At-RA requires RARα binding to the *Gfi1* promoter region, and that GFI1 expression suppresses both Th17 and Th9 differentiation. These results suggest that At-RA induction of GFI1 is involved in the At-RA regulation of T cell differentiation.

2.2 Materials and Methods

2.2.1 Mouse strains and generation.

C57BL/6J mice (stock 002216), Rag1-/- mice (stock 002216), distal LCK-cre mice (stock 012837), and RARα-flox mice (stock 033021) were purchased from Jackson Laboratory (Bar Harbor, ME). LCK-cre mice were mated with RARα-flox mice to generate the T cell specific conditionally-deleted $\Delta RAR\alpha^{Lck}$ mice strain. The RARα-Tg strain was generated by the Transgenic Mouse Core Facility at Purdue University, using the human RARα gene under the human CD2 promoter to drive T cell specific overexpression of RARα. Transgenic mice were generated on the C57BL/6J background. The *Gfi1*$^{fl/fl}$ CD4-cre mice were generously provided by Dr. Jinfang Zhu. Mice were generally 6-8 weeks of age when used for experiments. Both male and female mice were used, with sex-matched animals used for individual experiments. All animal protocols were approved by either the Purdue Animal Care and Use Committee (PACUC) or the University of Michigan Institutional Animal Care and Use Committee (IACUC).

2.2.2 Cell isolation and culture.

Naïve T cells were routinely isolated to >95% purity with magnetic separation using an autoMACS separator and mouse naïve $CD4^+$ T cell kit (Miltenyi Biotec, Somerville, MA). For *in vitro* culture, cells were cultured in complete RPMI-1640 media containing charcoal-stripped FBS. Cells were activated using plate-bound anti-CD3 (5 μg/mL) and anti-CD28 (2 μg/mL) (BioXcell, Lebanon, NH). For Th17-polarizing culture, cytokines and antibodies included mIL-6 (20 ng/mL), mIL-1ß (10 ng/mL), mIL-21 (10 ng/mL), mIL-23 (10 ng/mL), mTNFα (10 ng/mL), hTGFß-1 (5 ng/mL), anti-IFNγ (10 μg/mL), and anti-IL-4 (10 μg/mL). Th9-polarizing culture included hIL-2 (100 U/mL), hIL-4 (30 ng/mL), hTGFß-1 (2 ng/mL), mTNFα (10 ng/mL), and anti-IFNγ (10 μg/mL). Cytokines and antibodies were purchased from Biolegend (San Diego, CA). Cells were

cultured in the presence of all-trans retinoic acid (At-RA), Ro41-5253 (Sigma Aldrich, St. Louis, MO), SI-2, or GSK126 (Cayman Chemical, Ann Arbor, MI) as indicated.

2.2.3 T cell transfer colitis model.

Recipient Rag1-/- mice were maintained in a conventional facility for one week prior to T cell transfer and for the remainder of the experiment. Naïve T cells were magnetically sorted and 5 x 10^5 cells per mouse were injected retroorbitally in 100 μL PBS. Mice were monitored for body weight change and stool score. Once the endpoint of 20% weight loss from initial weight or 5 weeks was reached, mice were euthanized and assessed for intestinal inflammation and T cell phenotype by flow cytometry. Tissues were processed to prepare single cell suspensions for flow cytometry as previously described.[109]

2.2.4 Flow cytometry.

Single cell suspensions from mouse tissues and *in vitro* cultures were assessed by flow cytometry for surface and intracellular markers using Canto II (BD Biosciences; San Jose, CA) or NovoCyte flow cytometers (ACEA Biosciences; San Diego, CA). Antibodies used were purchased from Biolegend or Tonbo Biosciences. For intracellular staining of cytokines, cells were stained for surface markers, followed by activation with phorbol 12-myristate 13-acetate (PMA; 50 ng/mL; Sigma Aldrich), ionomycin (0.5-1.0 μg/mL; Sigma Aldrich), and monensin (2 mM; Sigma Aldrich) for 3-6 hours. Cells were fixed with 1% paraformaldehyde for at least 2 hours, then permeabilized with saponin buffer and stained for intracellular cytokines. For transcription factor staining, FoxP3 Fix/Perm reagents (Tonbo Biosciences; San Diego, CA) were used per manufacturer guidelines.

2.2.5 RNAseq analysis of transcriptome.

RNA was extracted from 24-hour cultures of naïve T cells in the Th17-polarizing culture condition, with or without 10 nM At-RA, using RNeasy Mini spin kit (Qiagen; Venlo, The Netherlands). The Purdue Genomics Facility prepared libraries using the TruSeq Stranded kit (Illumina, San Diego, CA). Paired, 100 bp reads were sequenced using a HiSeq2500 on high-throughput mode. Before library preparation the dscDNA quality was checked using an Agilent Bioanalyzer with the High Sensitivity DNA Chip. Reads were trimmed using Trimmomatic v. 0.32 (Bolger, Lohse, & Usadel, 2014) and assessed with FastQC v. 0.11.2 (Andrews, 2010) and FastX-Toolkit v. 0.0.13.2 (Gordon & Hannon, 2010). Differentially expressed genes (DEGs) were selected by $-0.5 > \log2FC > 0.5$ and t-test p-value < 0.05 for comparisons of RARα and At-RA effects. A list of 2742 DEGs was used for subsequent heatmap generation and sample correlation (GenePattern) and pathway analysis using the Database for Annotation, Visualization, and Integrated Discovery (DAVID).[110,111] Principle component analysis (PCA) was performed using the list of DEGs.

2.2.6 ChIPseq and ChIP PCR analysis of epigenetic modifications.

Naïve T cells were cultured for 16 hours in the Th17-polarizing condition, then samples were prepared for sequencing using the magnetic SimpleChIP enzymatic chromatin IP kit (Cell Signaling; Danvers, MA). For ChIPseq, indexed libraries were generated using the ThruPLEX DNA-seq kit (Takara; Mountain View, CA) with 13 cycles of amplification and 1 x 50 bp sequencing was performed on a NovaSeq 6000 (Illumina; San Diego, CA). Trimming, FastQC, and alignment was performed; and bigwig files of the samples minus matched input samples were created in Galaxy.[112] Further analysis of enrichment regions was performed using the -2kb to +2kb region surrounding the TSS of DEGs from the RNAseq data. For enrichment scores, read counts

within these regions were normalized for read depth and reduced by the read count in the respective input sample. Bigwig files were visualized and plotted using Integrated Genome Browser (IGB).[113] For ChIP PCR experiments, cultures were performed as described for ChIPseq, with the exception that antibodies for RARα and SRC3 were used for immunoprecipitation and qPCR was performed for enrichment of sites in the *Gfi1* locus.

2.2.7 Quantitative reverse-transcription PCR (qRT-PCR).

RNA expression was measured using Ribosol-extracted RNA, with cDNA synthesis done using the High Capacity cDNA Reverse Transcription Kit (Thermo Fisher; Grand Island, NY). Quantitative reverse-transcription PCR was performed using the Maxima® SYBR Green/ROX qPCR Master Mix (Thermo Fisher) on an Eppendorf Mastercycler. Oligonucleotides used are listed in Table 2.1.

2.2.8 Dual luciferase reporter assay.

To assess transcriptional activity of RARE sites for validation of RARα activity in mouse strains, naïve T cells were cultured with anti-CD3, anti-CD28, and hIL-2 for 16 hours, then 4 x 10^6 cells were co-transfected with pGL3-RARE (Addgene #13458) and pRL-CMV (Promega) using the Mouse T Cell Nucleofector kit and Nucleofector 2b device (Lonza; Houston, TX), rested for 4 hours in Lonza recovery media with or without 10 nM At-RA, and restimulated for 6 hours with anti-CD3, anti-CD28, and hIL-2 with or without 10 nM At-RA. Cells were lysed with passive lysis buffer and luminescence of both Renilla and Firefly luciferases were measured using the Dual Luciferase kit (Promega; Madison, WI) on either a SpectraMax i3x (Molecular Devices; San Jose, CA) or Synergy HT (BioTek; Winooski, VT) plate reader. For assessing the activity of the *Gfi1* promoter, Gibson cloning was used to generate pGL4.10 plasmids containing the promoter region

(-10 to -1085 of TSS), with additional mutations of putative RARα binding sites. Luciferase assays were repeated as before, with the protocol modified to use the Th9-polarizing culture condition.

2.2.9 Statistics.

Statistical significance was tested using GraphPad Prism v7.0. Differences between two groups were compared using Student's t-test. For three or more groups, one-way ANOVA with Bonferroni's multiple testing correction was used. For comparisons with two factors (e.g. At-RA and RARα), two-way ANOVA with Bonferroni's multiple testing correction was used. P values <0.05 were considered significant. All error bars indicate SEM.

2.3 Results

2.3.1 Transgenic and conditional knockout mice have predicted RARα expression and function.

Generation of $\Delta Rara^{Lck}$ and RARα-Tg mouse strains was performed using the cre-lox system and transgenic overexpression under the CD2 promoter (Figure 2.1). Validation of conditional knock-out or overexpressing RARα mouse strains included isolation of naïve T helper cells and assessment of mRNA transcripts present by qRT-PCR. $\Delta Rara^{Lck}$ naïve $CD4^+$ T cells had nearly undetectable levels of RARα expression; while RARα-Tg naïve $CD4^+$ T cells expressed approximately seven times as much RARα as did the WT cells (Figure 2.1B). RARα protein expression in total $CD4^+$ splenocytes demonstrated increased protein levels of RARα in the RARα-Tg cells (Figure 2.2C). Functional assessment of RARα and At-RA in binding to RARE sites indicated that $\Delta Rara^{Lck}$ $CD4^+$ T cells lost the ability to upregulate transcription upon At-RA exposure, whereas RARα-Tg $CD4^+$ T cells displayed enhanced transcriptional upregulation in the presence of At-RA (Figure 2.1D).

RARα expression and At-RA have divergent effects on Th17, Th9, and Treg differentiation *in vitro.*

The known effect of At-RA on suppressing Th17 and Th9 differentiation and the effect of inducing Treg differentiation were enhanced in RARα-Tg cells and absent in ΔRara^{Lck} cells. Surprisingly, high levels of RARα enhanced Th17 differentiation and suppressed Treg differentiation. Loss of RARα enhanced Treg differentiation and suppressed Th17 and Th9 differentiation (Figure 2.2A). These results indicate the roles of RARα and At-RA can be divergent rather than additive.

2.3.2 T-cell transfer model of colitis.

Injection of naïve T cell injection into Rag1-/- recipient mice is an established model of colitis.[114–116] Utilizing naïve T cells isolated from WT, ΔRara^{Lck}, and RARα-Tg mice, we used this model to assess the role of T-cell specific RARα in colitis induction. Higher RARα expression level correlated with more rapid colitis formation, as indicated by body weight loss (Figure 2.2B) and colon shortening (Figure 2.2C). The T cell profile at the endpoint indicated that higher RARα led to higher percentages and absolute numbers of Th17 cells in spleen, mesenteric lymph node, and colon tissue (Figure 2.2D).

2.3.3 Steady-state T cell populations in RARα mice strains.

We assessed how T-cell specific loss or overexpression of RARα affected T cell populations in the steady state. T helper cell percentage of CD3 was not affected in spleen, mesenteric lymph node, small intestine lamina propria, or large intestine lamina propria. There was a decrease in T helper CD62L^{hi} cell percentage and corresponding increase in CD44^{hi} cell percentage in the ΔRara^{Lck} spleen. RARα-Tg mice also had higher percentage of CD44^{hi} cells in the mesenteric lymph node (Figure 2.3). Absolute numbers of T helper cells indicated fewer cells

in the spleen and small intestine of ΔRara^{Lck} mice, but there was an increase of CD44^{hi} cells in the mesenteric lymph node of these mice. The populations of Th1 and Th17 cells had no changes in percentage, although ΔRara^{Lck} mice had reduced numbers of Th1 cells in the small intestine and Th17 cells in the spleen and small intestine (Figure 2.4). RARα-Tg mice had increased numbers of Th17 cells in the large intestine. Treg percentages of CD4^{+} cells were increased in ΔRara^{Lck} spleen and small intestine, while RARα-Tg mice had increased Treg percentages in secondary lymphoid tissues, but decreased percentages in small and large intestine lamina propria (Figure 2.5).

The thymocyte populations were also assessed, as defects in T cell maturation might occur from altered RARα expression. The ΔRara^{Lck} mice had a significant increase in the double negative (CD4^{-}, CD8^{-}) population and a decrease in the double positive (CD4^{+}, CD8^{+}) population. The RARα-Tg mice also had a reduction in double positive cell percentage, but with compensatory increases in both single positive (CD4^{+} and CD8^{+}) populations (Figure 2.6).

2.3.4 Transcriptome analysis identifies gene groups regulated by RARα and At-RA.

Given divergent effects of RARα and At-RA in T cell differentiation, we sought to dissect their individual effects on the transcriptome of Th17 cells. In 24-hour, Th17-polarized cultures, we identified 2742 differentially expressed genes (assessed for At-RA and/or RARα effects) with -0.5 > log2FC > 0.5 and p-values <0.05 (Student's t-test). These genes were clustered by expression pattern (Pearson correlation), and 5 distinct gene groups were identified (Figure 2.7A). These genes were used assess sample similarities with a PCA plot (Figure 2.7B) and Pearson correlation of samples (Figure 2.7C). Duplicated samples always paired within groups, with minimal difference between ΔRara^{Lck} and ΔRara^{Lck} At-RA groups. The RARα-Tg At-RA group was most different from the other groups. Pathway analysis with the 2742 DEGs,

with At-RA and RARα effects separated, indicated overlap in the KEGG pathways affected by At-RA and RARα, although dissimilar effects on those pathways cannot be assessed by pathway analysis (Table 2.2).

2.3.5 Epigenetic modification at H3k27 is proportional to RARα expression.

Epigenetic modifications at H3k27 can indicate active transcription (acetylation) or repressed transcription (tri-methylation). These modifications can be performed by enzymes that have known protein interactions with RARα. In 16-hour, Th17-polarized cell cultures, we observed an overall increase in H3k27ac in the RARα-Tg cells among the 2742 DEGs (from RNAseq data); At-RA did not alter the overall H3k27ac level among all DEGs (Figure 2.8). Comparison of H3k27ac with RNAseq expression (log10-transformed FPKM) indicated a direct correlation between H3k27ac and RNA expression. RARα binding assessed with ChIPseq by Brown et al. demonstrates that the majority of DEGs have RARα binding near the TSS.[100] To assess the correlation between H3k27ac and RNA expression, we compared log2FC values of H3k27ac enrichment to the log2FC values of RNA expression from RNAseq data for each indicated comparison (Figure 2.9). Slopes in these graphs indicate the degree to which changes in H3k27ac enrichment correlate with changes in RNA expression. The At-RA effect was proportional to RARα expression, with RARα-Tg having the steepest slope and $\Delta Rara^{Lck}$ having the lowest slope. P-values test whether the slope is different from 0. The RARα effect was more pronounced in the RARα-Tg / WT comparison than the $\Delta Rara^{Lck}$/ WT comparison, indicating RARα-Tg are more epigenetically distinct from WT than $\Delta Rara^{Lck}$ are (Figure 2.9B). Assessment of the broad, repressive H3k27me3 modification also indicated overall higher levels of this modification in RARα-Tg cells, contrary to the expectation that high H3k27ac would lead to lower H3k27me3, albeit within a grouped gene dataset (Figure 2.10A). At-RA reduced

H3k27me3 in all three cell types, including $\Delta Rara^{Lck}$. Comparison of H3k27me3 to RNA expression demonstrated an indirect correlation, matching the known repressive function of H3k27me3. ChIPseq and RNAseq comparisons, similar to those with H3k27ac, demonstrated that RARα expression level correlated with greater epigenetic control of transcription by At-RA (Figure 2.11).

Higher levels of both H3K27 acetylation and methylation within the cumulative group of DEGs could mask effects within individual DEG group. To eliminate this possibility, each of the 5 DEG groups identified by similar patterns of RNA expression were assessed for enrichment of epigenetic modifications surrounding the TSS (Figure 2.12). Remarkably, patterns of acetylation and methylation were relatively unchanged between groups, with both H3K27ac and H3K27me3 modifications increased in cells with higher RARα expression.

2.3.6 Epigenetic modifications and RNA expression in grouped DEGs.

Genes from each DEG group were assessed for patterns in RNA expression and epigenetic modification. Within group 1, IL-9 expression was increased in RARα-Tg cells, and strongly suppressed by At-RA (Figure 2.13A-B). The increase in IL-9 in RARα-Tg cells indicates that RARα and At-RA may have opposite roles in controlling Th9 differentiation. ChIPseq analysis of the *Il9* locus indicates increased H3k27ac modification in the absence of At-RA. IRF4 is an essential factor for Th9 differentiation as it binds to the *Il9* promoter.[117] We observed that At-RA decreased the expression of *Irf4*, correlating with a decrease in H3k27ac (Figure 2.13C-D). This regulation could potentially explain At-RA suppression of IL-9, but not the RARα effect. *Ahr* expression exhibited a similar pattern, with strong suppression of RNA expression and H3k27ac by At-RA (Figure 2.13E-F).

Genes within group 2 had RARα-induced expression in the absence of At-RA, but with suppression by At-RA (Figure 2.14). Patterns of both H3K27ac and me3 demonstrated activating and repressive epigenetic modifications matching RNA expression patterns. Within this group, IL-7R, IL-21, and SRC are all genes with functional relevance for Th17 cells.

Group 3 contains the majority of the classically upregulated genes of At-RA (Figure 2.15). FOXO3, IRF8, and GFI1 all have repressive functions on differentiation of effector T helper cells.[118–124] *Gfi1* expression was strongly-upregulated by At-RA, proportional to RARα expression level, while expression in the absence of At-RA was very low. Epigenetic modification at the *Gfi1* locus indicated strong At-RA- and RARα-dependent regulation of H3k27ac. These genes, and GFI1 in particular, demonstrate the ability of At-RA to regulate T helper cell differentiation through transcriptional regulation.

Group 4 genes had a pattern of At-RA upregulation of gene expression only in conditions with high RARα (Figure 2.16). These genes, including TGFB1, TNFRSF9 (CD137), and BATF3 represent genes that may be regulated by At-RA only in high At-RA concentrations or with high RARα availability.

Loss of RARα resulted in increased expression only in group 5 DEGs (Figure 2.17). A weak pattern of upregulation by At-RA was present in some genes. These genes, including SMAD3, KLF2, and S1PR1, represent genes with relevance to T helper cells that may be repressed by RARα.

To further assess patterns of *Gfi1* expression in cultures, we measured expression at 24- and 72-hours of culture in Th17-polarized cultures. *Gfi1* expression was most induced by At-RA at the earlier time point in WT cells, while RARα-Tg cells treated with At-RA maintained high expression at 72 hours as well (Figure 2.18A). Sequence analysis of the *Gfi1* promoter identified

3 putative RARα binding sites [(A/G)G(G/T)TCA] (Figure 2.18B). We created a luciferase reporter plasmid with the -10 to -1085 bp of TSS promoter region containing either native or mutated RARα binding sites [(A/G)G(G/T)**A**CA]. Promoter activity was induced by At-RA with native RARα binding sites; however, mutation of the RARα binding sites led to increased promoter activity and loss of responsiveness to At-RA (Figure 2.18C). This indicates that RARα binding in the *Gfi1* promoter in the absence of At-RA is suppressive of *Gfi1* expression.

2.3.7 Reciprocal RARα and SRC3 binding in Gfi1 locus is At-RA-dependent.

Binding of RARα and one of its cofactors, the histone acetyltransferase SRC3, were assessed in the presence and absence of At-RA. Binding of RARα and SRC3 was absent in sites lacking the RARα binding motifs. Binding of RARα in site #4 containing two RARα binding motifs was demonstrated in the absence of At-RA, while SRC3 binding was observed at the same site only in the presence of At-RA. Thus, the repressive binding of RARα to the GFI1 promoter occurs only in the absence of At-RA, and reciprocal binding of SRC3 at the same site in the presence of At-RA explains At-RA induction of H3k27 acetylation and *Gfi1* expression.

2.3.8 GFI1 downregulates Th9 and Th17 differentiation.

Given the known effects of GFI1 on the differentiation of other T cell subsets, Th9 differentiation may also be regulated by GFI1. Forced expression of GFI1 using retroviral transduction decreased Th9 and Th17 differentiation in WT cells (Figure 2.15A). Using *Gfi1*$^{fl/fl}$-CD4-cre mice, we assessed Th9 and Th17 differentiation in 0, 1, and 10 nM At-RA concentrations. In the absence of At-RA, no differences in Th17 differentiation were observed, but at the low concentration of At-RA, loss of GFI1 increased Th17 differentiation. Higher Th9 differentiation in *Gfi1*$^{fl/fl}$-CD4-cre cells was demonstrated in all concentrations of At-RA (Figure 2.15B).

2.4 Discussion

Vitamin A plays important roles in immune function and homeostasis, but clarifying individual effects of the active metabolite, At-RA, and its major nuclear receptor, RARα, has been challenging as these two factors are often confounded in the analysis of their individual effects. Epigenetic regulation of effector T cells by At-RA and RARα is expected to involve both factors, yet their individual effects may not be fully represented in previous studies. Utilizing mice with conditional knock out or overexpression of RARα in T cell populations, we addressed the factors of At-RA and RARα individually and jointly in a study of how epigenetic modification is linked to transcriptome.

Evidence of divergent roles of At-RA and RARα on effector T cells was first demonstrated with *in vitro* differentiation studies. Known At-RA effects on suppression of Th17 and Th9 differentiation and inducing Treg differentiation were noted and determined to be RARα-dependent. However, the effect of RARα on T cell differentiation in the absence of At-RA was observed to be opposite of the At-RA effect, with increased RARα leading to increased Th17 and Th9 differentiation and less Treg differentiation. In the T-cell transfer model of colitis, RARα-overexpressing cells were more capable of inducing colitis, and they generated higher percentages and numbers of Th17 cells in secondary lymphoid tissues and colonic lamina propria. Given the heightened sensitivity to At-RA that increased RARα expression provides, an increase in Th17 cells indicates a relatively low concentration of At-RA in inflamed colonic tissue, in agreement with studies demonstrating reduced At-RA concentrations in colitis due to altered synthesizing and metabolizing enzyme expression at local tissue sites and positive roles of At-RA in preventing colitis.[17,125] Thus the effects of RARα on effector T cells appear to be distinct from At-RA, although conditional upon At-RA concentrations.

In its role as a transcription factor, RARα binds to DNA motifs and recruits a variety of activating or repressing cofactors to alter transcription. The transcriptome of T cells in a Th17-polarized culture condition showed that RARα expression level heightened the At-RA effect on transcriptome (Groups 1, 3, and 4). At-RA-independent RARα effects were also observed in the upregulation and downregulation of genes (Groups 2 and 5, respectively). The epigenetic modifications at H3k27, both acetylation and tri-methylation, can be facilitated by RARα-interacting proteins.[38–40] Thus, differences in these epigenetic modifications can link RARα and At-RA to transcriptome modification. Within DEGs, overall levels of both H3k27ac and H3k27me3 were increased in the RARα-Tg cells, indicating that epigenetic modifications are increased with more RARα expression. At-RA demonstrated a RARα-independent effect on decreasing H3k27me3, indicating the potential role of other nuclear factors such as RARß, RARγ, or RXRs in suppressing methyltransferase activity or a role of At-RA in inducing demethylase activity through a RARα-independent mechanism. Correlation of log2FC in both epigenetic modifications at the TSS and RNA expression identified stronger associations of At-RA effects on epigenetic modifications with higher RARα expression for both H3k27ac and H3k27me3 modifications. In the absence of At-RA, RARα-Tg cells demonstrated positive effects of H3k27ac on transcriptional expression and negative effects of H3k27me3 on transcriptional regulation. Loss of RARα led to a weaker association of H3k27ac with transcription and a slight positive association of H3k27me3 with increased transcription. These results indicate that both At-RA and RARα have roles in epigenetic regulation, with RARα expression level correlating with the At-RA effect size, and RARα epigenetic effects that occur in the absence of At-RA.

Epigenetic regulation of Th9 cell differentiation by retinoic acid and RARα has recently been proposed to include RARα-dependent, At-RA downregulation of IL-9 expression through recruitment of the suppressive Nrip1 to an enhancer region 23kb upstream of the TSS.[79] In contrast to this study, we found that RARα itself, in the absence of At-RA, had a positive effect on inducing Th9 cells, with correlating increases in H3k27ac at both the promoter and -23kb enhancer region. Th9 cells require IRF4 binding to the *Il9* locus for induction.[117] We identified *Irf4* downregulation by At-RA, but the effect of RARα on IRF4 expression was insufficient to explain the positive RARα effect on Th9 differentiation. Notable At-RA induction of the transcriptional repressor, *Gfi1,* was also identified. Putative RARα binding sites in the *Gfi1* promoter region indicated RARα binding may be necessary to mediate At-RA upregulation of GFI1 expression. Promoter activity with native RARα binding sites demonstrated the induction of promoter activity by At-RA; however, mutated RARα binding sites led to equivocal promoter activity with the WT promoter. This indicates a suppressive effect of RARα binding in the absence of At-RA on the activity of the GFI1 promoter. RARα binding to sites within the *Gfi1* locus indicated RARα binding to a pair of RARα binding motifs only in the absence of At-RA. Reciprocal binding of the histone acetyltransferase SRC3 at the same site in the presence of At-RA provides a mechanism for At-RA induced acetylation at H3k27 and induction of *Gfi1* expression.

While GFI1 is known to affect other T helper cell differentiation, its effect on Th9 differentiation had yet to be tested.[123,126,127] To this end, we forced expression of GFI1 and demonstrated a suppressive effect on Th9 and Th17 differentiation. Analysis of T cell differentiation in *Gfi1*$^{fl/fl}$ CD4-cre cells demonstrated that GFI1 suppressed Th9 and Th17

differentiation at low At-RA concentrations, indicating At-RA induction of *Gfi1* expression can partially explain reduced Th9 and Th17 differentiation.

Individual and cumulative roles of At-RA and RARα on the epigenetic modification and transcriptome of effector T cells are responsible for changes in differentiation and function. The divergent nature of At-RA and RARα effects as demonstrated at low At-RA concentrations indicates the complexity of regulation that vitamin A exerts upon the immune system. Future studies of vitamin A effects on immune function must consider retinoic acid receptor functions that occur in the absence of vitamin A metabolites. In particular, RARα effects on Th9 and Th17 cells may contribute to pathology in T cell-mediated inflammatory or allergic diseases, such as colitis, airway inflammation, and food allergy.

Table 2.1. Oligonucleotide sequences.

Oligonucleotides	
Endogenous RARα-F 5’ TCAGCCCCTCACCCTCCAAT 3’	RARα-Tg genotyping
Endogenous RARα-R 5’ CTCACCTTACAGCCCTCACA 3’	RARα-Tg genotyping
Transgenic RARα-F 5’ GATGCTGATGAAGATCACAG 3’	RARα-Tg genotyping
Transgenic RARα-R 5’ GGACAATGAGTTTTCTGCTG 3’	RARα-Tg genotyping
Cre-F 5’ 5’ CGGTCGATGCAACGAGTGATGAGG 3’	$\Delta Rara^{LCK}$ genotyping
Cre-R 5’ CCAGAGACGGAAATCCATCGCTCG 3’	$\Delta Rara^{LCK}$ genotyping
oIMR7338 5’ CTAGGCCACAGAATTGAAAGATCT 3’	$\Delta Rara^{LCK}$ genotyping
oIMR7339 5’ GTAGGTGGAAATTCTAGCATCATCC 3’	$\Delta Rara^{LCK}$ genotyping
Flox-RARα-F 5’ TCAGCCCCTCACCCTCCAAT 3’	$\Delta Rara^{LCK}$ genotyping
Flox-RARα-R 5’CTCACCTTACAGCCCTCACA 3’	$\Delta Rara^{LCK}$ genotyping
Gfi1-F 5’ AAGAAGGCGCACAGCTATCA 3’	qRT-PCR
Gfi1-R 5’ CAGTGACTTCTCCGACGCTG 3’	qRT-PCR
Rara-F 5’ CCTGCCCCGCATCTACAAG 3’	qRT-PCR
Rara-R 5’ GGTTCCGGGTCACCTTGTT 3’	qRT-PCR
Actb-F 5’ AGAAGAGCTACGAGCTGCCTGAC 3’	qRT-PCR
Actb-R 5’ TACTCCTGCTTGCTGATCCACAT 3’	qRT-PCR

Table 2.2. KEGG pathway analysis. KEGG pathways enriched in differentially expressed gene lists from RNAseq data. Using lists of differentially expressed genes derived from comparisons of individual factors (RARα or At-RA), KEGG pathway analysis was performed with DAVID.

		KEGG Pathway	Gene Count	p-value
Without At-RA	Increased expression with higher RARα	Inflammatory bowel disease	10	0.000005
		FoxO signaling pathway	12	0.000213
		Cytokine-cytokine receptor interaction	15	0.001133
		Cell adhesion molecules (CAMs)	11	0.003622
		Adherens junction	6	0.023145
		T cell receptor signaling pathway	7	0.026634
	Decreased expression with higher RARα	Insulin signaling pathway	9	0.002481
		Cytokine-cytokine receptor interaction	12	0.002555
		Adherens junction	5	0.033180
		N-Glycan biosynthesis	4	0.049505
With At-RA	Increased expression with higher RARα	Cytokine-cytokine receptor interaction	16	0.000007
		Inflammatory bowel disease	8	0.000019
		Toll-like receptor signaling pathway	7	0.003148
		T cell receptor signaling pathway	7	0.003148
		NF-kappa B signaling pathway	6	0.012430
		TGF-beta signaling pathway	5	0.033141
	Decreased expression with higher RARα	Inflammatory bowel disease	8	0.001446
		cAMP signaling pathway	15	0.001638
		Adherens junction	8	0.004552
		cGMP-PKG signaling pathway	12	0.007420
		Cell adhesion molecules (CAMs)	11	0.018655
		Metabolic pathways	49	0.025900

	KEGG Pathway	Gene Count	p-value
Increased by At-RA	Inflammatory bowel disease	16	<0.000001
	FoxO signaling pathway	22	0.000031
	Cell adhesion molecules (CAMs)	23	0.000181
	Cytokine-cytokine receptor interaction	29	0.000413
	T cell receptor signaling pathway	16	0.000740
	Jak-STAT signaling pathway	17	0.010624
	Chemokine signaling pathway	21	0.010736
	cAMP signaling pathway	21	0.011320
	Colorectal cancer	10	0.011733
	Notch signaling pathway	8	0.023056
	TNF signaling pathway	13	0.025399
	TGF-beta signaling pathway	11	0.026303
	Fatty acid metabolism	8	0.028128
Decreased by At-RA	Cytokine-cytokine receptor interaction	28	<0.000001
	Arginine and proline metabolism	9	0.000242
	Inflammatory bowel disease	9	0.000884
	Jak-STAT signaling pathway	14	0.001483
	TNF signaling pathway	11	0.004330
	Rap1 signaling pathway	16	0.007208
	Chemokine signaling pathway	15	0.007911
	Biosynthesis of amino acids	8	0.015667
	Central carbon metabolism in cancer	7	0.022686
	Neurotrophin signaling pathway	10	0.025195
	p53 signaling pathway	7	0.027738

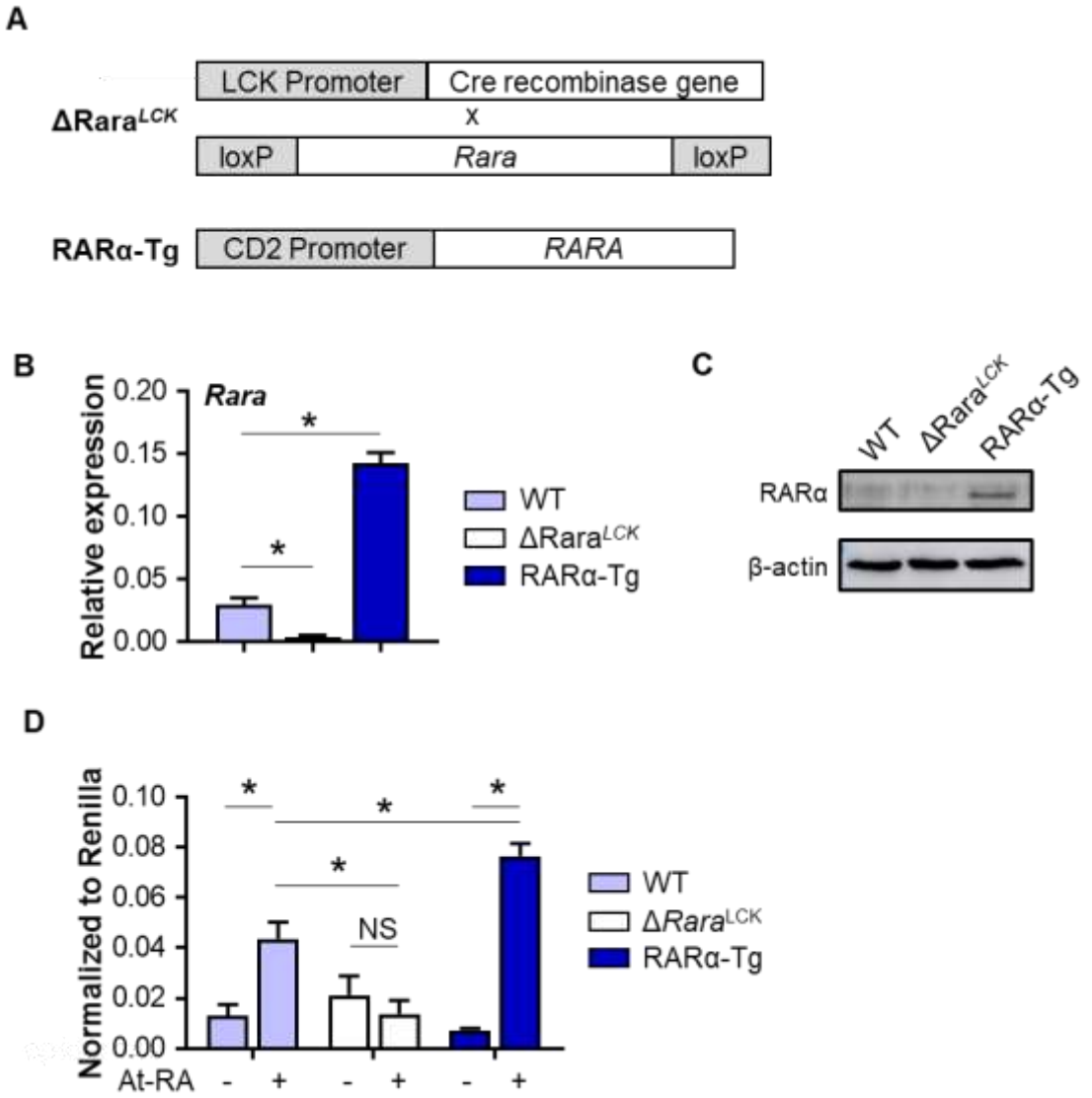

Figure 2.1. RARα expression and function altered in murine RARα strains. (A) For selective modification of RARα expression in T cells two mice strains were utilized. The ΔRaraLCK strain utilizes the cre-lox system and a mouse strain with the Rara exon 3 flanked by loxP sites to selectively delete expression in T cells. The RARα-Tg strain utilizes the CD2 promoter to selectively overexpress the human RARA transcript in T cells. (B) Naïve T cells were isolated from RARα mice splenocytes (>95% purity) and used to isolate RNA and synthesize cDNA, followed by qRT-PCR for Rara. (C) Total T helper cells were isolated from RARα mice splenocytes and the expression of RARα protein level by Western Blot was performed. (D) RARα function in binding to RARE sites to initiate transcription was assessed using a dual-luciferase assay. Naïve T cells were isolated and cultured in Tnp condition with charcoal-treated FBS cRPMI for 1 day. Cells were then harvested and chilled for 1 hour, then transfected with 10 μg of pGL3-RARE and 0.5 μg of pRL-CMV. Cells were split and rested for 4 hours in Amaxa media (with or without At-RA) and then restimulated for 6 hours in Tnp condition (with or without At-RA). Dual-luciferase assay was performed immediately. * $p<0.05$ by one-way ANOVA w/Bonferroni (A) or two-way ANOVA w/Bonferroni (C). Error bars indicate SEM.

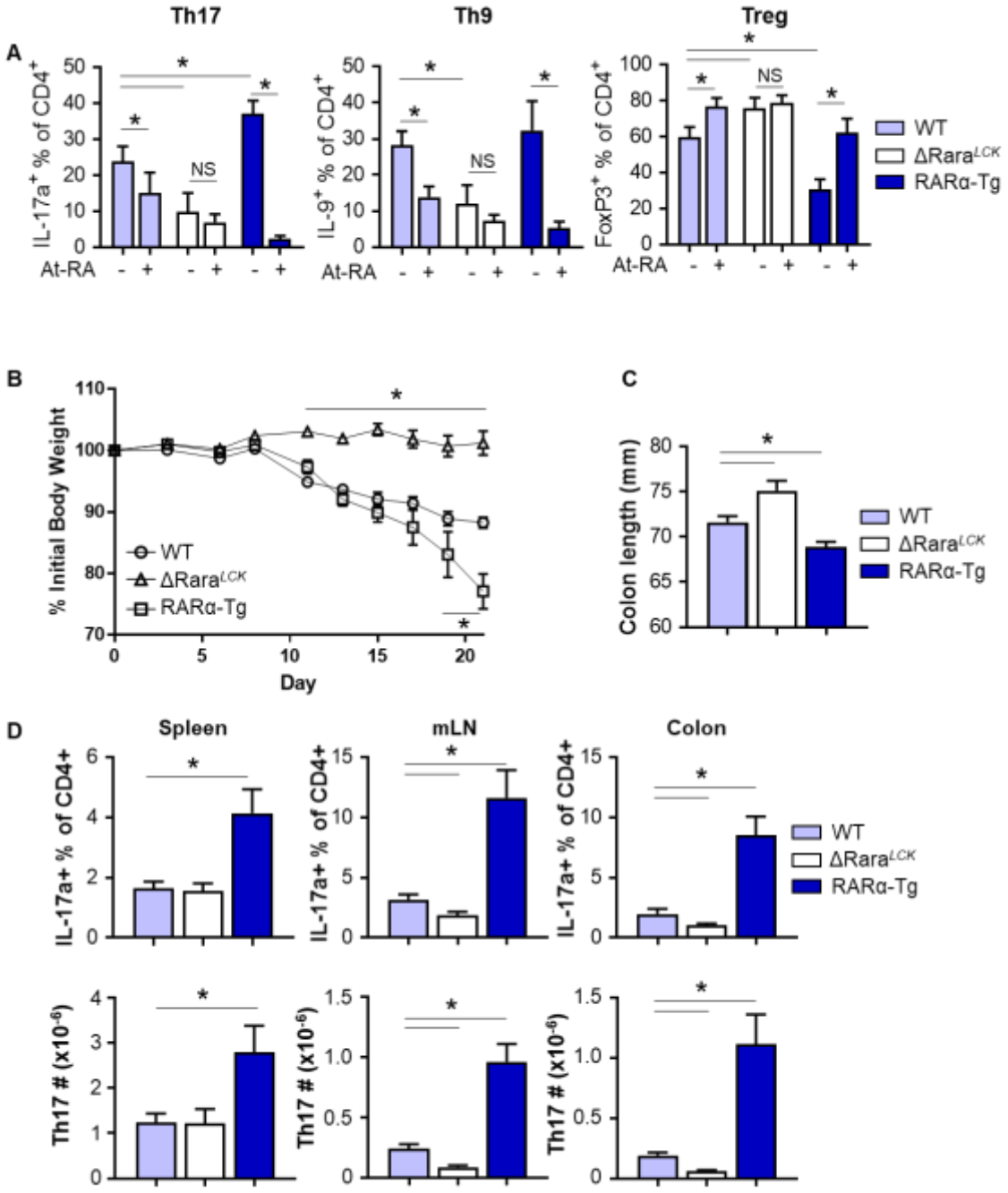

Figure 2.2. Divergent roles of RARα and At-RA on T helper cell *in vitro* differentiation and T-cell transfer colitis. (A) Naïve T helper cells were activated in Th17-, Treg-, or Th9-polarizing conditions for 4 days followed by flow cytometry analysis of intracellular FoxP3, IL-17a, or IL-9 expression. (B) Body weight change from initial in T-cell transfer model of colitis. (C) Colon length at the termination of the experiment. (D) Th17 cell percentages and numbers at the termination of the experiment. * $p<0.05$. Statistical analysis by repeated measures ANOVA w/Bonferroni for A and one-way ANOVA for B-C. * $p<0.05$; n=3. Stats by two-way ANOVA w/Bonferroni. * $p<0.05$; n=3-4.

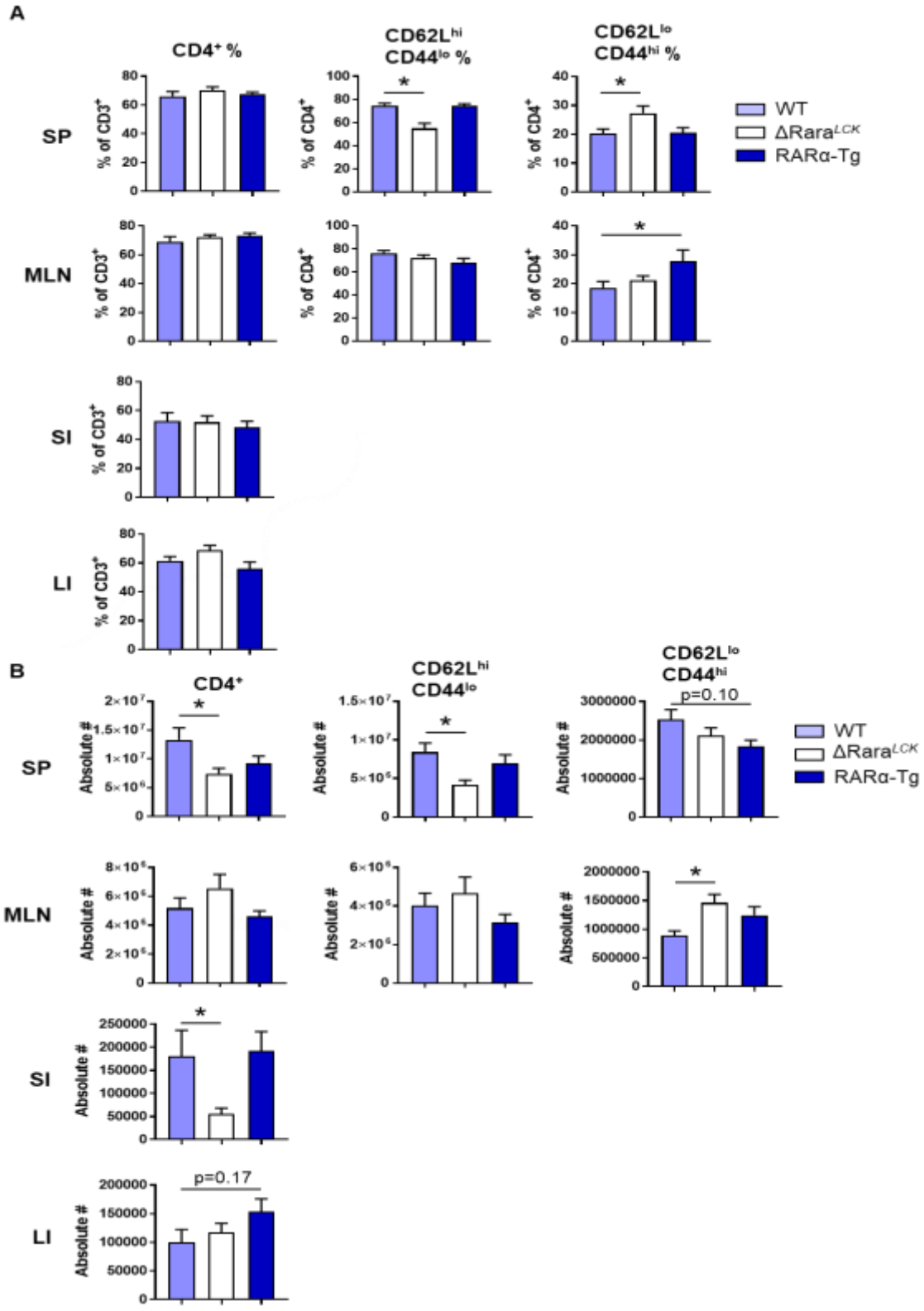

Figure 2.3. Steady state T helper cell populations in RARα mouse strains. (A) Percentages of indicated populations in $CD3^+$ or $CD4^+$ populations of lymphocytes. (B) Absolute numbers of indicated populations of T helper cells per tissue.

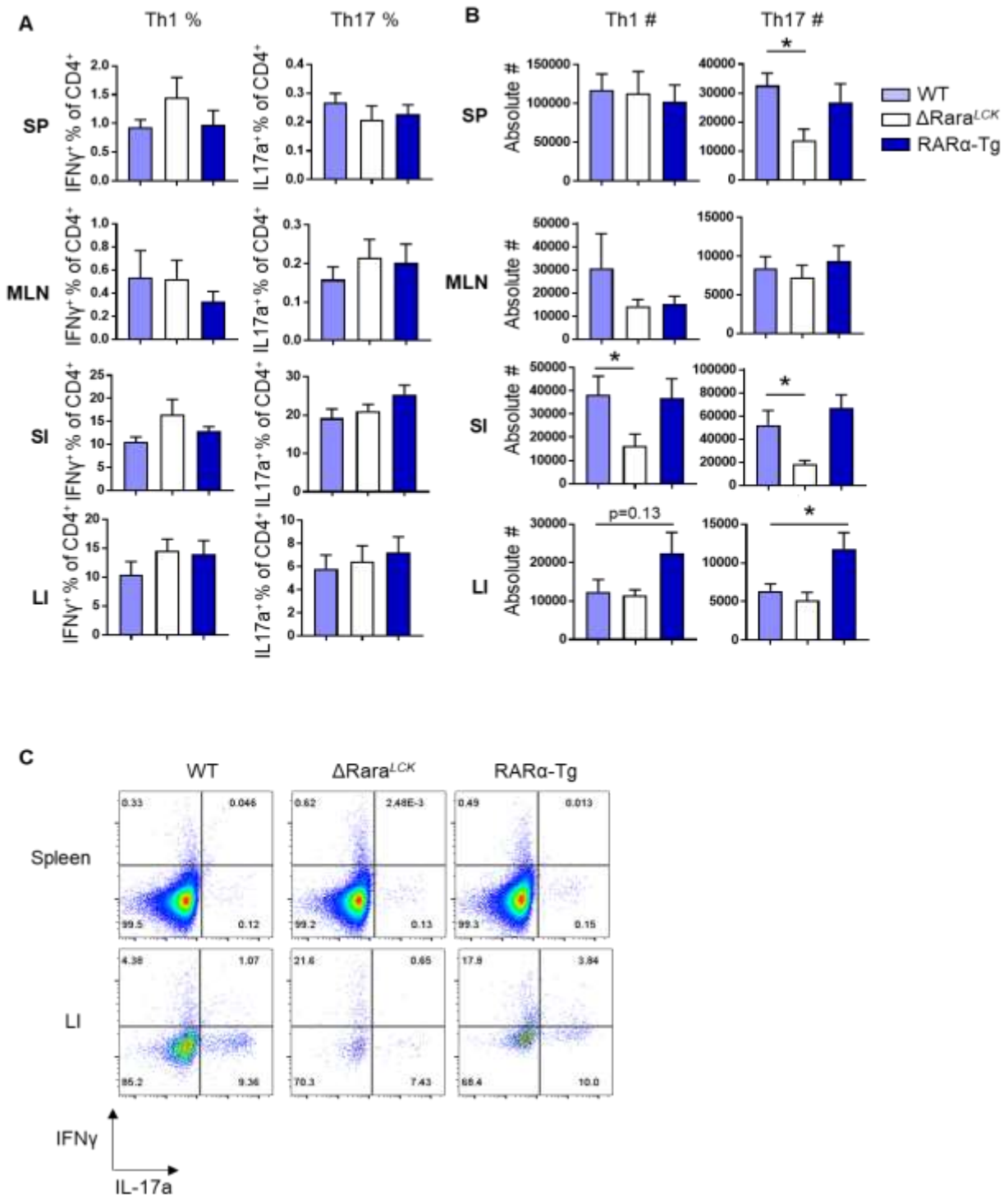

Figure 2.4. Steady state Th1 and Th17 populations in RARα mouse strains. Th1 and Th17 cells were analyzed by intracellular flow cytometry for cytokine expression. (A) Percentages and absolute counts in the spleen, mesenteric LN, small intestine lamina propria, and large intestine lamina propria are shown for 6-8 week old mice in steady state conditions. (B) Representative flow cytometry dot plots. Results are combined from 3 independent experiments. n=6-7. * $p<0.05$. Statistical analysis by one-way ANOVA w/Bonferroni.

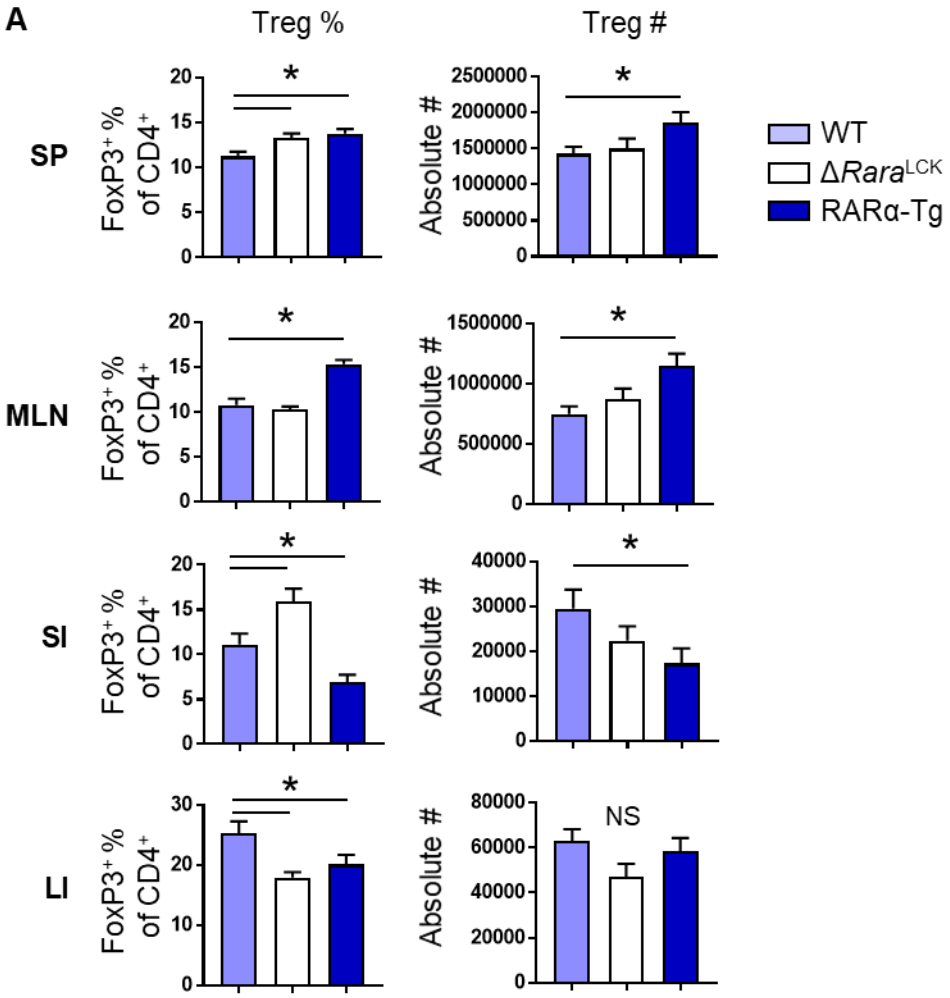

Figure 2.5. Steady state Treg populations in RARα mouse strains. Total T helper cell counts and Treg percentages and absolute counts in the spleen, mesenteric LN, small intestine lamina propria, and large intestine lamina propria were assessed in 6-8 week-old mice in steady state conditions. Results are combined from at least 3 independent experiments. n=6-13. * $p<0.05$. Statistical analysis by one-way ANOVA w/Bonferroni.

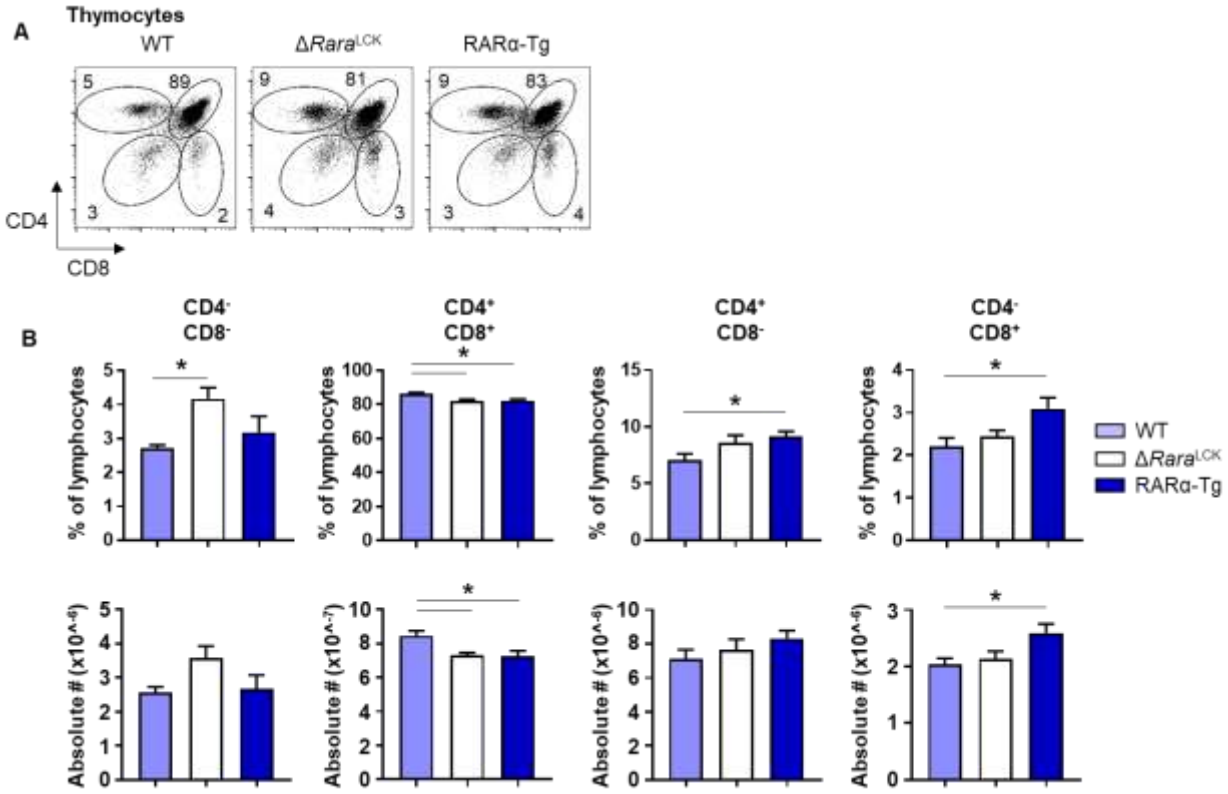

Figure 2.6. Thymocyte T cell populations from 6-8 week old mice. Representative data (A) and combined data (B) from 5 independent experiments. WT n=8, ΔRara^{LCK} n=17, RARα-Tg n=12. Statistical analysis by one-way ANOVA with Bonferroni correction.

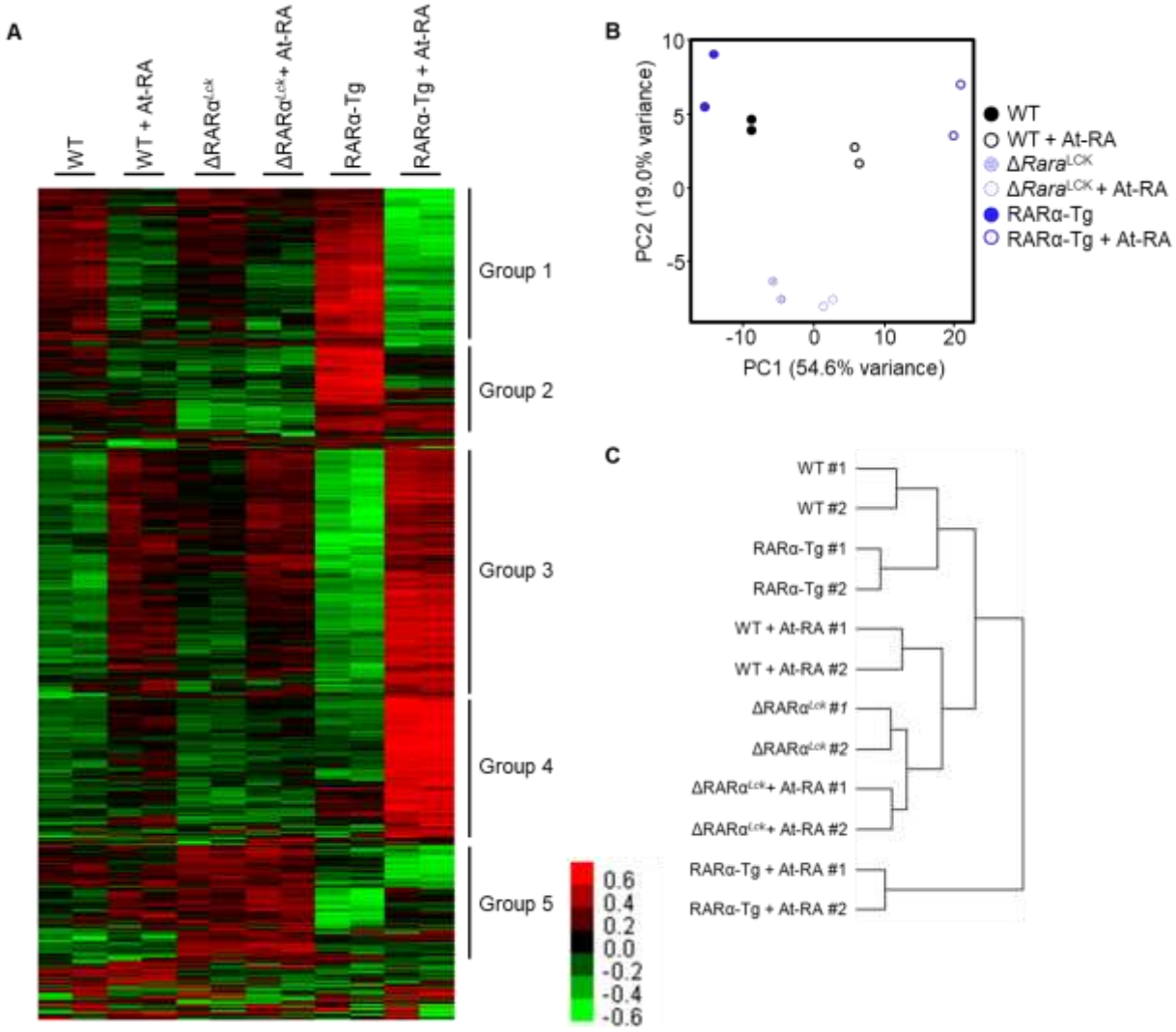

Figure 2.7. Transcriptome analysis of RARα and At-RA effects on Th17-polarized cell cultures. (A) Treeview plot of 2742 differentially expressed genes with -0.5 > log2 FC > 0.5 and p-value < 0.05 (t-test) for at least one comparison. [Genepattern, normalized expression by row, city-block clustering in rows. (B) PCA plot with differentially expressed genes. (C) Pearson correlation of samples, using list of 2742 DEGs. (Genepattern).

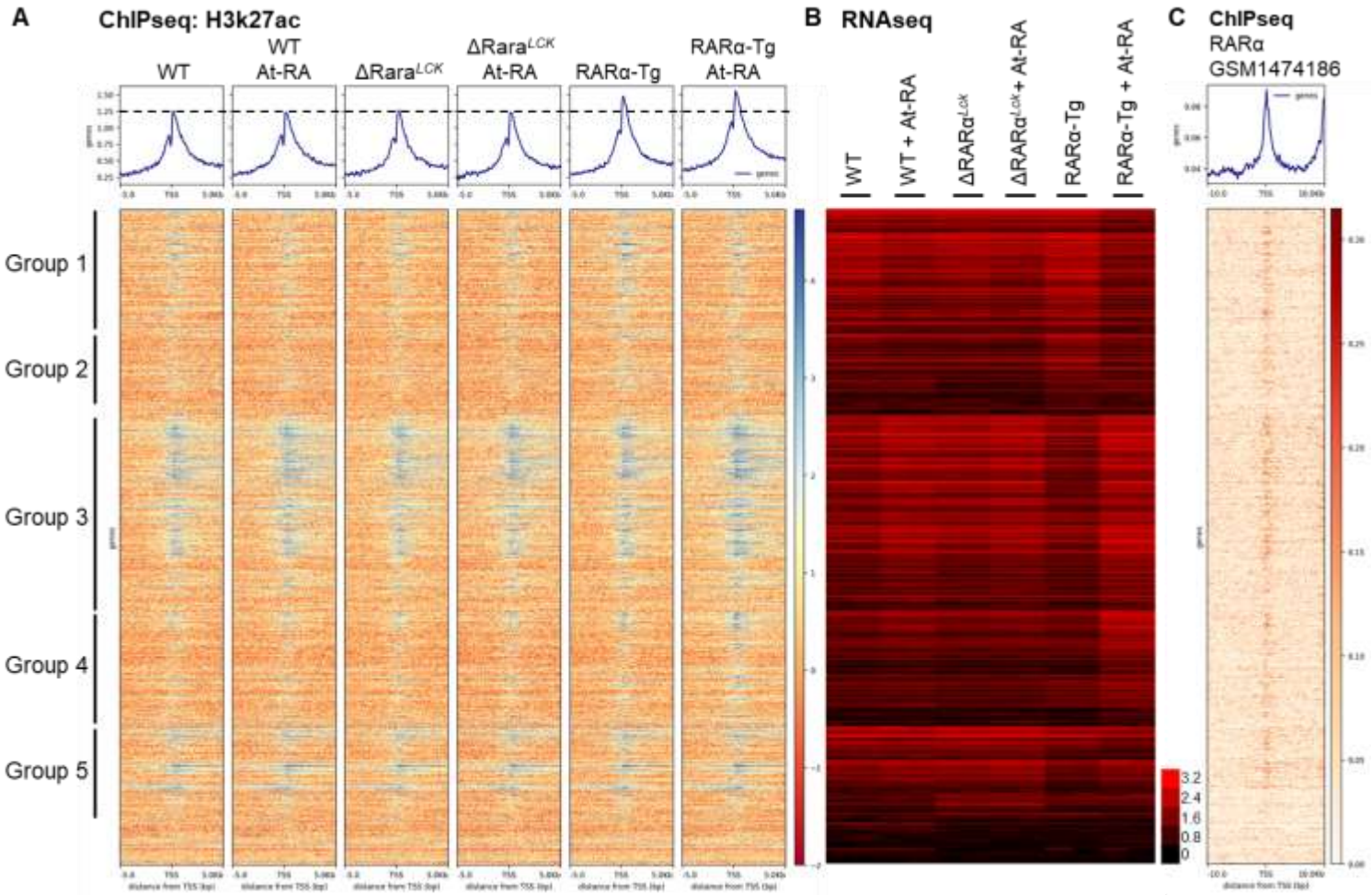

Figure 2.8. H3k27ac epigenetic modifications are amplified by RARα expression. (A) H3k27ac modification in 16-hr Th17-polarized cultures, arranged in the order of RNAseq DEGs, and compared with log10 transformed FPKM values of RNAseq data and RARα binding in the TSS region (Brown et al. 2015, GSM1474186). (B) Enrichment of H3k27ac in the TSS region (-2kb to +2kb) from ChIPseq data compared to RNAseq gene expression for the At-RA effect. (C) Enrichment of H3k27ac in the TSS region (-2kb to +2kb) from ChIPseq data compared to RNAseq gene expression for the RARα effect.

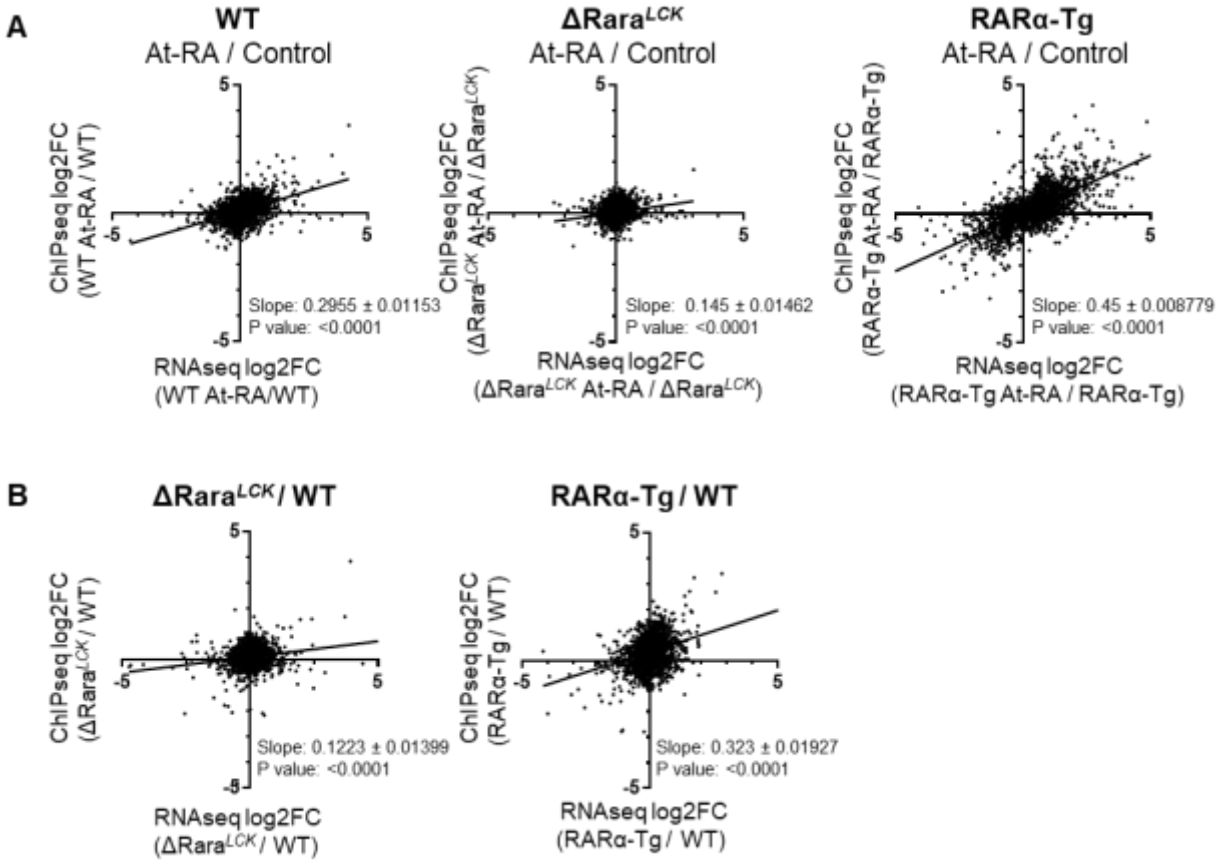

Figure 2.9. RARα expression amplifies epigenetic effects of H3k27ac on transcription. (A) Log2FC enrichment of H3k27ac in the TSS region (-2kb to +2kb) from ChIPseq data compared to log2FC RNAseq gene expression for the At-RA effect. (C) Log2FC enrichment of H3k27ac in the TSS region (-2kb to +2kb) from ChIPseq data compared to log2FC RNAseq gene expression for the RARα effect.

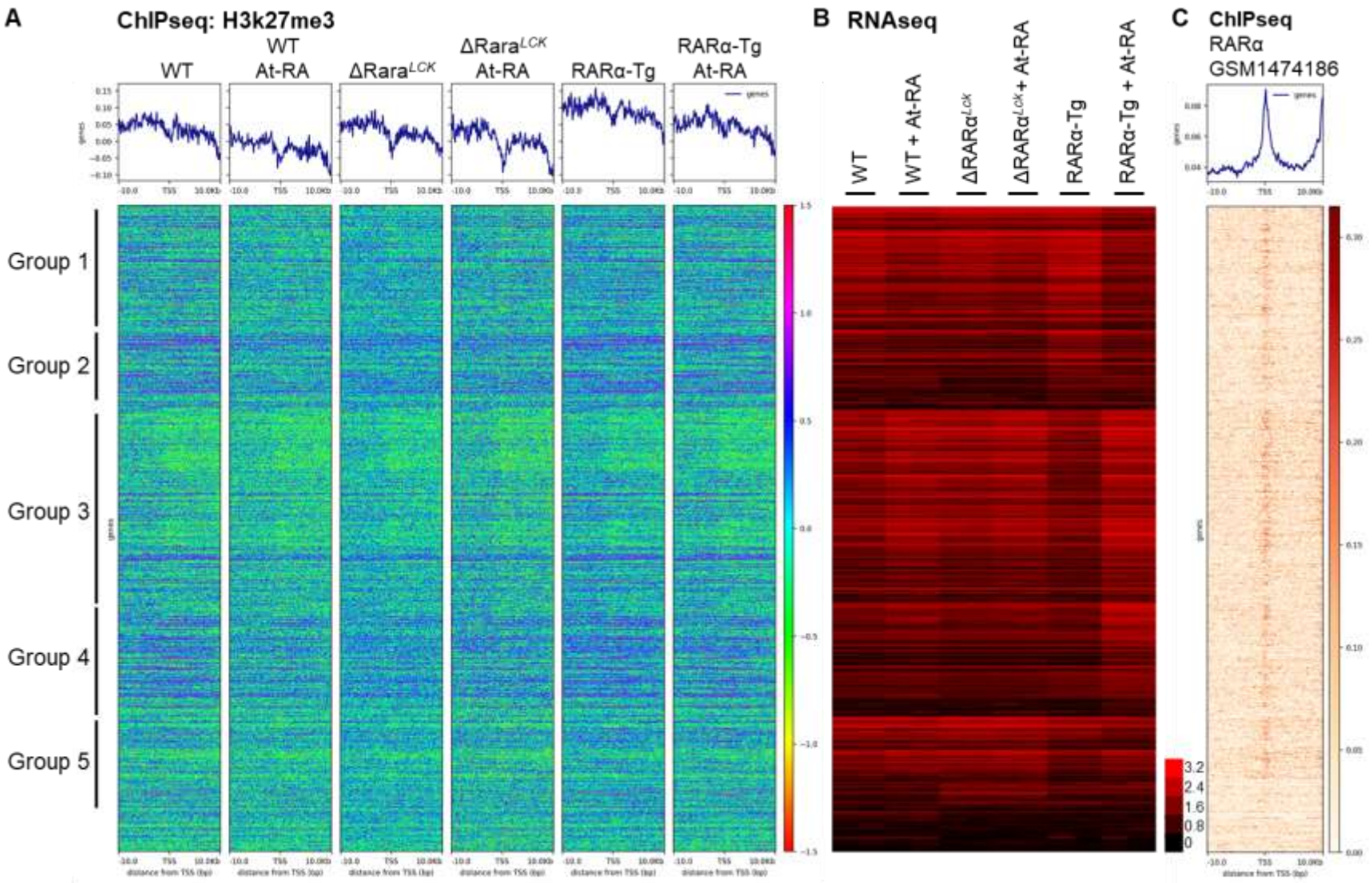

Figure .2.10. H3k27me3 epigenetic modifications parallel RNA expression and are upregulated by RARα. (A) H3k27me3 modification in 16-hr Th17-polarized cultures, arranged in the order of RNAseq DEGs, and compared with log10 transformed FPKM values of RNAseq data and RARα binding in the TSS region (Brown et al. 2015, GSM1474186).

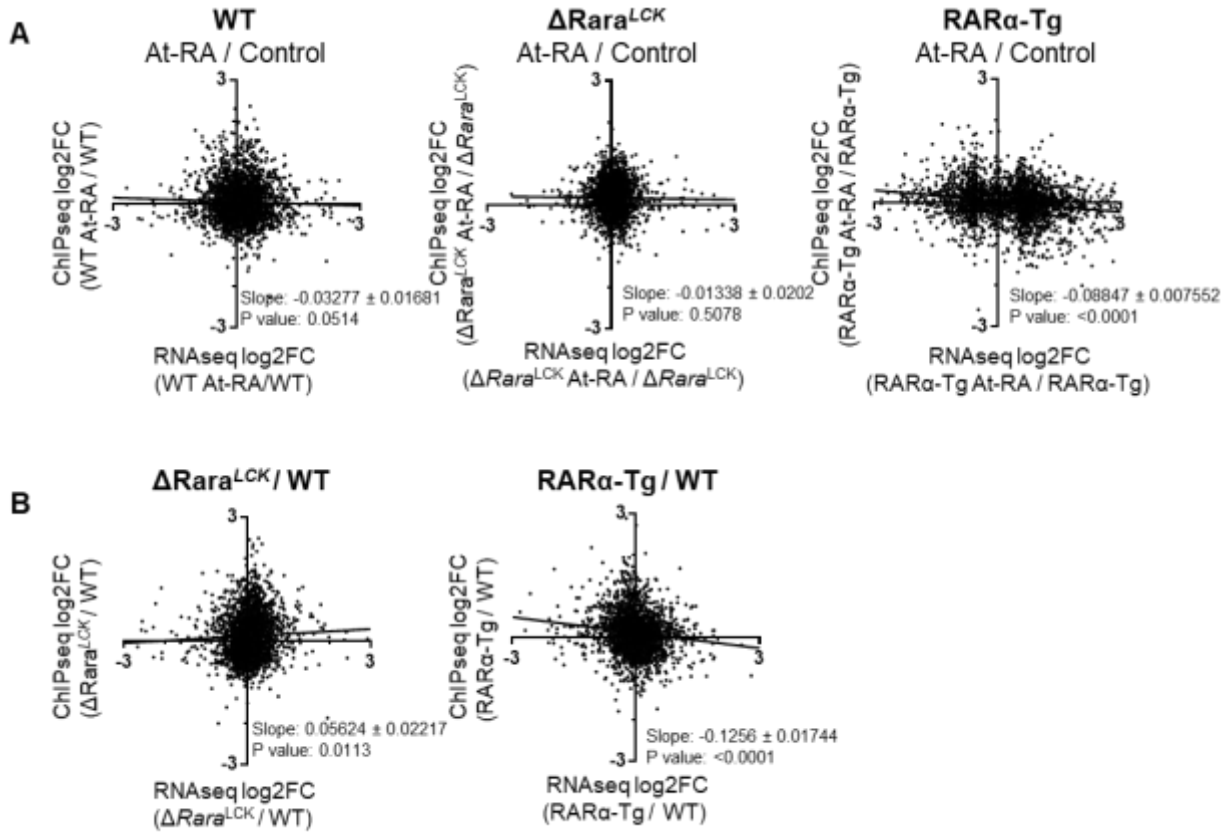

Figure 2.11. RARα expression amplifies epigenetic effects of H3k27me3 on transcriptome. (A) Log2FC enrichment of H3k27me3 in the TSS region (-2kb to +2kb) from ChIPseq data compared to log2FC RNAseq gene expression for the At-RA effect for WT, ΔRara^{LCK}, and RARα-Tg comparisons. (C) Log2FC enrichment of H3k27me3 in the TSS region (-2kb to +2kb) from ChIPseq data compared to log2FC RNAseq gene expression for the RARα effect.

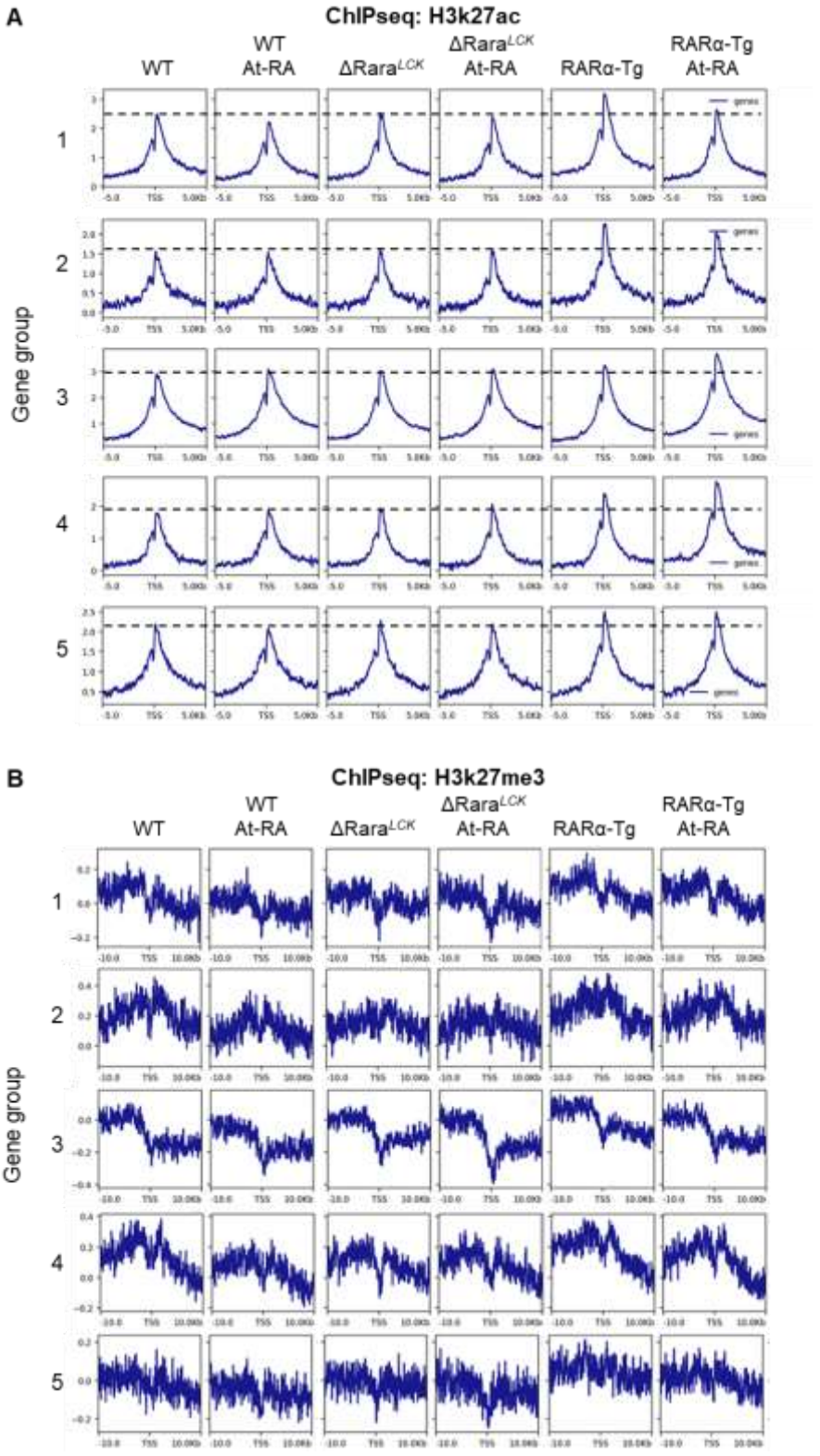

Figure 2.12. Epigenetic modification patterns are linked to RARα expression level regardless of differential RNA expression. (A) H3k27ac peaks in the +/- 5kb region of TSS, separated into DEG groups. (B) H3k27me3 peaks in the +/- 10kb region of TSS, separated into DEG groups.

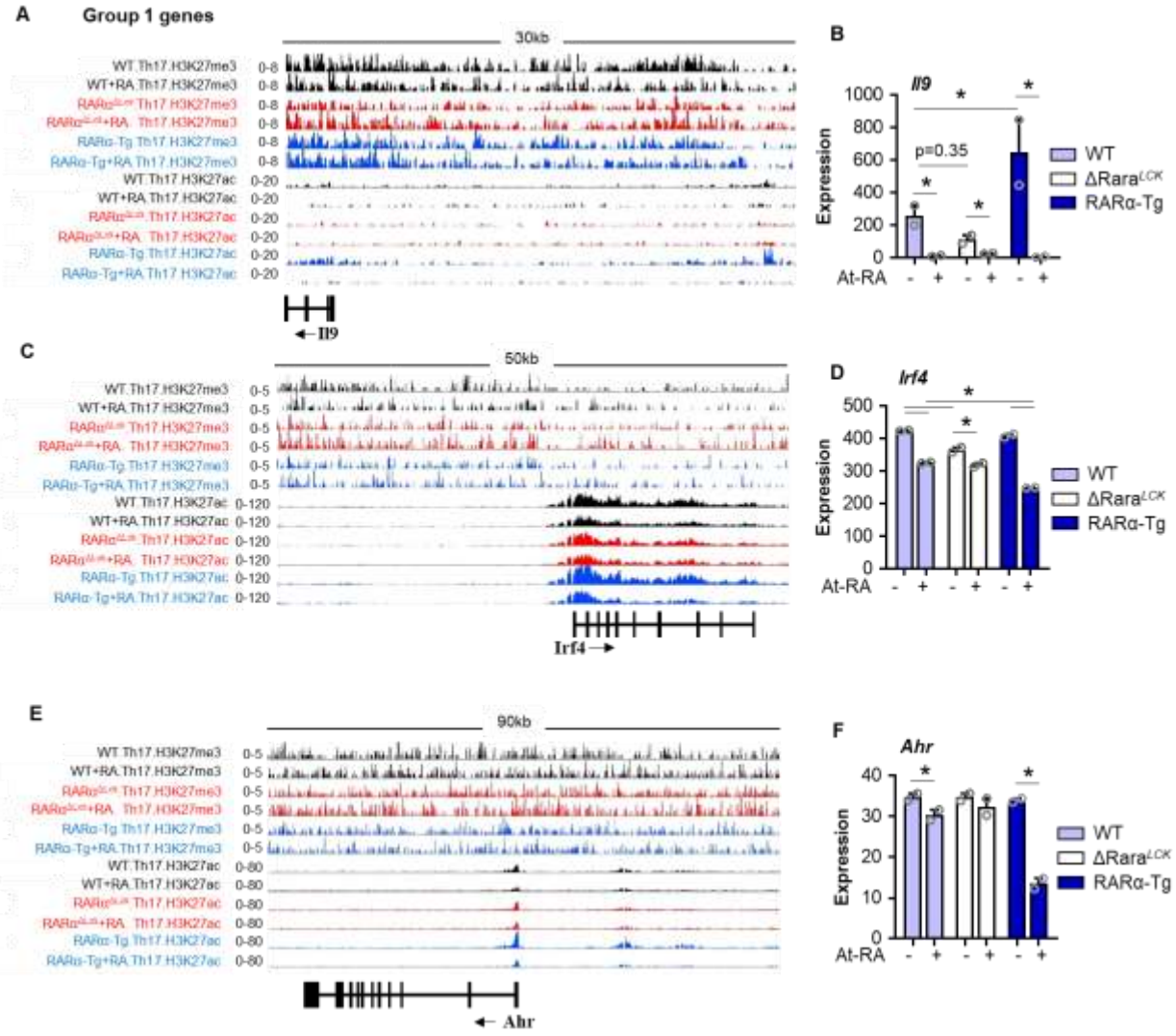

Figure 2.13. At-RA induces suppressive epigenetic landscape in group 1 DEGs (Il9, Irf4, and Ahr). (A) ChIPseq data of Il9 region. (B) RNAseq expression of Il9. (C) ChIPseq data of Irf4 region. (D) RNAseq expression of Irf4. (E) ChIPseq data of Ahr region. (F) RNAseq expression of Ahr. Statistics by 2-way ANOVA with Bonferroni correction.

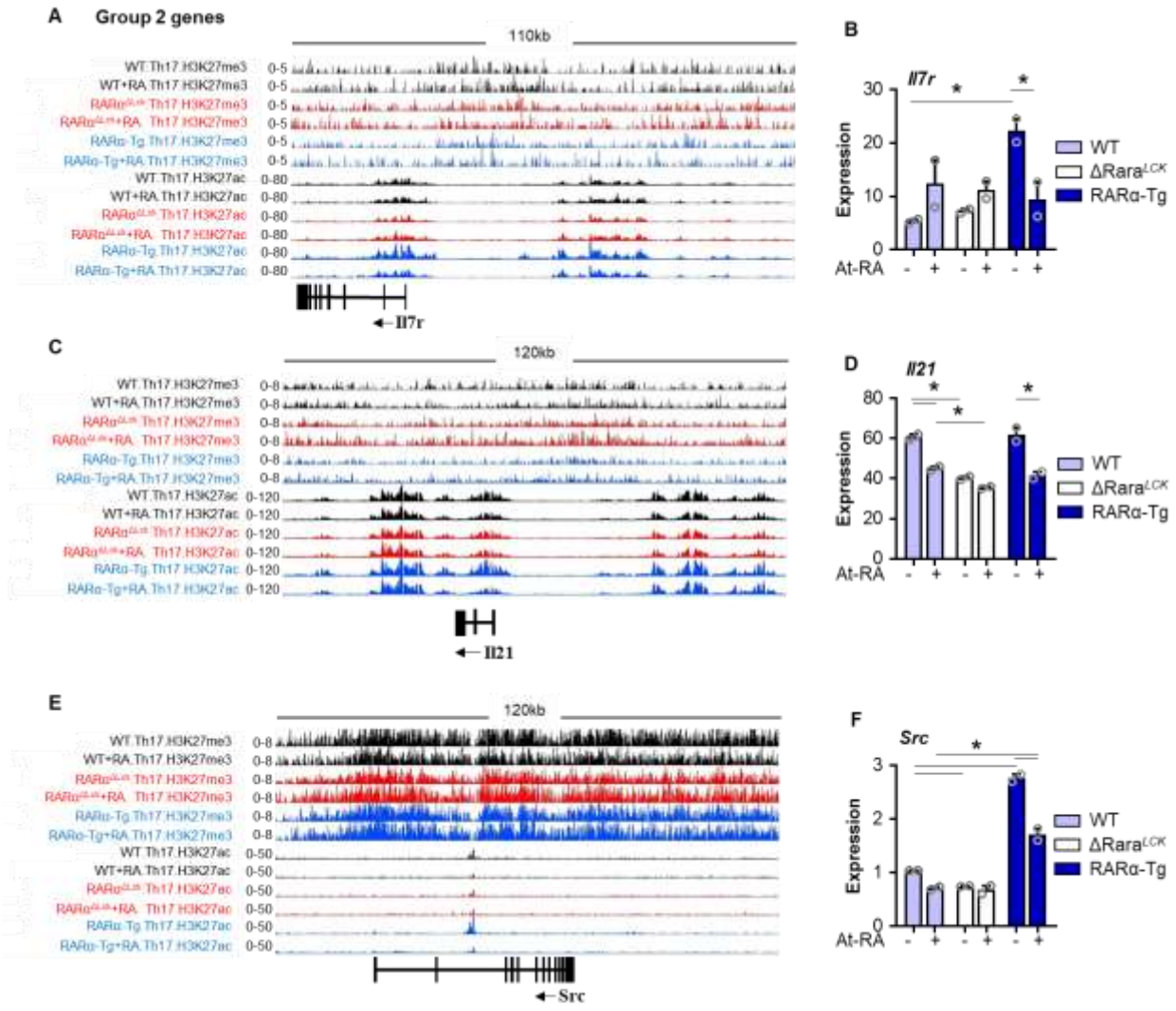

Figure.2.14. RARα promotes active, while At-RA promotes repressive epigenetic modifications in group 2 DEGs (Il7r, Il21, and Src). (A) ChIPseq data of Il7r region. (B) RNAseq expression of Il7r. (C) ChIPseq data of Il21 region. (D) RNAseq expression of Il21. (E) ChIPseq data of Src region. (F) RNAseq expression of Src. Statistics by 2-way ANOVA with Bonferroni correction.

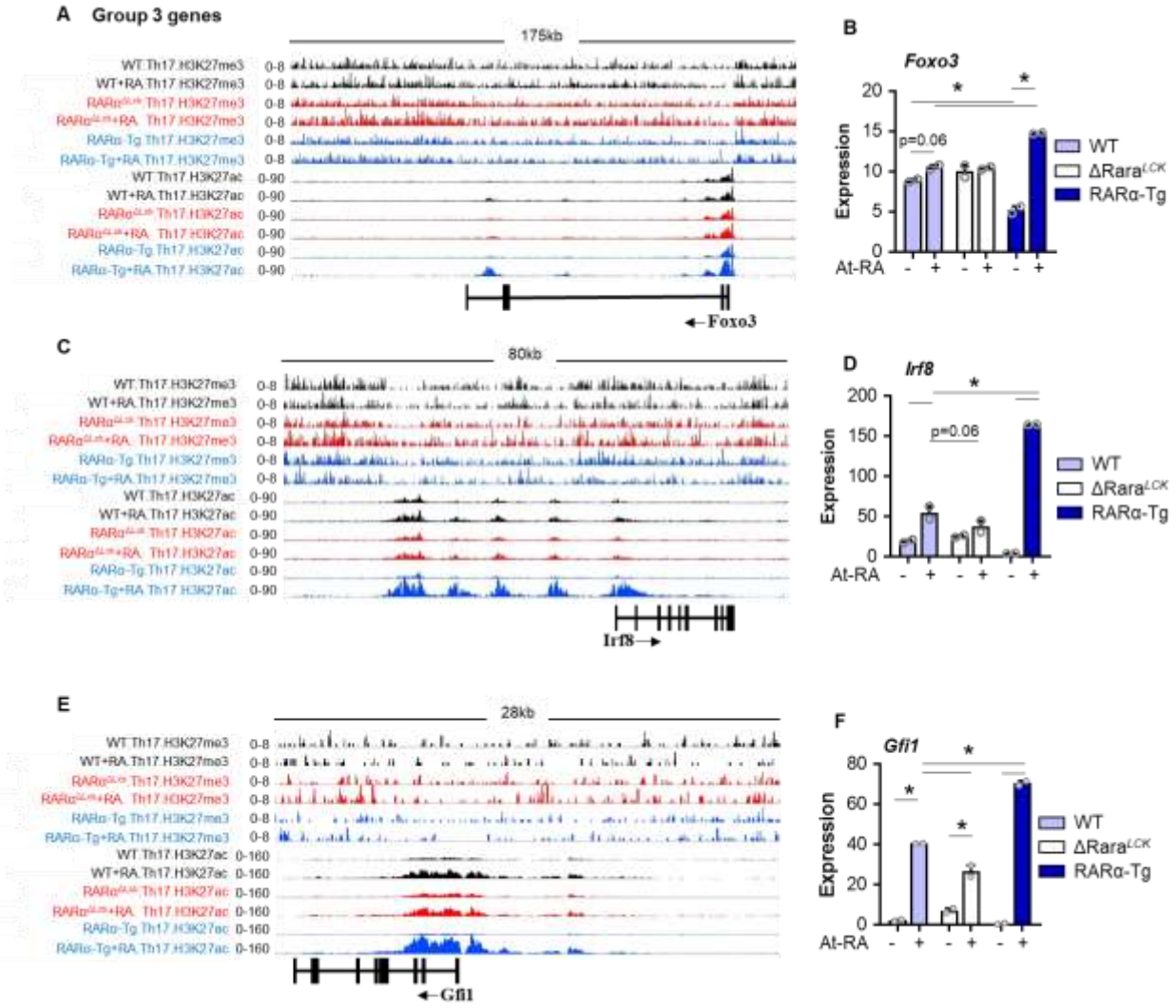

Figure.2.15. RARα promotes repressive, while At-RA promotes active epigenetic modifications in group 3 DEGs (Foxo3, Irf8, and Gfi1). (A) ChIPseq data of Foxo3 region. (B) RNAseq expression of Foxo3. (C) ChIPseq data of Irf8 region. (D) RNAseq expression of Irf8. (E) ChIPseq data of Gfi1 region. (F) RNAseq expression of Gfi1. Statistics by 2-way ANOVA with Bonferroni correction.

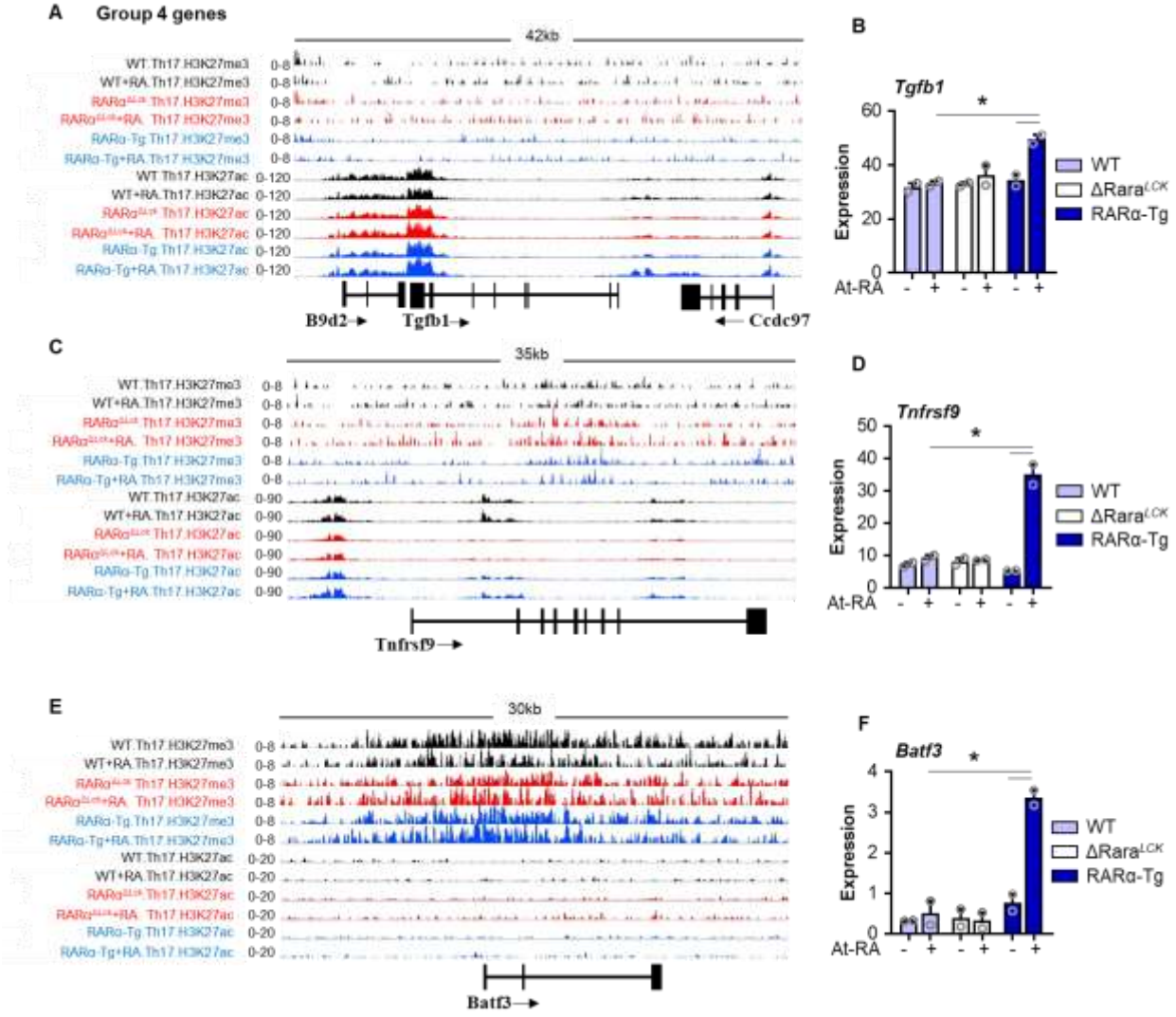

Figure 2.16. At-RA induces active epigenetic modifications in group 4 DEGs (Tgfb1, Tnfrsf9, and Batf3) in the presence of high RARα expression. (A) ChIPseq data of Tgfb1 region. (B) RNAseq expression of Tgfb1. (C) ChIPseq data of Tnfrsf9 region. (D) RNAseq expression of Tnfrsf9. (E) ChIPseq data of Batf3 region. (F) RNAseq expression of Batf3. Statistics by 2-way ANOVA with Bonferroni correction.

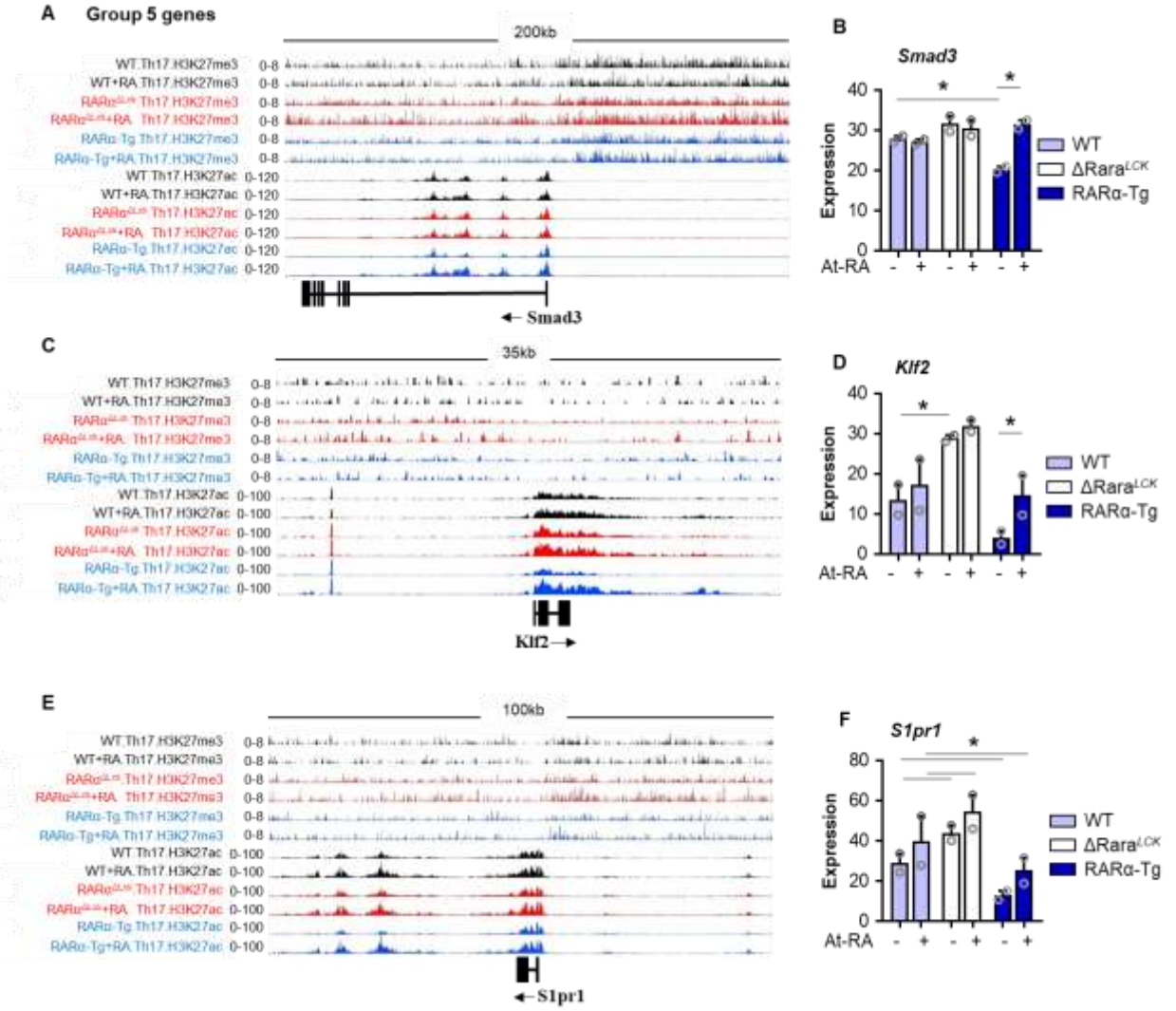

Figure 2.17. Loss of RARα deregulates At-RA-dependent epigenetic modifications in group 5 DEGs (Smad3, Klf2, and S1pr1). (A) ChIPseq data of Smad3 region. (B) RNAseq expression of Smad3. (C) ChIPseq data of Klf2 region. (D) RNAseq expression of Klf2. (E) ChIPseq data of S1pr1 region. (F) RNAseq expression of S1pr1. Statistics by 2-way ANOVA with Bonferroni correction.

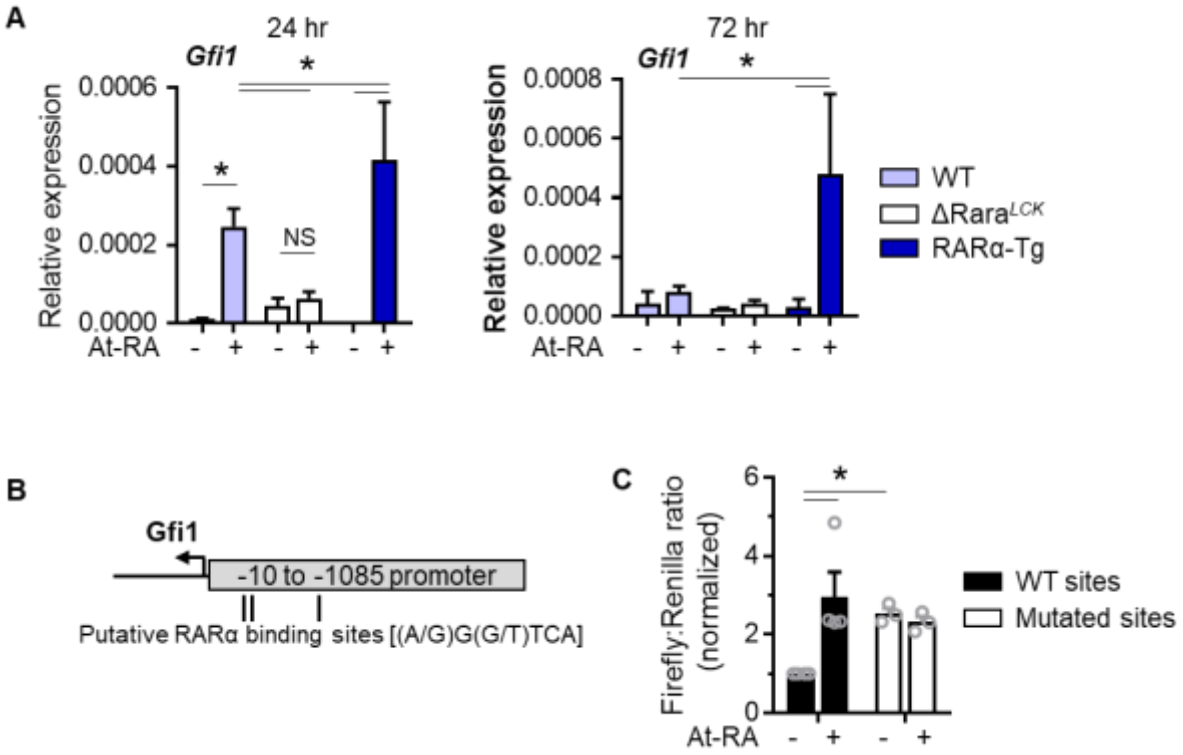

Figure 2.18. At-RA and RARα control *Gfi1* expression by epigenetic regulation. (A) *Gfi1* expression by qRT-PCR in 24- and 72-hour cultures of Th17-polarized cells. (B) GFI1 promoter region used in construction of pGL4.10_Gfi1 plasmids for dual luciferase assay. (C) Dual luciferase assay of GFI1 promoter activity in the presence or absence of At-RA, with promoter containing intact or mutated putative RARα binding sites. n=3-5 from at least 3 independent experiments. Statistics by 2-way ANOVA with Bonferroni correction. * $p < 0.05$.

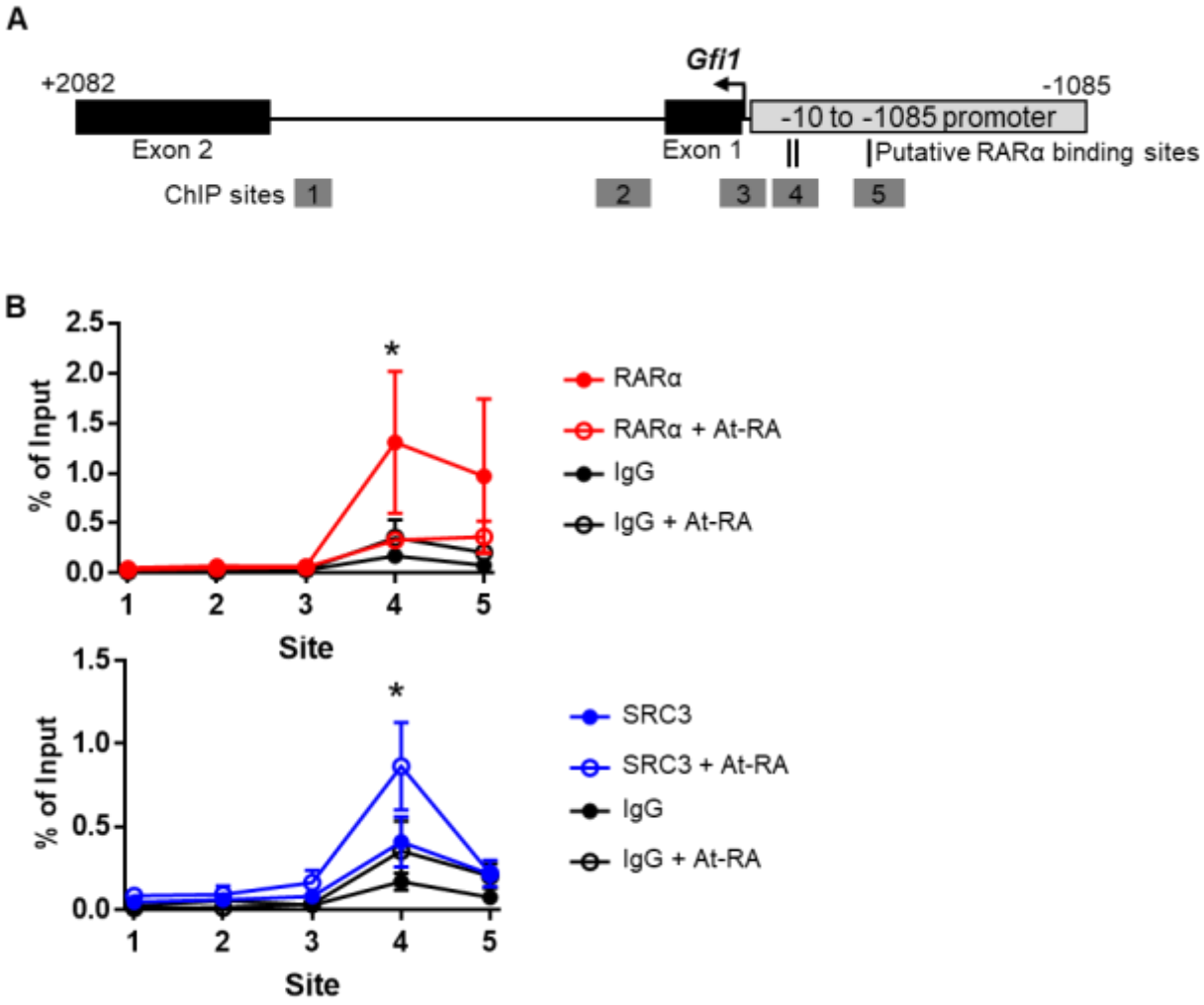

Figure 2.19. RARα binds *Gfi1* promoter in the absence of At-RA. (A) *Gfi1* locus with putative RARα bindings sites and ChIP primer sites identified. (B) ChIP of *Gfi1* locus sites in 16-hour cultures of Th17-polarized WT naïve T helper cells. At-RA use at 10 nM concentration. Immunoprecipitation with antibodies to normal rabbit IgG, RARα, and SRC3. Results from 3 independent experiments. Statistics by 2-way ANOVA with Bonferroni correction. * $p < 0.05$.

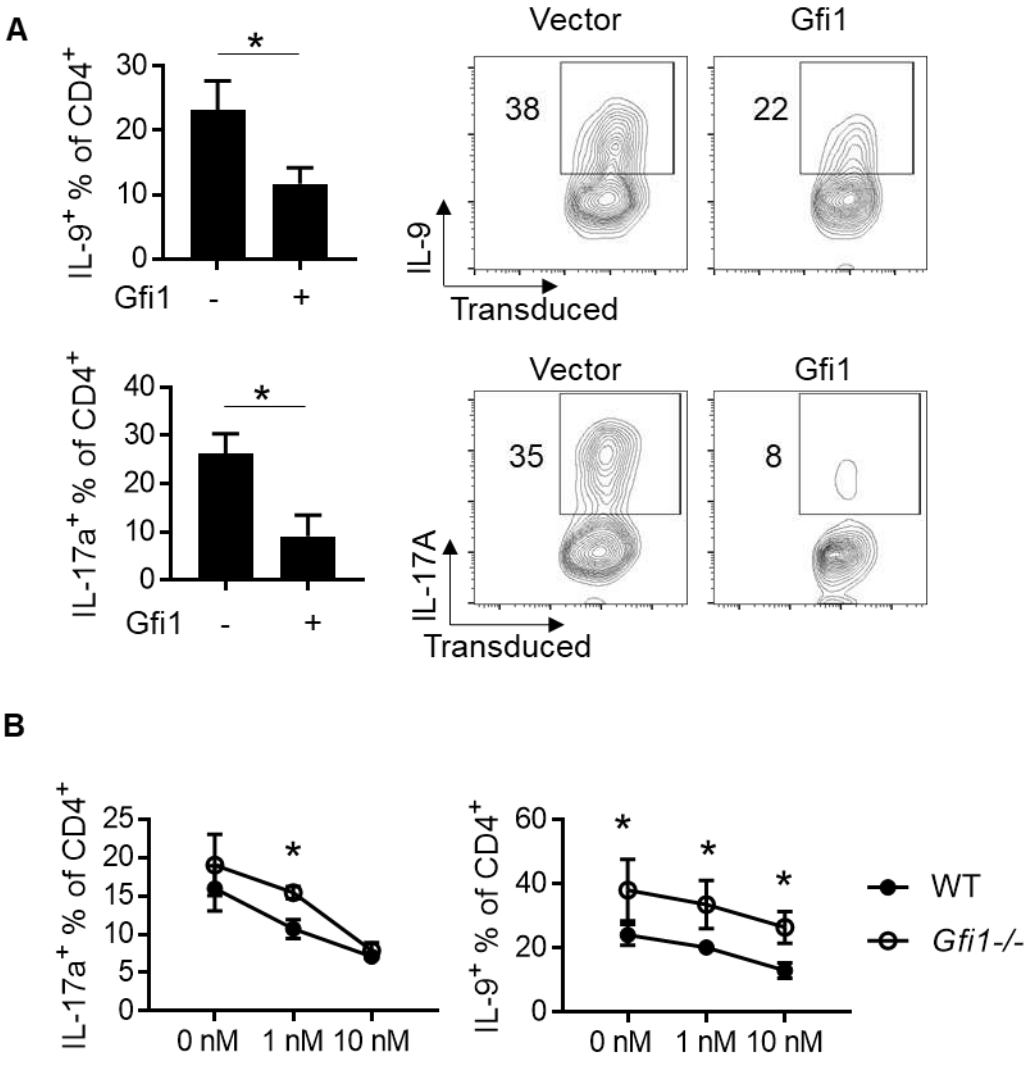

Figure 2.20. GFI1 expression reduces Th9 and Th17 differentiation. (A) Forced Gfi1 expression by retroviral transduction reduces Th9 and Th17 differentiation. (B) Th9 and Th17 differentiation in Δ*Gfi1*^{CD4} cells. Representative or combined data from 4 individual experiments. Statistics by paired t-test (A) or two-way ANOVA with Bonferroni correction (B). * $p < 0.05$.

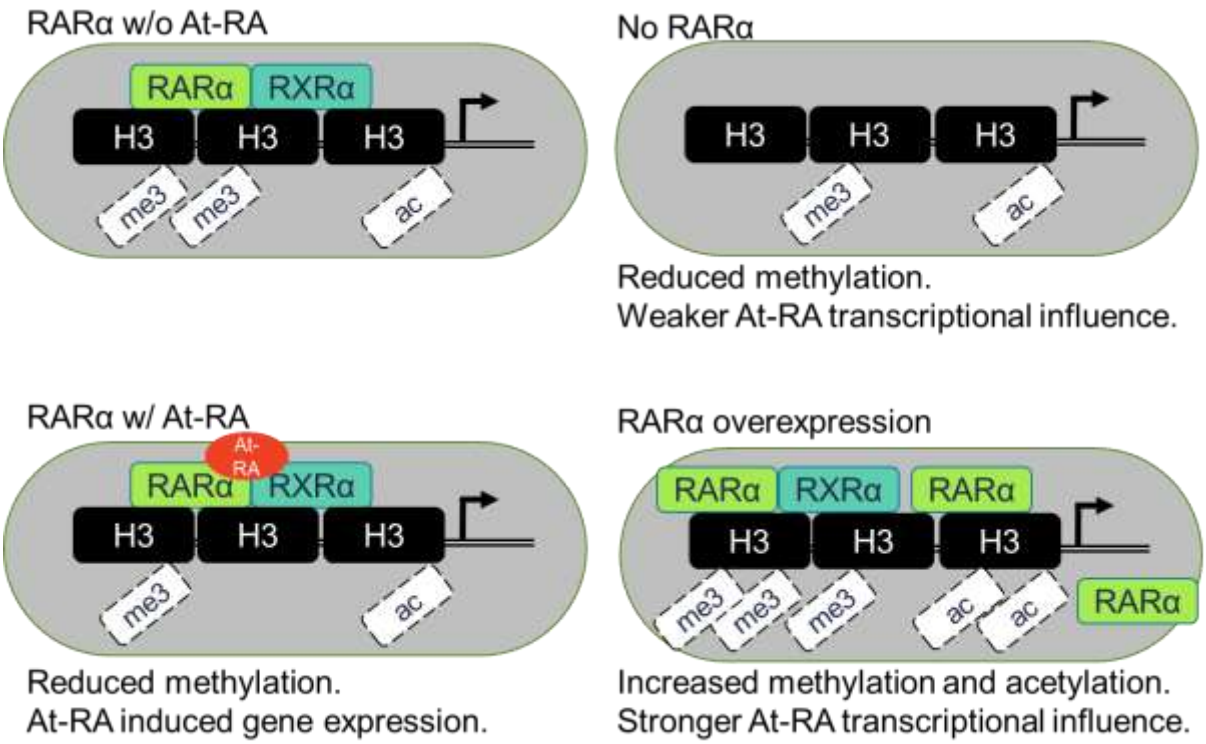

Figure 2.21. Model of epigenetic regulation by RARα and At-RA.

3. RETINOIC ACID RECEPTOR ALPHA REGULATION OF AKT/MTOR SIGNALING BOOSTS T HELPER CELL METABOLISM IN THE ABSENCE OF RETINOIC ACID

3.1 Introduction

Challenges to the immune system stimulate increased cell proliferation as numbers of effector cells expand to combat a perceived threat. The high metabolic demands of an active immune response are held in check by pathways that assimilate inputs from cytokine signaling, antigen receptor signaling, and co-stimulatory molecule signaling.[128,129] The phosphatidyl-inositide-3 kinase (PI3K), protein kinase B (Akt), and mammalian target of rapamycin (mTOR) pathway is activated upon T cell receptor (TCR) stimulation and co-stimulation through CD28, inducible costimulatory (ICOS), or additional costimulatory molecules.[73–75] Sequential upregulation of glycolysis and anabolic metabolism regulate not only proliferation, but also differentiation of numerous T helper subsets, including Th1, Th2, Th17, Treg, and Tfh cells.[72–78] How additional regulation of these signaling pathways and downstream effects on T helper cell immunometabolism, differentiation, and function occurs in the context of vitamin A remains an important topic for study.

T helper cells exhibit profound regulation by the vitamin A metabolite, all-trans retinoic acid (At-RA), and retinoic acid receptor α (RARα). At-RA suppresses Th17 cell differentiation and induces Treg differentiation.[61,63,64,95,96] Additional T helper cell subsets are also affected in either supportive (e.g. Th1 and Th2) or suppressive (e.g. Th9) manners, and homing to intestinal tissues is induced by At-RA upregulation of chemokine receptors CCR9 and Itgα4β7.[71,79,97–100] RARα has been identified as the major mediator of At-RA effects through transcriptional regulation; RARβ and RARγ also interact with At-RA, although their expression in T helper cells

is minimal. The interaction of RARα with PI3K, most distinctly the p85 regulatory component, was demonstrated in neuroblastoma and fibroblast cells, with differential regulation of protein binding by At-RA.[52] In binding to the catalytic p110 subunit, p85 acts to stabilize, activate, and localize the protein complex, yet p85 also maintains repressive functions on PI3K by monomeric p85 competition with p85-p110 dimers for binding phosphorylation targets and p85 upregulation of PI3K-repressive phosphatase and tensin homolog (PTEN) activity.[130–133] Mice with loss of p85 demonstrated increased pAkt and decreased PTEN activity, although additional targets of PI3K, insulin receptor substrate proteins (IRS-1 and IRS-2), had lower levels of phosphorylation, indicating p85 regulation of PI3K may be dependent upon substrate or cellular localization of the PI3K complex.[130] Interaction of the RARα with the PI3K complex or individual components, such as p85, and with the Akt complex suggests a novel regulatory mechanism by which vitamin A metabolites and receptors could regulate immune responses in a non-genomic fashion.

In this study, we utilized mouse strains with T-cell specific knockout or overexpression of RARα to probe the roles of RARα and At-RA on T cell metabolism, signaling pathway activation, and protein interactions with signaling pathway components. We report that RARα expression promotes T cell metabolism upon TCR signaling, with corresponding increases in Akt and mTOR pathway activity. Conversely, At-RA reduced signaling pathway activation and aspects of cellular proliferation in a RARα-dependent manner, indicating antithetical roles of RARα and At-RA on immunometabolism. Nuclear localization of RARα was induced by At-RA, with defective or absent ligand binding resulting in enhanced cytoplasmic localization. Interaction of RARα with p85 in both nuclear and cytoplasmic compartments indicates involvement of RARα with the PI3K pathway, with At-RA shifting cellular localization of RARα-p85 complexes. These results

demonstrate RARα and At-RA interact with signaling pathways and metabolic regulation in a non-genomic manner to influence T helper cell proliferation and function.

3.2 Materials and Methods

3.2.1 Mouse strains and generation.

C57BL/6J mice (stock 002216), distal LCK-cre mice (stock 012837), and RARα-flox mice (stock 033021) were purchased from Jackson Laboratory (Bar Harbor, ME). LCK-cre mice were mated with RARα-flox mice to generate the T cell specific conditionally-deleted $\Delta RAR\alpha^{Lck}$ mice strain. T-cell specific overexpression of RARα was tested using the RARα-Tg strain generated by the Transgenic Mouse Core Facility at Purdue University and described previously. Mice were generally 6-8 weeks of age when used for experiments. Both male and female mice were used, with sex-matched mice used for individual experiments. All animal protocols were approved by either the Purdue Animal Care and Use Committee (PACUC) or the University of Michigan Institutional Animal Care and Use Committee (IACUC).

3.2.2 Cell isolation and culture.

Naïve T cells were magnetically isolated to >95% with an autoMACS separator and mouse naïve $CD4^+$ T cell kit (Miltenyi Biotec, Somerville, MA). For *in vitro* culture, cells were cultured in complete RPMI-1640 media containing charcoal-stripped FBS. Plate-bound anti-CD3 (5 μg/mL) and anti-CD28 (2 μg/mL; both BioXcell, Lebanon, NH) were used for activation *in vitro*, with cytokines according to indicated culture conditions. For nonpolarized (Tnp) culture, hIL-2 (100 U/mL) was added. For Th17-polarizing culture, cytokines included mIL-6 (20 ng/mL), mIL-1ß (10 ng/mL), mIL-21 (10 ng/mL), mIL-23 (10 ng/mL), mTNFα (10 ng/mL), hTGFß-1 (5 ng/mL),

anti-IFNγ (10 μg/mL), and anti-IL-4 (10 μg/mL). Cytokines were purchased from Biolegend (San Diego, CA). Cells were cultured in the presence of all-trans retinoic acid (At-RA) as indicated.

3.2.3 XTT proliferation assay.

Naïve T helper cells were cultured at 1 x 10^6/mL in indicated polarization conditions for 72 hours. Proliferation was assessed with the XTT kit (ATCC; Manassas, VA) using absorbance measurements ($A_{450} - A_{690}$) on a Synergy HT (BioTek; Winooski, VT) plate reader following 2-hour incubation of cultures with activated XTT reagent.

3.2.4 Flow cytometry.

Surface and intracellular phenotyping was performed using Canto II (BD Biosciences; San Jose, CA) or NovoCyte flow cytometers (ACEA Biosciences; San Diego, CA). Antibodies used were purchased from Biolegend or Tonbo Biosciences. For intracellular staining of cytokines, cells were stained for surface markers, followed by activation with phorbol 12-myristate 13-acetate (PMA; 50 ng/mL; Sigma Aldrich), ionomycin (1.0 μg/mL; Sigma Aldrich), and monensin (2 mM; Sigma Aldrich) for 3-6 hours. Cells were fixed with 1% paraformaldehyde for at least 2 hours, then permeabilized with saponin buffer and stained for intracellular cytokines. For transcription factor staining, FoxP3 Fix/Perm reagents (Tonbo Biosciences; San Diego, CA) were used per manufacturer guidelines. For phosphorylated Akt and S6 staining, cells were fixed with BD Biosciences Phosflow™ Fix/Perm buffer and permeabilized with BD Phosflow™ Perm III buffer and stained with anti-pAkt (pS473; BD Biosciences) or pS6 (pS235/236; Cell Signaling; Danvers, MA).

3.2.5 Mitochondrial mass measurement and imaging.

In vitro cultures of naïve T helper cells in Th17-polarizing condition media were harvested at 24 hours of culture and stained with Mitotracker Green (Thermo Fisher; Grand Island, NY), TRITC (Sigma Aldrich, St. Louis, MO), and assessed by flow cytometry for mitochondrial mass by Mitotracker Green intensity and cell size by forward scatter. Cells from the same cultures were additionally stained with DRAQ5 (Thermo Fisher), spun onto glass slides, and imaged using a Leica SP5 laser scanning confocal microscope with 63x objective.

3.2.6 Mitochondrial stress test.

Mitochondrial metabolism was tested in 24-hour cultures of naïve T cells in the Th17-polarizing condition in cRPMI containing charcoal-stripped FBS, with or without 10 nM At-RA. Cells were harvested, washed, and resuspended using XF media (10 mM glucose, 2 mM glutamine, 1 mM pyruvate, pH 7.4) and 5 x 10^5 cells per well were added to a Cell-Tak coated 24-well plate. Plate was centrifuged (400g for 4 minutes) and incubated at 37C in an ambient incubator for 30 minutes prior to metabolic analysis. A Seahorse XFe24 analyzer with the Mito Stress Test kit (Agilent; Santa Clara, CA) was used for analysis.

3.2.7 Metabolic regulation upon T cell activation.

For analysis of metabolic upregulation following TCR stimulation, naïve T helper cells were isolated and cultured at 5 x 10^5 cells per well in a Cell-Tak coated 24-well plate using XF media containing 25 mM glucose, 2 mM glutamine, and 1 mM pyruvate. Plate was centrifuged (400g for 4 minutes) and incubated at 37C in an ambient incubator for 30 minutes prior to metabolic analysis. Metabolic measurements were collected using a Seahorse XFe24 analyzer. Baseline metabolic rates were measured, followed by an injection of mouse T-activator CD3/CD28 dynabeads (2:1 bead to cell ratio; Thermo Fisher) with hIL-2 (100 U/mL) to induce TCR

stimulation and cellular activation. Subsequent injections of oligomycin (1 μM) to suppress oxidative phosphorylation and 2-deoxyglucose (50 mM) to suppress glycolysis were used to calculate the glycolysis contribution to metabolism. The ΔECAR and ΔOCR rates were calculated as the change from baseline readings to the average of the three readings preceding oligomycin injection (~75 minutes after activation).

3.2.8 FLAG-RARα expression and imaging.

The pMSCV-Thy1.1 retroviral transduction system was used to produce retroviral supernatant encoding FLAG-RARα from Platinum E cells. Plasmids expressing native, nucleotide-binding defective (ΔNB, C105G mutation), or ligand-binding defective (ΔLB, G303E mutation) were cloned using Gibson assembly from plasmids generously donated by Akira Kakizuka. Naïve T helper cells were culture for 16 hours in cRPMI with plate-bound anti-CD3 (5 μg/mL) and anti-CD28 (2 μg/mL), then transduced with retroviral supernatants in the presence of polybrene (8 μg/mL) by spin transduction (90 minutes, 2300 rpm, 32C). Cells were rested for 1-2 hours after transduction, then reactivated in fresh Th17-polarizing culture media with or without 10 nM At-RA for 20 hours after transduction. Cells were then harvested and stained for surface Thy1.1, fixed with 1% paraformaldehyde for 1 hour, and permeabilized with flow cytometry perm buffer (Tonbo Biosciences; San Diego, CA) and stained with BV421 anti-FLAG (Biolegend) and DRAQ5. Cells were then spun onto a Cell-Tak coated glass slide and imaged with a Nikon A1 laser scanning confocal microscope with 60x objective. Cellular localization of FLAG-RARα was calculated using ImageJ analysis of FLAG-RARα signal.

3.2.9 Immunoprecipitation and Western Blot.

EL4 cells were cultured for 24 hours in cRPMI containing charcoal-stripped FBS, with or without At-RA (20 nM). Fractionated protein lysates were prepared with NE-PER^{TM} nuclear and

cytoplasmic extraction reagents (Thermo Scientific) and used for immunoprecipitation with anti-RARα (Cell Signaling) and SDS-PAGE with subsequent Western Blot analysis for p85.

Statistics. Statistical significance was tested using GraphPad Prism v7.0. Differences between two groups were compared using Student's t-test. For three or more groups, one-way ANOVA with Bonferroni's multiple testing correction was used. For comparisons with two factors (e.g. At-RA and RARα), two-way ANOVA with Bonferroni's multiple testing correction was used. P values <0.05 were considered significant. All error bars indicate SEM.

3.3 Results

3.3.1 RARα and At-RA effects on *in vitro* T cell proliferation.

Mice with T-cell specific loss of RARα demonstrated reduced populations of T cells in some tissues, notably intestinal tissues. Therefore, we assessed proliferation of T helper cells *in vitro* upon TCR activation in Th17-, Treg-, or Tnp-polarizing culture conditions using WT, $\Delta Rara^{LCK}$, and RARα-Tg naïve T cells in the presence or absence of 10 nM At-RA (Figure 3.1). RARα deficiency significantly decreased the proliferation of cells in all conditions, while RARα overexpression significantly increased T cell proliferation in all conditions. No effect of At-RA on cell proliferation *in vitro* was observed.

3.3.2 *In vitro* T cell size and mitochondrial mass is enhanced by RARα expression.

Consistent with increased proliferation, RARα expression level correlated with overall cell size and mitochondrial mass when measured by flow cytometry and confocal microscopy (Figure 3.2). Naïve T cells cultured for 24 hours in Th17-polarized condition demonstrated changes in cell size and mitochondrial mass matching 72-hour proliferation data. Increases in

cell size and mitochondrial mass in the RARα-Tg cells were decreased by At-RA, an effect that was absent in both WT and ΔRara^{LCK} cells.

3.3.3 Mitochondrial metabolism is increased in line with RARα expression.

Mitochondrial metabolism, as a key source of energy for activated T cells, was assessed using 24-hour Th17-polarized cultures, with or without 10 nM At-RA in both initial culture and during metabolic measurements (Figure 3.3). Baseline oxidative respiration of 24-hour cultured cells was decreased in ΔRara^{LCK} cells and increased in RARα-Tg cells. Forced reliance upon mitochondrial metabolism with the addition of oligomycin, an ATP-synthase inhibitor, followed by FCCP, a mitochondrial membrane depolarizer, demonstrates maximum respiratory capacity and spare respiratory capacity are increased together with basal levels of mitochondrial respiration. Corresponding increases in mitochondrial mass and respiration indicate the role of RARα, and to a lesser degree, At-RA, in controlling proliferation through mitochondrial metabolism.

3.3.4 RARα affects metabolism in naïve T cells following TCR stimulation.

Assessment of *in vitro*-polarized cells indicates metabolic changes in activated T cells, but it does not address naïve T helper cell metabolism prior to and immediately after TCR stimulation. Naïve T cells from WT, ΔRara^{LCK}, and RARα-Tg mice were isolated and assessed for basal metabolism and metabolic changes upon TCR stimulation with anti-CD3/CD28 dynabeads and IL-2 (Figure 3.4A-C). Basal metabolic rates measured with extracellular acidification rate (ECAR) and OCR were not altered by RARα or At-RA (Fig. 4B). The change in metabolism rates from activation to the average of the three measurements preceding oligomycin injection (ΔECAR and ΔOCR) were calculated, with ΔECAR rates decreased in ΔRara^{LCK} cells and increased in RARα-Tg cells, with no effect of At-RA (Figure 3.4C). The

maximum glycolysis rate, measured upon oligomycin injection, also indicated decreases in $\Delta Rara^{LCK}$ cells and increases in RARα-Tg cells. Together, this data indicates that while naïve T cell metabolism is not altered by RARα, the upregulation of metabolic pathways upon TCR stimulation are enhanced by RARα expression level and not significantly affected by the presence of At-RA at the time of activation.

3.3.5 RARα expression promotes mTOR signaling upon TCR activation.

The regulation of metabolism upon TCR stimulation relies on numerous signaling pathways that interact with T cell receptor signaling, including the mTOR pathway. To assess the involvement of the mTOR pathway in RARα-mediated metabolic effects, naïve T cells were cultured in Th17-polarized condition for up to 48 hours, and phosphorylation of S6, as an indicator of mTOR activity, was assessed by flow cytometry staining at indicated time points (Figure 3.5A-C). The percentage of $pS6^+$ cells increases in WT cells upon T cell activation and continues to increase to at least 72 hours post activation. As early as 3 hours post activation, differences in the percentages of $pS6^+$ cells were observed, with decreases in $\Delta Rara^{LCK}$ cells and increases in RARα-Tg cells. At-RA suppressed mTOR activity in WT and RARα-Tg cells, noted at 48 hour and 12 hour times post activation, respectively. Thus, activation of the mTOR signaling pathway by TCR stimulation is altered by RARα expression level and correlates with changes in metabolism.

3.3.6 RARα expression promotes Akt signaling upon TCR activation, with partial suppression by At-RA.

As a mediator of TCR activation signals and an upstream signaling pathway of mTOR, the Akt signaling pathway also is integral for T cell activation and metabolism. The effect of RARα and At-RA on Akt activation was measured in splenocytes from WT, $\Delta Rara^{LCK}$, and

RARα-Tg mice (Figure 3.6A-B). After 16 hours of culture in complete cRPMI without activation, and with or without 10 nM At-RA, splenocytes were activated in Th17-polarized culture media for 15 minutes, followed by flow cytometric assessment of phosphorylated Akt (Ser473) in live T helper cells. Increased pAkt levels were seen in all activated cells, compared to their unstimulated controls. Phosphorylated Akt levels were decreased in $\Delta Rara^{LCK}$ cells and increased in RARα-Tg cells. Additionally, At-RA suppressed pAkt levels in WT and RARα-Tg cells but not $\Delta Rara^{LCK}$ cells. This regulation of Akt and mTOR signaling by RARα and At-RA, with downstream effects on T cell metabolism, represents previously undiscovered roles of RARα and At-RA in immune regulation.

3.3.7 Ligand binding controls RARα cellular localization.

Protein localization of RARα within the cell determines where it can interact with signaling pathway components. Cellular localization of RARα assessed by microscopy of primary T cells indicated a majority of RARα protein is localized to the nucleus, and nuclear localization is induced by At-RA binding (Figure 3.7A-B). Mutation in the nucleotide-binding region (ΔNB) did not affect cellular localization. Mutation of the ligand-binding site did however reduce nuclear localization and At-RA-induced nuclear localization. The presence of RARα in the cytoplasmic compartment indicates the potential for RARα involvement with cytoplasmic components of signaling pathways that are involved in signal transduction arising from TCR stimulation and resulting in metabolic changes.

3.4 Discussion

While classically known as a transcription factor and mediator of At-RA transcriptional regulation, RARα may regulate other, nongenomic aspects of cellular homeostasis. In our study,

increases of proliferation, metabolism, and cell signaling pathways were insufficiently explained by functions of RARα as a transcription factor. As such, we sought to identify additional mechanisms for RARα involvement in these effects.

Proliferation of T helper cells *in vitro* was promoted by the level of RARα expression, regardless of the polarization condition. Cell size and mitochondrial mass measured after one day of culture were similarly increased by RARα. Metabolic pathways utilized by T helper cells include glycolysis and mitochondrial oxidative phosphorylation, with upregulation of both upon TCR stimulation to feed anabolic metabolism. In Th17-polarizing culture conditions, mitochondrial oxidation was increased by RARα after one day in culture. The upregulation of metabolism in naïve cells upon TCR stimulation was assessed, and RARα expression correlated with an increased rate of glycolysis in the first hour after TCR stimulation, whereas increases in mitochondrial oxidation rates were relatively unchanged in that time, indicating a delay in the responsiveness of mitochondrial metabolism to T cell activation, comparative to glycolysis. Basal levels of metabolism in naïve T cells, both ECAR and OCR, were unchanged by the expression of RARα. Therefore, RARα is demonstrated to promote T cell metabolism and proliferation upon T cell activation, with enhanced metabolism occurring within the first hour of activation.

How RARα mediates a rapid effect on T helper cell proliferation and metabolism upon activation is challenging to explain through traditional roles of RARα on transcription, but it could be mediated by RARα regulation of signaling pathways upstream of metabolism. The mTOR signaling pathway uses environmental cues, such as cytokines and TCR signaling, to invoke changes to cellular functions including metabolism, proliferation, autophagy, and differentiation.[75] The activity of mTORC1, assessed with pS6 status, in T cells at various time

points after activation indicated that the mTOR pathway was regulated by RARα and At-RA. Activation of the mTOR pathway by Akt signaling occurs following T cell activation. Regulation of the Akt signaling pathway was also demonstrated by RARα and also by At-RA, in a RARα-dependent manner. Signal transduction from TCR stimulation through Akt to mTOR involves the PI3K complex, which is responsible for phosphorylating Akt into its active state. Interaction of RARα with PI3K proteins was previously demonstrated in neuroblastoma and fibroblast cell lines, therefore PI3K presented both the potential to bind RARα and the regulatory capacities demonstrated in T helper cells with altered RARα. Further identification of protein interactions between RARα and the p85 regulatory component of PI3K, with pinpointed cellular localization of interacting complexes in the presence and absence of At-RA, would demonstrate the mechanism of RARα effects on the PI3K/Akt/mTOR pathway. The basis of protein interaction between RARα and signaling pathway components, as well as the resulting effects on the stability and activity of the PI3K, Akt, and mTOR complexes is required to elucidate the effects of this novel, nongenomic role of RARα in regulation of immune cell metabolism, proliferation, and differentiation.

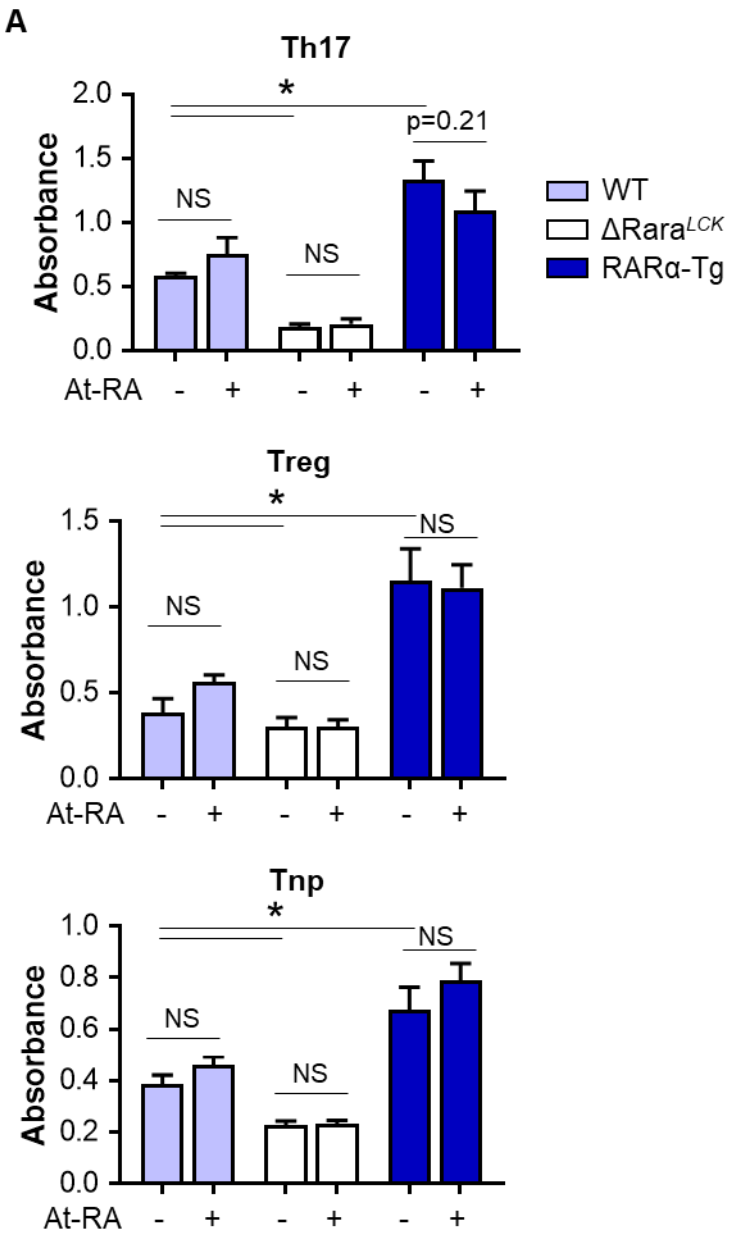

Figure 3.1. RARα and At-RA effects on *in vitro* T cell proliferation. (A) Proliferation of Th17-, Treg-, or Tnp-polarized cultures was measured using the XTT assay at 72 hours of culture. * $p<0.05$; n=3. Stats by two-way ANOVA w/Bonferroni. * $p<0.05$; n=3-4.

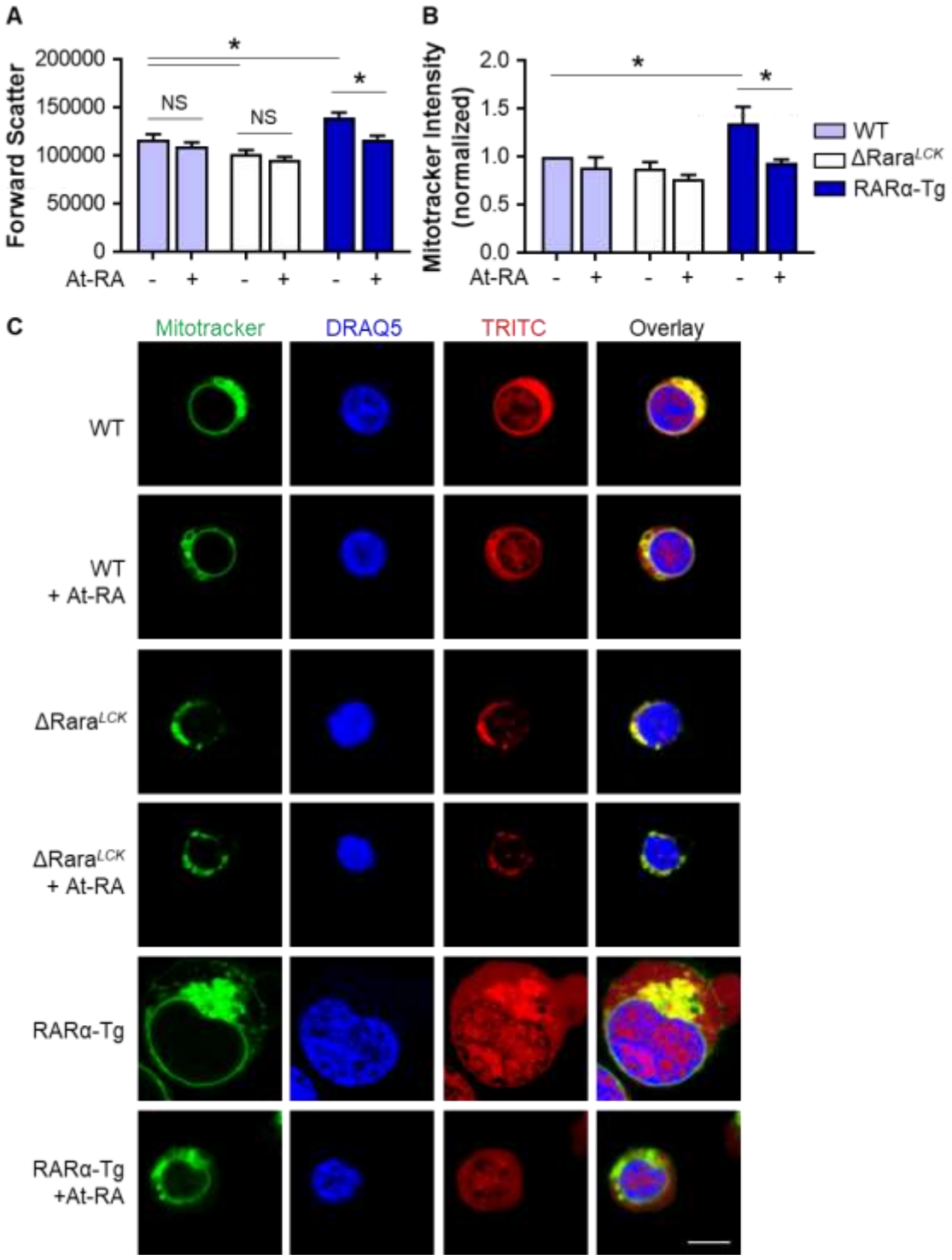

Figure 3.2. *In vitro* T cell size and mitochondrial mass is enhanced by RARα expression. (A) Cell size was assessed by flow cytometric analysis of forward scatter in cultures at 24 hours. (B) Mitochondrial mass was measured by mean Mitotracker Green staining intensity by flow cytometry. (C) Confocal images of cells used in (A) and (B). Scale bar is 5 microns. * $p<0.05$; n=3. Statistical analysis by two-way ANOVA w/Bonferroni.

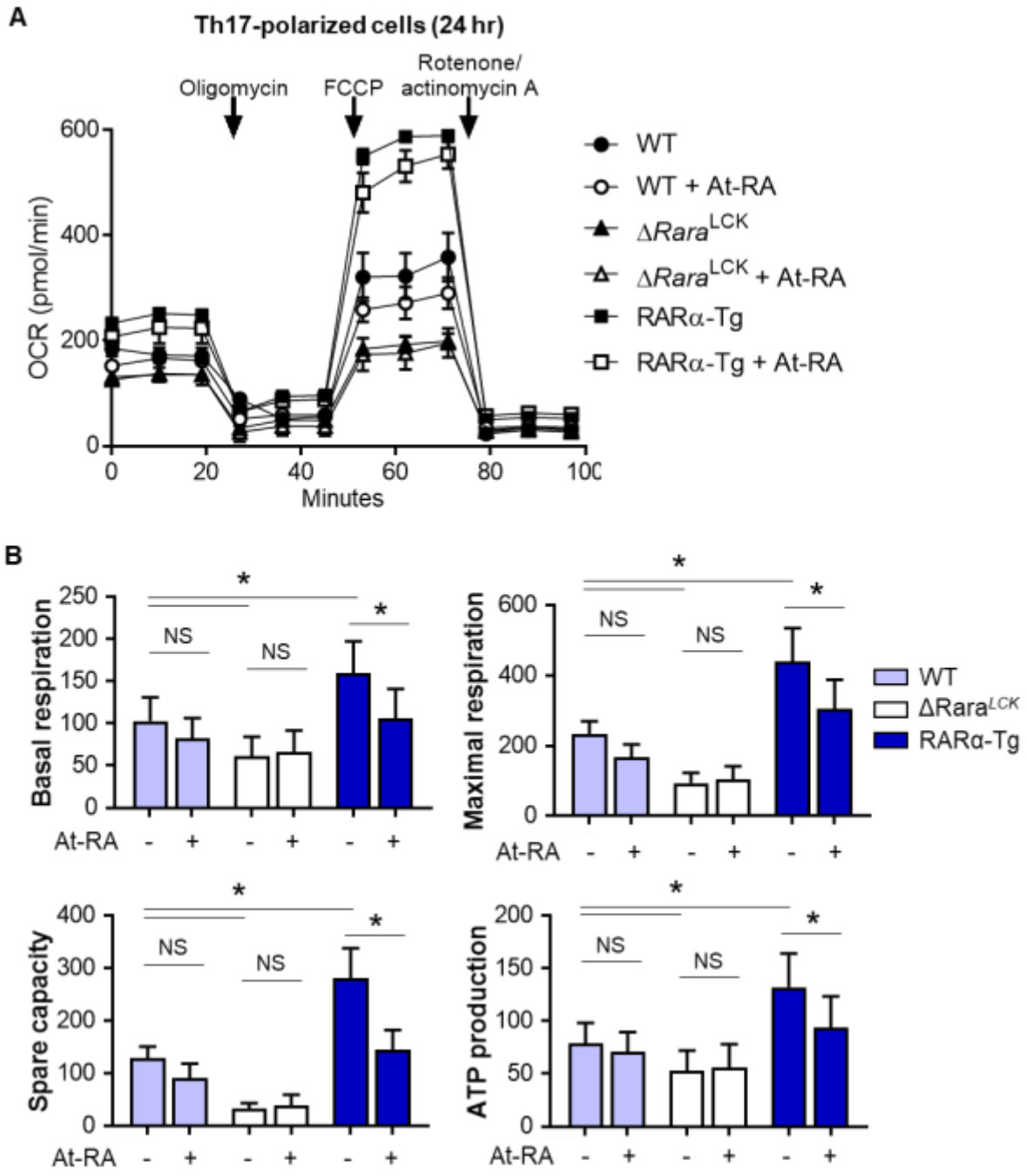

Figure 3.3. Mitochondrial metabolism is increased by RARα in Th17-polarized cells. Naïve T cell cultures in Th17-polarized condition were assessed for mitochondrial metabolism at 24 hours of culture. (A) Oxygen consumption rate (OCR) of cells was measured using a Seahorse XFe24 analyzer. (B) Measurements of metabolism were calculated from OCR measurements. Data are either representative (A) or combined from 3 independent experiments (B) * $p<0.05$; n=3. Statistical analysis by two-way ANOVA w/Bonferroni.

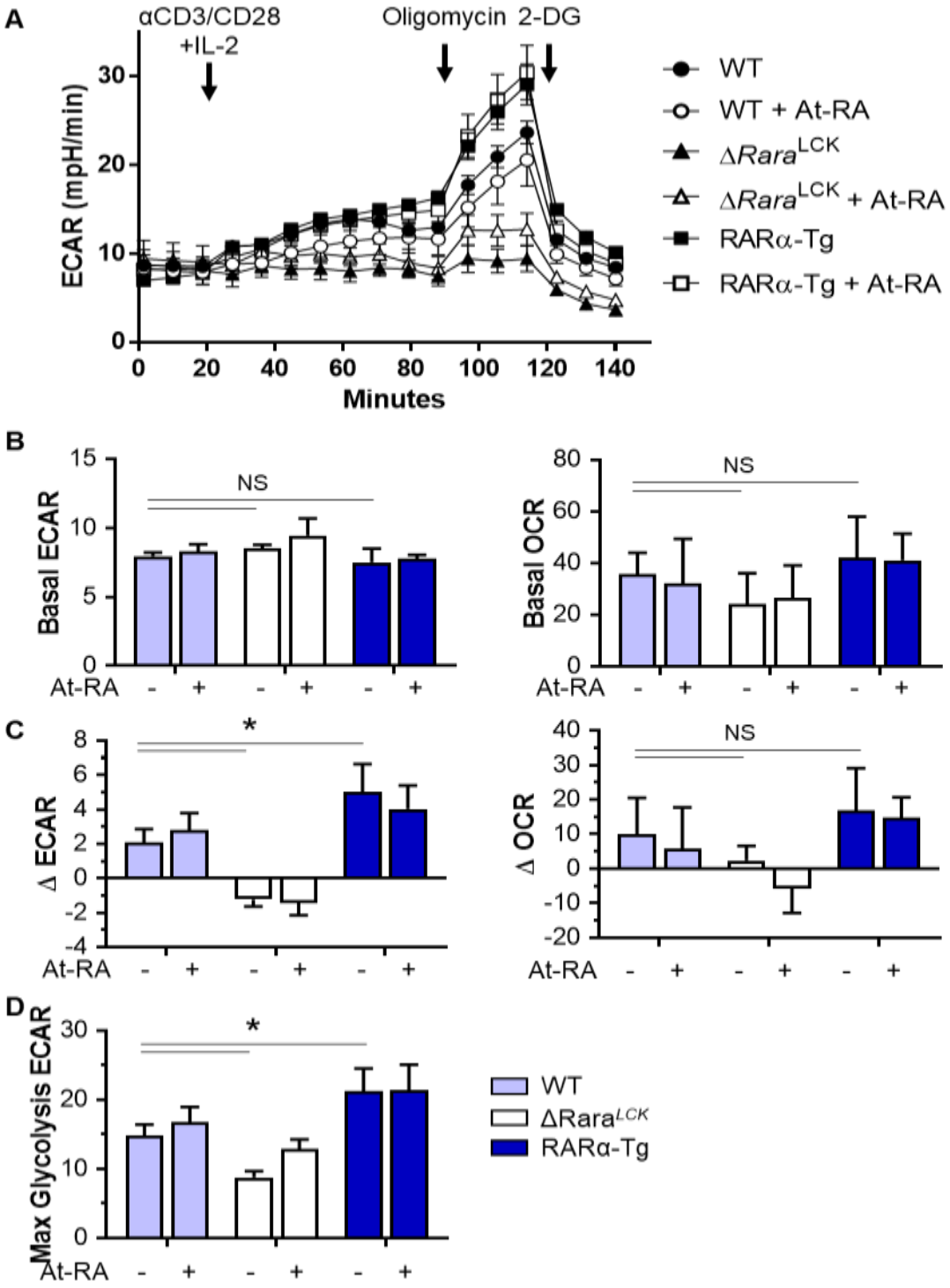

Figure 3.4. RARα affects metabolism in naïve T cells following TCR stimulation. (A) ECAR of naïve T cells during TCR activation. (B) Basal ECAR and OCR of naïve T cells prior to TCR stimulation. (C) Change in ECAR and OCR from basal to 70 minutes following TCR activation. (D) Maximum glycolysis rates measured following oligomycin administration. Results are from a single representative experiment (A) or combined data from three independent experiments. * $p<0.05$. Statistical analysis by two-way ANOVA w/Bonferroni.

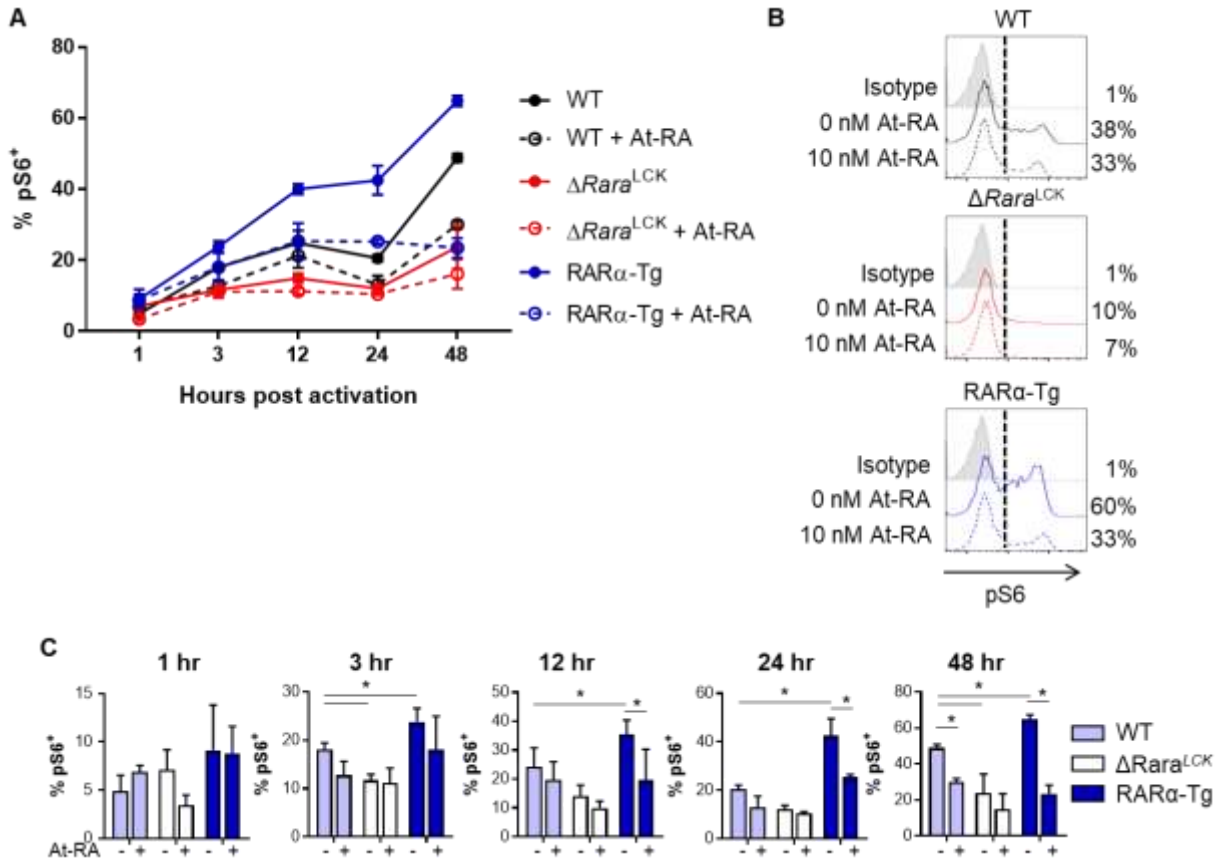

Figure 3.5. RARα expression promotes mTOR signaling upon TCR activation, with partial suppression by RA. (A-C) Naive T cells were activated for the indicated time period in the presence or absence of At-RA (10nM). Cells were harvested and stained for pS6 by flow cytometry. 4 independent experiments combined. n=4. Stats by two-way ANOVA w/Bonferroni.

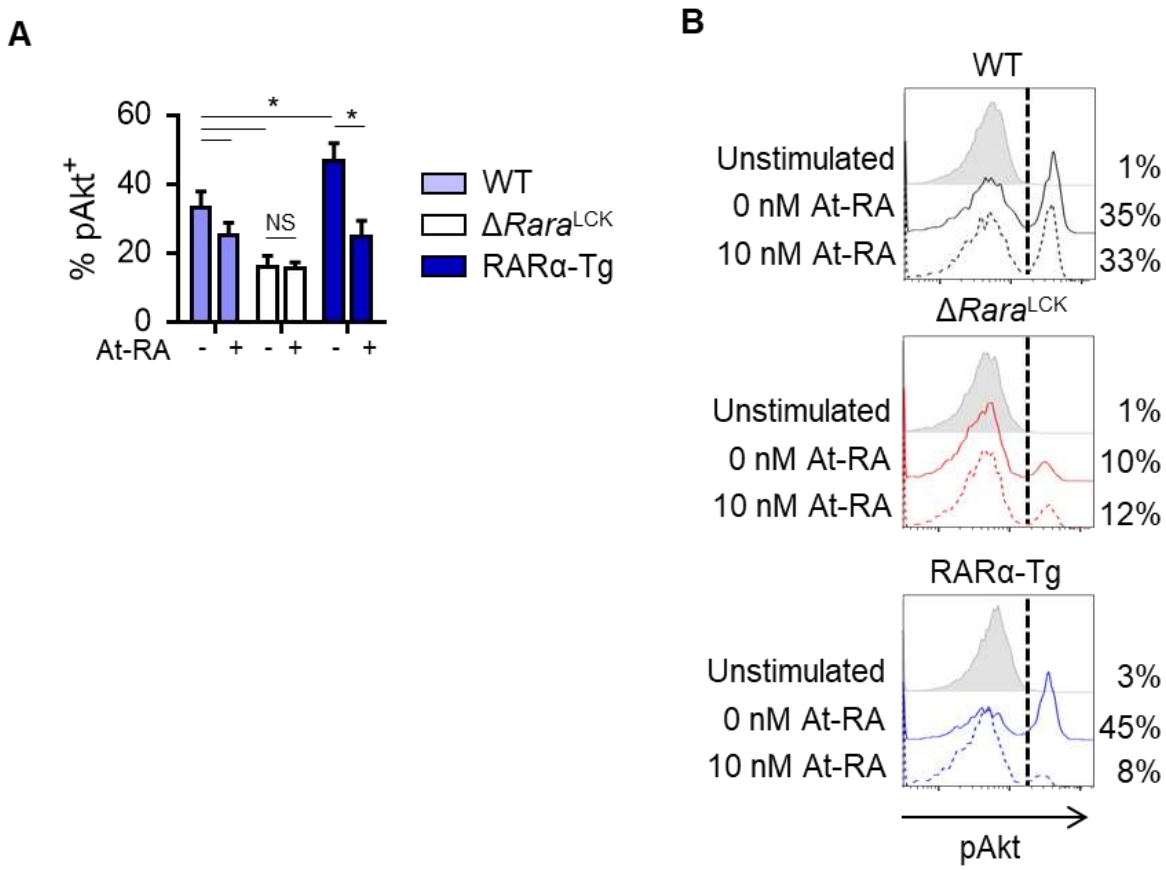

Figure 3.6. RARα expression promotes Akt signaling upon TCR activation, with partial suppression by RA. (A-C) Splenocytes were rested in cRPMI for 16 hours with or without At-RA (10 nM), then activated for 15 minutes in a Th17-polarizing culture with or without RA; cells were then stained for pAkt. 4+ independent experiments combined. n=4-8. Stats by two-way ANOVA w/Bonferroni.

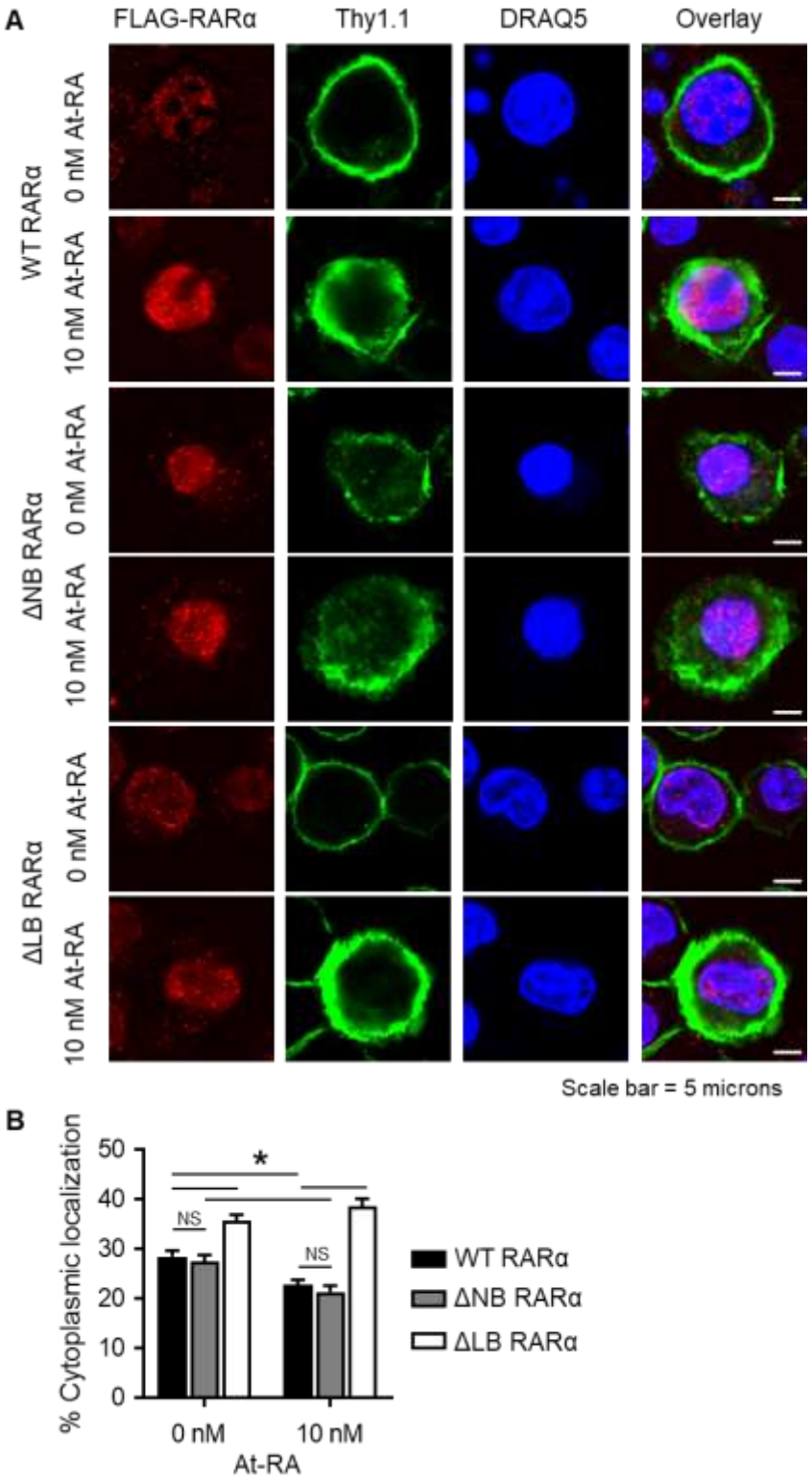

Figure 3.7. Ligand binding controls RARα cellular localization. (A) Microscopy of FLAG-RARα in retrovirally-transduced Th17-polarized cell cultures. (B) FLAG-RARα signal localization in the cytoplasmic compartment was measured from confocal images. (C) Western blot analysis of RARα in nuclear and cytoplasmic fractions of primary CD4+ T cells.

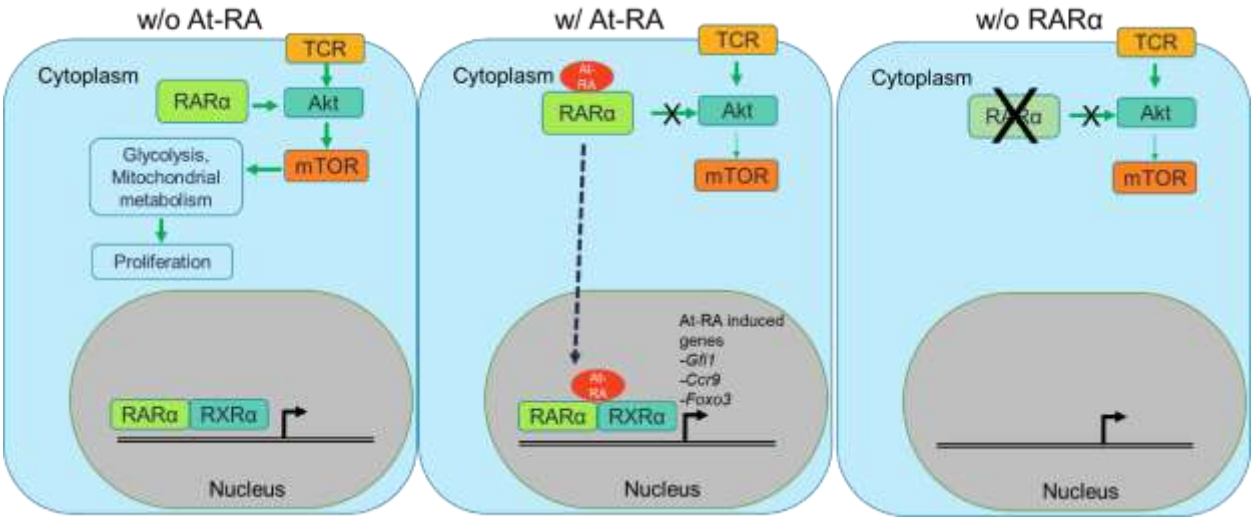

Figure 3.8. Model of non-genomic regulation of Akt/mTOR by RARα and At-RA.

REFERENCES

1. Semba RD. On the 'Discovery' of Vitamin A. *Ann Nutr Metab*. 2012;61(3):192-198. doi:10.1159/000343124
2. Zile MH. Function of Vitamin A in Vertebrate Embryonic Development. *J Nutr*. 2001;(December 2000):1401-1404.
3. Heavner W, Pevny L. Eye development and retinogenesis. *Cold Spring Harb Perspect Biol*. 2012;4(12). doi:10.1101/cshperspect.a008391
4. Wiseman EM, Bar-El Dadon S, Reifen R. The vicious cycle of vitamin a deficiency: A review. *Crit Rev Food Sci Nutr*. 2017;57(17):3703-3714. doi:10.1080/10408398.2016.1160362
5. Wirth J, Petry N, Tanumihardjo S, et al. Vitamin A Supplementation Programs and Country-Level Evidence of Vitamin A Deficiency. *Nutrients*. 2017;9(3):190. doi:10.3390/nu9030190
6. Kedishvili NY. Enzymology of retinoic acid biosynthesis and degradation. *J Lipid Res*. 2013;54(7):1744-1760. doi:10.1194/jlr.R037028
7. Blomhoff R, Blomhoff HK. Overview of retinoid metabolism and function. *J Neurobiol*. 2006;66(7):606-630. doi:10.1002/neu.20242
8. D'Ambrosio DN, Clugston RD, Blaner WS, D'Ambrosio DN, Clugston RD, Blaner WS. Vitamin A Metabolism: An Update. *Nutrients*. 2011;3(1):63-103. doi:10.3390/nu3010063
9. Kumar S, Sandell LL, Trainor PA, Koentgen F, Duester G. Alcohol and aldehyde dehydrogenases: Retinoid metabolic effects in mouse knockout models. *Biochim Biophys Acta - Mol Cell Biol Lipids*. 2012;1821(1):198-205. doi:10.1016/j.bbalip.2011.04.004
10. Heyman RA, Mangelsdorf DJ, Dyck JA, et al. 9-cis retinoic acid is a high affinity ligand for the retinoid X receptor. *Cell*. 1992;68(2):397-406. doi:10.1016/0092-8674(92)90479-V
11. Kliewer SA, Umesono K, Noonan DJ, Heyman RA, Evans RM. Convergence of 9-cis retinoic acid and peroxisome proliferator signalling pathways through heterodimer formation of their receptors. *Nature*. 1992;358(6389):771-774. doi:10.1038/358771a0
12. Blaner WS. Cellular metabolism and actions of 13-cis-retinoic acid. *J Am Acad Dermatol*. 2001;45(5):S129-S135. doi:10.1067/MJD.2001.113714

13. Larange A, Cheroutre H. Retinoic Acid and Retinoic Acid Receptors as Pleiotropic Modulators of the Immune System. *Annu Rev Immunol*. 2016;34(1):369-394. doi:10.1146/annurev-immunol-041015-055427
14. Sun C-M, Hall JA, Blank RB, et al. Small intestine lamina propria dendritic cells promote de novo generation of Foxp3 T reg cells via retinoic acid. *J Exp Med*. 2007;204(8):1775-1785. doi:10.1084/jem.20070602
15. Grizotte-Lake M, Zhong G, Duncan K, et al. Commensals Suppress Intestinal Epithelial Cell Retinoic Acid Synthesis to Regulate Interleukin-22 Activity and Prevent Microbial Dysbiosis. *Immunity*. 2018;49(6):1103-1115.e6. doi:10.1016/j.immuni.2018.11.018
16. Thomas S, Prabhu R, Balasubramanian KA. Retinoid metabolism in the rat small intestine. *Br J Nutr*. 2005;93(1):59-63. doi:10.1079/bjn20041306
17. Bhattacharya N, Yuan R, Prestwood TRR, et al. Normalizing Microbiota-Induced Retinoic Acid Deficiency Stimulates Protective CD8+ T Cell-Mediated Immunity in Colorectal Cancer. *Immunity*. 2016;45(3):641-655. doi:10.1016/j.immuni.2016.08.008
18. KANE MA, CHEN N, SPARKS S, NAPOLI JL. Quantification of endogenous retinoic acid in limited biological samples by LC/MS/MS. *Biochem J*. 2005;388(1):363-369. doi:10.1042/BJ20041867
19. O'Byrne SM, Wongsiriroj N, Libien J, et al. Retinoid Absorption and Storage Is Impaired in Mice Lacking Lecithin:Retinol Acyltransferase (LRAT). *J Biol Chem*. 2005;280(42):35647-35657. doi:10.1074/jbc.M507924200
20. Allenby G, Bocquel MT, Saunders M, et al. Retinoic acid receptors and retinoid X receptors: interactions with endogenous retinoic acids. *Proc Natl Acad Sci U S A*. 1993;90(1):30-34. doi:10.1073/pnas.90.1.30
21. Petkovich M, Brand NJ, Krust A, Chambon P. A human retinoic acid receptor which belongs to the family of nuclear receptors. *Nature*. 1987;330(6147):444-450. doi:10.1038/330444a0
22. Donovan M, Olofsson B, Gustafson A-L, Dencker L, Eriksson U. The cellular retinoic acid binding proteins. *J Steroid Biochem Mol Biol*. 1995;53(1-6):459-465. doi:10.1016/0960-0760(95)00092-E

23. Napoli JL. Cellular retinoid binding-proteins, CRBP, CRABP, FABP5: Effects on retinoid metabolism, function and related diseases. *Pharmacol Ther*. 2017;173:19-33. doi:10.1016/J.PHARMTHERA.2017.01.004
24. Majumdar A, Petrescu AD, Xiong Y, Noy N. Nuclear translocation of cellular retinoic acid-binding protein II is regulated by retinoic acid-controlled SUMOylation. *J Biol Chem*. 2011;286(49):42749-42757. doi:10.1074/jbc.M111.293464
25. Schug TT, Berry DC, Shaw NS, Travis SN, Noy N. Opposing Effects of Retinoic Acid on Cell Growth Result from Alternate Activation of Two Different Nuclear Receptors. *Cell*. 2007;129(4):723-733. doi:10.1016/j.cell.2007.02.050
26. Shaw N, Elholm M, Noy N. Retinoic Acid is a High Affinity Selective Ligand for the Peroxisome Proliferator-activated Receptor β/δ. *J Biol Chem*. 2003;278(43):41589-41592. doi:10.1074/jbc.C300368200
27. Napoli JL. Cellular retinoid binding-proteins, CRBP, CRABP, FABP5: Effects on retinoid metabolism, function and related diseases. *Pharmacol Ther*. 2017. doi:10.1016/j.pharmthera.2017.01.004
28. Liu R-Z, Graham K, Glubrecht DD, Germain DR, Mackey JR, Godbout R. Association of FABP5 Expression With Poor Survival in Triple-Negative Breast Cancer: Implication for Retinoic Acid Therapy. *Am J Pathol*. 2011;178(3):997-1008. doi:10.1016/J.AJPATH.2010.11.075
29. Liu R-Z, Garcia E, Glubrecht DD, Poon HY, Mackey JR, Godbout R. CRABP1 is associated with a poor prognosis in breast cancer: adding to the complexity of breast cancer cell response to retinoic acid. *Mol Cancer*. 2015;14(1):129. doi:10.1186/s12943-015-0380-7
30. Saari JC, Nawrot M, Kennedy BN, et al. Visual Cycle Impairment in Cellular Retinaldehyde Binding Protein (CRALBP) Knockout Mice Results in Delayed Dark Adaptation. *Neuron*. 2001;29(3):739-748. doi:10.1016/S0896-6273(01)00248-3
31. Xue Y, Shen SQ, Jui J, et al. CRALBP supports the mammalian retinal visual cycle and cone vision. *J Clin Invest*. 2015;125(2):727-738. doi:10.1172/JCI79651
32. Uhlen M, Fagerberg L, Hallstrom BM, et al. Tissue-based map of the human proteome. *Science (80-)*. 2015;347(6220):1260419-1260419. doi:10.1126/science.1260419

33. Heng TSP, Painter MW, Consortium TIGP, et al. The Immunological Genome Project: networks of gene expression in immune cells. *Nat Immunol 2008 910*. October 2008.
34. Santos NC, Kim KH. Activity of retinoic acid receptor-alpha is directly regulated at its protein kinase A sites in response to follicle-stimulating hormone signaling. *Endocrinology*. 2010;151(5):2361-2372. doi:10.1210/en.2009-1338
35. Piskunov A, Rochette-Egly C. A retinoic acid receptor RARα pool present in membrane lipid rafts forms complexes with G protein αQ to activate p38MAPK. *Oncogene*. 2012;31(28):3333-3345. doi:10.1038/onc.2011.499
36. Rochette-Egly C, Germain P. Dynamic and combinatorial control of gene expression by nuclear retinoic acid receptors (RARs). *Nucl Recept Signal*. 2009;7(1):nrs.07005. doi:10.1621/nrs.07005
37. Marshall H, Studer M, Pöpperl H, et al. A conserved retinoic acid response element required for early expression of the homeobox gene Hoxb-1. *Nature*. 1994;370(6490):567-571. doi:10.1038/370567a0
38. Zhang Y, Liang J, Li Q. Coordinated regulation of retinoic acid signaling pathway by KDM5B and polycomb repressive complex 2. *J Cell Biochem*. 2014;115(9):1528-1538. doi:10.1002/jcb.24807
39. Giannì M, Parrella E, Raska I, et al. P38MAPK-dependent phosphorylation and degradation of SRC-3/AIB1 and RARα-mediated transcription. *EMBO J*. 2006;25(4):739-751. doi:10.1038/sj.emboj.7600981
40. Ferry C, Gianni M, Lalevée S, et al. SUG-1 plays proteolytic and non-proteolytic roles in the control of retinoic acid target genes via its interaction with SRC-3. *J Biol Chem*. 2009;284(12):8127-8135. doi:10.1074/jbc.M808815200
41. Girard N, Tremblay M, Humbert M, et al. RAR -PLZF oncogene inhibits C/EBP function in myeloid cells. *Proc Natl Acad Sci*. 2013;110(33):13522-13527. doi:10.1073/pnas.1310067110
42. Urvalek AM, Gudas LJ. Retinoic acid and histone deacetylases regulate epigenetic changes in embryonic stem cells. *J Biol Chem*. 2014;289(28):19519-19530. doi:10.1074/jbc.M114.556555

43. Zheng B, Han M, Shu Y, et al. HDAC2 phosphorylation-dependent Klf5 deacetylation and RARα acetylation induced by RAR agonist switch the transcription regulatory programs of p21 in VSMCs. *Cell Res*. 2011;21(10):1487-1508. doi:10.1038/cr.2011.34
44. Kada N, Suzuki T, Aizawa K, et al. Acyclic retinoid inhibits functional interaction of transcription factors Krüppel-like factor 5 and retinoic acid receptor-alpha. *FEBS Lett*. 2008;582(12):1755-1760. doi:10.1016/j.febslet.2008.04.040
45. Zheng B, Han M, Shu Y, et al. HDAC2 phosphorylation-dependent Klf5 deacetylation and RARα acetylation induced by RAR agonist switch the transcription regulatory programs of p21 in VSMCs. *Cell Res*. 2011;21(10):1487-1508. doi:10.1038/cr.2011.34
46. Hashimoto-Hill S, Friesen L, Kim M, Kim CH. Contraction of intestinal effector T cells by retinoic acid-induced purinergic receptor P2X7. *Mucosal Immunol*. 2017;10(4):912-923. doi:10.1038/mi.2016.109
47. Dey N, De PK, Wang M, et al. CSK Controls Retinoic Acid Receptor (RAR) Signaling: a RAR-c-SRC Signaling Axis Is Required for Neuritogenic Differentiation. *Mol Cell Biol*. 2007;27(11):4179-4197. doi:10.1128/MCB.01352-06
48. Stavridis MP, Collins BJ, Storey KG. Retinoic acid orchestrates fibroblast growth factor signalling to drive embryonic stem cell differentiation. *Development*. 2010;137(6):881-890. doi:10.1242/dev.043117
49. Cheung Y-T, Lau WK-W, Yu M-S, et al. Effects of all-trans-retinoic acid on human SH-SY5Y neuroblastoma as in vitro model in neurotoxicity research. *Neurotoxicology*. 2009;30(1):127-135. doi:10.1016/j.neuro.2008.11.001
50. BOST F, CARON L, MARCHETTI I, DANI C, MARCHAND-BRUSTEL Y LE, BINÉTRUY B. Retinoic acid activation of the ERK pathway is required for embryonic stem cell commitment into the adipocyte lineage. *Biochem J*. 2015;361(3):621-627. doi:10.1042/bj3610621
51. Al Tanoury Z, Piskunov A, Rochette-Egly C. Vitamin A and retinoid signaling: genomic and nongenomic effects. *J Lipid Res*. 2013;54(7):1761-1775. doi:10.1194/jlr.R030833
52. Masiá S, Alvarez S, de Lera AR, Barettino D. Rapid, Nongenomic Actions of Retinoic Acid on Phosphatidylinositol-3-Kinase Signaling Pathway Mediated by the Retinoic Acid Receptor. *Mol Endocrinol*. 2007;21(10):2391-2402. doi:10.1210/me.2007-0062

53. Moran AE, Hogquist KA. T-cell receptor affinity in thymic development. *Immunology*. 2012;135(4):261-267. doi:10.1111/j.1365-2567.2011.03547.x

54. Macpherson AJ, Hooper L V, Littman DR. Interactions Between the Microbiota and the Immune System. *Science (80-)*. 2012;336(June):1268-1273. doi:10.1126/science.1223490

55. Kespohl M, Vachharajani N, Luu M, et al. The Microbial Metabolite Butyrate Induces Expression of Th1-Associated Factors in CD4+ T Cells. *Front Immunol*. 2017;8:1036. doi:10.3389/fimmu.2017.01036

56. Ivanov II, Atarashi K, Manel N, et al. Induction of Intestinal Th17 Cells by Segmented Filamentous Bacteria. *Cell*. 2009;139(3):485-498. doi:10.1016/j.cell.2009.09.033

57. Park J, Kim M, Kang SG, et al. Short-chain fatty acids induce both effector and regulatory T cells by suppression of histone deacetylases and regulation of the mTOR-S6K pathway. *Mucosal Immunol*. 2015;8(1):80-93. doi:10.1038/mi.2014.44

58. Haghikia A, Jörg S, Duscha A, et al. Dietary Fatty Acids Directly Impact Central Nervous System Autoimmunity via the Small Intestine. *Immunity*. 2015;43(4):817-829. doi:10.1016/j.immuni.2015.09.007

59. Kim CH. Control of Innate and Adaptive Lymphocytes by the RAR-Retinoic Acid Axis. *Immune Netw*. 2018;18(1):1-13. doi:10.4110/in.2018.18.e1

60. Wang C, Kang SG, HogenEsch H, Love PE, Kim CH. Retinoic Acid Determines the Precise Tissue Tropism of Inflammatory Th17 Cells in the Intestine. *J Immunol*. 2010;184(10):5519-5526. doi:10.4049/jimmunol.0903942

61. Cha H-R, Chang S-Y, Chang J-H, et al. Downregulation of Th17 Cells in the Small Intestine by Disruption of Gut Flora in the Absence of Retinoic Acid. *J Immunol*. 2010;184(12):6799-6806. doi:10.4049/jimmunol.0902944

62. Takeuchi H, Yokota-Nakatsuma A, Ohoka Y, et al. Retinoid X Receptor Agonists Modulate Foxp3+ Regulatory T Cell and Th17 Cell Differentiation with Differential Dependence on Retinoic Acid Receptor Activation. *J Immunol*. 2013;191(7):3725-3733. doi:10.4049/jimmunol.1300032

63. Mucida D, Park Y, Kim G, et al. Reciprocal TH17 and regulatory T cell differentiation mediated by retinoic acid. *Science*. 2007;317(5835):256-260. doi:10.1126/science.1145697

64. Elias KM, Laurence A, Davidson TS, et al. Retinoic acid inhibits Th17 polarization and enhances FoxP3 expression through a Stat-3 / Stat-5 independent signaling pathway. *Blood*. 2008;111(3):1013-1020. doi:10.1182/blood-2007-06-096438.K.M.E.
65. Schambach F, Schupp M, Lazar MA, Reiner SL. Activation of retinoic acid receptor-α favours regulatory T cell induction at the expense of IL-17-secreting T helper cell differentiation. *Eur J Immunol*. 2007;37(9):2396-2399. doi:10.1002/eji.200737621
66. Zhou X, Kong N, Wang J, et al. Cutting edge: all-trans retinoic acid sustains the stability and function of natural regulatory T cells in an inflammatory milieu. *J Immunol*. 2010;185(5):2675-2679. doi:10.4049/jimmunol.1000598
67. Xiao S, Jin H, Korn T, et al. Retinoic Acid Increases Foxp3+ Regulatory T Cells and Inhibits Development of Th17 Cells by Enhancing TGF- -Driven Smad3 Signaling and Inhibiting IL-6 and IL-23 Receptor Expression. *J Immunol*. 2008;181(4):2277-2284. doi:10.4049/jimmunol.181.4.2277
68. Coombes JL, Siddiqui KRR, Arancibia-Cárcamo C V., et al. A functionally specialized population of mucosal CD103+ DCs induces Foxp3+ regulatory T cells via a TGF-β– and retinoic acid–dependent mechanism. *J Exp Med*. 2007;204(8):1757-1764. doi:10.1084/JEM.20070590
69. Cha H-R, Chang S-Y, Chang J-H, et al. Downregulation of Th17 Cells in the Small Intestine by Disruption of Gut Flora in the Absence of Retinoic Acid. *J Immunol*. 2010;184(12):6799-6806. doi:10.4049/jimmunol.0902944
70. Kang SSGS, Wang C, Matsumoto S, Kim CH. High and Low Vitamin A Therapies Induce Distinct FoxP3+ T-Cell Subsets and Effectively Control Intestinal Inflammation. *Gastroenterology*. 2009;137(4):1391-1402. doi:10.1053/j.gastro.2009.06.063
71. Hall JA, Cannons JL, Grainger JR, et al. Essential Role for Retinoic Acid in the Promotion of CD4+ T Cell Effector Responses via Retinoic Acid Receptor Alpha. *Immunity*. 2011;34(3):435-447. doi:10.1016/j.immuni.2011.03.003
72. Zeng H, Cohen S, Guy C, et al. mTORC1 and mTORC2 Kinase Signaling and Glucose Metabolism Drive Follicular Helper T Cell Differentiation. *Immunity*. 2016;45(3):540-554. doi:10.1016/j.immuni.2016.08.017

73. Gigoux M, Shang J, Pak Y, et al. Inducible costimulator promotes helper T-cell differentiation through phosphoinositide 3-kinase. *Proc Natl Acad Sci*. 2009;106(48):20371-20376. doi:10.1073/pnas.0911573106
74. Rathmell JC, Elstrom RL, Cinalli RM, Thompson CB. Activated Akt promotes increased resting T cell size, CD28-independent T cell growth, and development of autoimmunity and lymphoma. *Eur J Immunol*. 2003;33(8):2223-2232. doi:10.1002/eji.200324048
75. Waickman AT, Powell JD. mTOR, metabolism, and the regulation of T-cell differentiation and function. *Immunol Rev*. 2012;249(1):43-58. doi:10.1111/j.1600-065X.2012.01152.x
76. Sauer S, Bruno L, Hertweck A, et al. T cell receptor signaling controls Foxp3 expression via PI3K, Akt, and mTOR. *Proc Natl Acad Sci*. 2008;105(22):7797-7802. doi:10.1073/pnas.0800928105
77. Delgoffe GM, Kole TP, Zheng Y, et al. Article The mTOR Kinase Differentially Regulates Effector and Regulatory T Cell Lineage Commitment. 2009. doi:10.1016/j.immuni.2009.04.014
78. Yang J, Lin X, Pan Y, et al. Critical roles of mTOR Complex 1 and 2 for T follicular helper cell differentiation and germinal center responses. *Elife*. 2016;5. doi:10.7554/eLife.17936
79. Schwartz DM, Farley TK, Richoz N, et al. Retinoic Acid Receptor Alpha Represses a Th9 Transcriptional and Epigenomic Program to Reduce Allergic Pathology. *Immunity*. 2019;50(1):106-120.e10. doi:10.1016/j.immuni.2018.12.014
80. Wu J, Zhang Y, Liu Q, Zhong W, Xia Z. All-trans retinoic acid attenuates airway inflammation by inhibiting Th2 and Th17 response in experimental allergic asthma. *BMC Immunol*. 2013;14(1):28. doi:10.1186/1471-2172-14-28
81. Bakdash G, Vogelpoel LT, van Capel TM, Kapsenberg ML, de Jong EC. Retinoic acid primes human dendritic cells to induce gut-homing, IL-10-producing regulatory T cells. *Mucosal Immunol*. July 2014. doi:10.1038/mi.2014.64
82. Iliev ID, Spadoni I, Mileti E, et al. Human intestinal epithelial cells promote the differentiation of tolerogenic dendritic cells. *Gut*. 2009;58(11):1481-1489. doi:10.1136/gut.2008.175166

83. Edele F, Molenaar R, Gütle D, et al. Cutting edge: instructive role of peripheral tissue cells in the imprinting of T cell homing receptor patterns. *J Immunol*. 2008;181(6):3745-3749. doi:10.4049/jimmunol.181.6.3745

84. Coombes JL, Siddiqui KRR, Arancibia-Cárcamo C V., et al. A functionally specialized population of mucosal CD103+ DCs induces Foxp3+ regulatory T cells via a TGF-beta and retinoic acid-dependent mechanism. *J Exp Med*. 2007;204(8):1757-1764. doi:10.1084/jem.20070590

85. Jaensson-Gyllenbäck E, Kotarsky K, Zapata F, et al. Bile retinoids imprint intestinal CD103+ dendritic cells with the ability to generate gut-tropic T cells. *Mucosal Immunol*. 2011;4(4):438-447. doi:10.1038/mi.2010.91

86. Galvin KC, Dyck L, Marshall NA, et al. Blocking retinoic acid receptor-α enhances the efficacy of a dendritic cell vaccine against tumours by suppressing the induction of regulatory T cells. *Cancer Immunol Immunother*. 2013;62(7):1273-1282. doi:10.1007/s00262-013-1432-8

87. Szatmari I, Pap A, Rühl R, et al. PPARγ controls CD1d expression by turning on retinoic acid synthesis in developing human dendritic cells. *J Exp Med*. 2006;203(10):2351-2362. doi:10.1084/jem.20060141

88. Chang S-Y, Cha H-R, Chang J-H, et al. Lack of Retinoic Acid Leads to Increased Langerin-Expressing Dendritic Cells in Gut-Associated Lymphoid Tissues. 2010. doi:10.1053/j.gastro.2009.11.006

89. Hashimoto-Hill S, Friesen L, Park S, Im S, Kaplan MH, Kim CH. RARα supports the development of Langerhans cells and langerin-expressing conventional dendritic cells. *Nat Commun*. 2018;9(1):3896. doi:10.1038/s41467-018-06341-8

90. Chang J, Thangamani S, Kim MH, Ulrich B, Morris SM, Kim CH. Retinoic acid promotes the development of Arg1-expressing dendritic cells for the regulation of T-cell differentiation. *Eur J Immunol*. 2013;43(4):1-12. doi:10.1002/eji.201242772

91. Cassani B, Villablanca EJ, De Calisto J, Wang S, Mora JR. Vitamin A and immune regulation: Role of retinoic acid in gut-associated dendritic cell education, immune protection and tolerance. *Mol Aspects Med*. 2012;33(1):63-76. doi:10.1016/j.mam.2011.11.001

92. Hall J a, Grainger JR, Spencer SP, Belkaid Y. The role of retinoic acid in tolerance and immunity. *Immunity*. 2011;35(1):13-22. doi:10.1016/j.immuni.2011.07.002

93. Beijer MR, Kraal G, Den Haan JMM. Vitamin A and dendritic cell differentiation. *Immunology*. 2014;142(1):39-45. doi:10.1111/imm.12228

94. Kim MH, Taparowsky EJ, Kim CH. Retinoic Acid Differentially Regulates the Migration of Innate Lymphoid Cell Subsets to the Gut. *Immunity*. 2015:1-13. doi:10.1016/j.immuni.2015.06.009

95. Benson MJ, Pino-Lagos K, Rosemblatt M, Noelle RJ. All-trans retinoic acid mediates enhanced T reg cell growth, differentiation, and gut homing in the face of high levels of co-stimulation. *J Exp Med*. 2007;204(8):1765-1774. doi:10.1084/jem.20070719

96. Kim CH. Host and microbial factors in regulation of T cells in the intestine. *Front Immunol*. 2013;4(June):141. doi:10.3389/fimmu.2013.00141

97. Maynard CL, Hatton RD, Helms WS, Oliver JR, Stephensen CB, Weaver CT. Contrasting roles for all-trans retinoic acid in TGF-beta-mediated induction of Foxp3 and Il10 genes in developing regulatory T cells. *J Exp Med*. 2009;206(2):343-357. doi:10.1084/jem.20080950

98. Iwata M, Eshima Y, Kagechika H. Retinoic acids exert direct effects on T cells to suppress Th1 development and enhance Th2 development via retinoic acid receptors. *Int Immunol*. 2003;15(8):1017-1025. doi:10.1093/intimm/dxg101

99. Stephensen CB, Rasooly R, Jiang X, et al. Vitamin A Enhances in Vitro Th2 Development Via Retinoid X Receptor Pathway. *J Immunol*. 2014;168(9):4495-4503. doi:10.4049/jimmunol.168.9.4495

100. Brown CCC, Esterhazy D, Sarde A, et al. Retinoic Acid Is Essential for Th1 Cell Lineage Stability and Prevents Transition to a Th17 Cell Program. *Immunity*. 2015;42(3):499-511. doi:10.1016/j.immuni.2015.02.003

101. Wang J, Yen A. A novel retinoic acid-responsive element regulates retinoic acid-induced BLR1 expression. *Mol Cell Biol*. 2004;24(6):2423-2443. doi:10.1128/MCB.24.6.2423-2443.2004

102. Prüfer K, Racz a, Lin GC, Barsony J. Dimerization with retinoid X receptors promotes nuclear localization and subnuclear targeting of vitamin D receptors. *J Biol Chem*. 2000;275(52):41114-41123. doi:10.1074/jbc.M003791200

103. Bugge TH, Pohl J, Lonnoy O, Stunnenberg HG. RXR alpha, a promiscuous partner of retinoic acid and thyroid hormone receptors. *EMBO J*. 1992;11(4):1409-1418. http://www.ncbi.nlm.nih.gov/pubmed/1314167%0Ahttp://www.pubmedcentral.nih.gov/articlerender.fcgi?artid=PMC556590.

104. Pelicci PG, Grignani F, De Matteis S, et al. Fusion proteins of the retinoic acid receptor-alpha recruit histone deacetylase in promyelocytic leukaemia. *Nature*. 1998;391(6669):815-818. doi:10.1038/35901

105. Takeshita A, Cardona GR, Koibuchi N, Suen CS, Chin WW. TRAM-1, a novel 160-kDa thyroid hormone receptor activator molecule, exhibits distinct properties from steroid receptor coactivator-1. *J Biol Chem*. 1997;272(44):27629-27634. doi:10.1074/jbc.272.44.27629

106. DiRenzo J, Söderstrom M, Kurokawa R, et al. Peroxisome proliferator-activated receptors and retinoic acid receptors differentially control the interactions of retinoid X receptor heterodimers with ligands, coactivators, and corepressors. *Mol Cell Biol*. 2015;17(4):2166-2176. doi:10.1128/mcb.17.4.2166

107. Villa R, Pasini D, Gutierrez A, et al. Role of the Polycomb Repressive Complex 2 in Acute Promyelocytic Leukemia. *Cancer Cell*. 2007;11(6):513-525. doi:10.1016/j.ccr.2007.04.009

108. Rampal R, Awasthi A, Ahuja V. Retinoic acid-primed human dendritic cells inhibit Th9 cells and induce Th1/Th17 cell differentiation. *J Leukoc Biol*. 2016;100(1):111-120. doi:10.1189/jlb.3vma1015-476r

109. Kang SG, Park J, Cho JY, Ulrich B, Kim CH. Complementary roles of retinoic acid and TGF-β1 in coordinated expression of mucosal integrins by T cells. *Mucosal Immunol*. 2011;4(1):66-82. doi:10.1038/mi.2010.42

110. Huang DW, Sherman BT, Lempicki RA. Systematic and integrative analysis of large gene lists using DAVID bioinformatics resources. *Nat Protoc*. 2009;4(1):44-57. doi:10.1038/nprot.2008.211

111. Reich M, Liefeld T, Gould J, Lerner J, Tamayo P, Mesirov JP. GenePattern 2.0. *Nat Genet*. 2006;38(5):500-501. doi:10.1038/ng0506-500

112. Afgan E, Baker D, Batut B, et al. The Galaxy platform for accessible, reproducible and collaborative biomedical analyses: 2018 update. *Nucleic Acids Res*. 2018;46(W1):W537-W544. doi:10.1093/nar/gky379

113. Helt GA, Nicol JW, Erwin E, et al. Genoviz software development kit: Java tool kit for building genomics visualization applications. *BMC Bioinformatics*. 2009;10(20):266. doi:10.1186/1471-2105-10-266

114. Mudter J, Wirtz S, Galle PR, Neurath MF. A New Model of Chronic Colitis in SCID Mice Induced by Adoptive Transfer of CD62L+ CD4+ T Cells: Insights into the Regulatory Role of Interleukin-6 on Apoptosis. *Pathobiology*. 2002;70(3):170-176. doi:10.1159/000068150

115. Eri R, McGuckin MA, Wadley R. T cell transfer model of colitis: A great tool to assess the contribution of T cells in chronic intestinal inflammation. *Methods Mol Biol*. 2012;844:261-275. doi:10.1007/978-1-61779-527-5_19

116. Ostanin D V., Bao J, Koboziev I, et al. T cell transfer model of chronic colitis: concepts, considerations, and tricks of the trade. *Am J Physiol Liver Physiol*. 2009;296(2):G135-G146. doi:10.1152/ajpgi.90462.2008

117. Staudt V, Bothur E, Klein M, et al. Interferon-Regulatory Factor 4 Is Essential for the Developmental Program of T Helper 9 Cells. *Immunity*. 2010;33(2):192-202. doi:10.1016/j.immuni.2010.07.014

118. Merkenschlager M, von Boehmer H. PI3 kinase signalling blocks Foxp3 expression by sequestering Foxo factors. *J Exp Med*. 2010;207(7):1347-1350. doi:10.1084/jem.20101156

119. Hedrick SM, Michelini RH, Doedens AL, Goldrath AW, Stone EL. FOXO transcription factors throughout T cell biology. *Nat Rev Immunol*. 2012;12(9):649-661. doi:10.1038/nri3278

120. Stienne C, Michieletto MF, Benamar M, et al. Foxo3 Transcription Factor Drives Pathogenic T Helper 1 Differentiation by Inducing the Expression of Eomes. *Immunity*. 2016;45(4):774-787. doi:10.1016/J.IMMUNI.2016.09.010

121. Humblin E, Thibaudin M, Chalmin F, et al. IRF8-dependent molecular complexes control the Th9 transcriptional program. *Nat Commun*. 2017;8(1):2085. doi:10.1038/s41467-017-01070-w

122. Glasmacher E, Agrawal S, Chang AB, et al. A genomic regulatory element that directs assembly and function of immune-specific AP-1-IRF complexes. *Science*. 2012;338(6109):975-980. doi:10.1126/science.1228309

123. Suzuki J, Maruyama S, Tamauchi H, et al. Gfi1, a transcriptional repressor, inhibits the induction of the T helper type 1 programme in activated CD4 T cells. *Immunology*. 2016;147(4):476-487. doi:10.1111/imm.12580

124. Zhu J, Davidson TS, Wei G, et al. Down-regulation of Gfi-1 expression by TGF-β is important for differentiation of Th17 and CD103 + inducible regulatory T cells. *J Exp Med*. 2009;206(2):329-341. doi:10.1084/jem.20081666

125. Penny HL, Prestwood TR, Bhattacharya N, et al. Restoring Retinoic Acid Attenuates Intestinal Inflammation and Tumorigenesis in APCMin/+ Mice. *Cancer Immunol Res*. 2016:917-927. doi:10.1158/2326-6066.CIR-15-0038

126. Shinnakasu R, Yamashita M, Kuwahara M, et al. Gfi1-mediated stabilization of GATA3 protein is required for Th2 cell differentiation. *J Biol Chem*. 2008;283(42):28216-28225. doi:10.1074/jbc.M804174200

127. Zhu J, Davidson TS, Wei G, et al. Down-regulation of Gfi-1 expression by TGF-β is important for differentiation of Th17 and CD103 + inducible regulatory T cells . *J Exp Med*. 2009;206(2):329-341. doi:10.1084/jem.20081666

128. Vander Heiden MG, Cantley LC, Thompson CB. Understanding the Warburg Effect: The Metabolic Requirements of Cell Proliferation. *Science (80-).* 2009;324(5930):1029-1033. doi:10.1126/science.1160809

129. Buck MD, Sowell RT, Kaech SM, Pearce EL. Metabolic Instruction of Immunity. *Cell*. 2017;169(4):570-586. doi:10.1016/j.cell.2017.04.004

130. Taniguchi CM, Tran TT, Kondo T, Luo J, Ueki K, Cantley LC. Correction for Taniguchi et al., Phosphoinositide 3-kinase regulatory subunit p85α suppresses insulin action via positive regulation of PTEN. *Proc Natl Acad Sci*. 2016;113(25):E3588-E3588. doi:10.1073/pnas.1607478113

131. Ueki K, Fruman DA, Brachmann SM, Tseng Y-H, Cantley LC, Kahn CR. Molecular Balance between the Regulatory and Catalytic Subunits of Phosphoinositide 3-Kinase Regulates Cell Signaling and Survival. *Mol Cell Biol*. 2009;22(3):965-977. doi:10.1128/mcb.22.3.965-977.2002

132. Luo J, Cantley LC. The negative regulation of phosphoinositide 3-kinase signaling by p85 and it's implication in cancer. *Cell Cycle*. 2005;4(10):1309-1312. doi:10.4161/cc.4.10.2062

133. Inoue G, Cheatham B, Emkey R, Kahn CR. Dynamics of Insulin Signaling in 3T3-L1 Adipocytes. *J Biol Chem*. 2002;273(19):11548-11555. doi:10.1074/jbc.273.19.11548

134. Friesen LR, Kuhn RE. Fluorescent microscopy of viable Batrachochytrium dendrobatidis. *J Parasitol*. 2012;98(3):509-512. doi:10.1645/GE-2973.1

135. Zimmerman MK, Friesen LR, Nice a., et al. Multi-center evaluation of analytical performance of the Beckman Coulter AU5822 chemistry analyzer. *Clin Biochem*. 2015:4-8. doi:10.1016/j.clinbiochem.2015.06.010

136. Hashimoto-Hill S, Friesen L, Kim M, Kim CH. Contraction of intestinal effector T cells by retinoic acid-induced purinergic receptor P2X7. *Mucosal Immunol*. 2016;(July):1-12. doi:10.1038/mi.2016.109

137. Kim M, Friesen L, Park J, Kim HM, Kim CH. Microbial metabolites, short-chain fatty acids, restrain tissue bacterial load, chronic inflammation, and associated cancer in the colon of mice. *Eur J Immunol*. 2018:1235-1247. doi:10.1002/eji.201747122

VITA

Leon R. Friesen

PhD Candidate, Interdisciplinary Biomedical Science

Purdue University

Education

BA (Microbiology), 2003-2008. Miami University, Oxford, Ohio.

BS (Medical Laboratory Science), 2003-2008. Miami University, Oxford, Ohio.

MS (Biology), 2009-2011. Wake Forest University, Winston-Salem, North Carolina.

PhD (Interdisciplinary Biomedical Sciences), 2013-present. Purdue University, West Lafayette, Indiana.

Positions and Employment

2/2008-8/2013 Medical Laboratory Scientist, Wake Forest Baptist Medical Center, Winston-Salem, NC

8/2009-6/2011 Graduate Student (MS), Dept. of Biology, Wake Forest University, Winston-Salem, NC

8/2013-present Graduate Student (PhD), Interdisciplinary Biomedical Sciences Program, Purdue University, West Lafayette, IN

Professional Organizations

2008-2013 American Society of Clinical Laboratory Scientists

2009-2013,

2018- American Society of Clinical Pathologists

2012-2014 International Clinical Cytometry Society

2016- American Association of Immunologists

Research Presentations

1. Friesen, LR. 2010. Designing research methods for studying *Batrachochytrium dendrobatidis*. Presented at the 37th Annual Immunoparasitology Workshop.
2. Friesen, LR. 2011. Quantitative, competitive PCR and fluorescent microscopy methods for the study of *Batrachochytrium dendrobatidis*. Presented in the Biology department seminar series at Wake Forest University.
3. Friesen, LR. 2016. Gut microbial metabolites alter T helper cells in *Trichuris muris* infection. Presented at the 43rd Annual Immunoparasitology Workshop.

Poster Presentations

1. Friesen, LR. 2010. Quantitative, competitive PCR for detection of *Batrachochytrium dendrobatidis*. Presented at the Wake Forest University Department of Biology Regional Conference.
2. Friesen, LR. 2016. Role of Vitamin A signaling in regulation of inflammatory colon cancer. Presented at the Purdue Institute of Inflammation, Immunology, and Infectious Disease Summer Symposium. ***Poster Award**
3. Friesen, LR. 2016. Role of Vitamin A signaling in regulation of inflammation and cancer in the GI tract. Presented at the annual Phi Zeta meeting at Purdue University.
4. Friesen, LR. 2018. Microbial metabolites, short-chain fatty acids, restain tissue bacterial load, chronic inflammation, and associated cancer in the colon of mice. Presented at the University of Michigan Immunology Retreat.
5. Friesen, LR. 2018. Microbial metabolites, short-chain fatty acids, restain tissue bacterial load, chronic inflammation, and associated cancer in the colon of mice. PISA (American Society of Investigative Pathology).
6. Friesen, LR. 2018. RARα and retinoic acid alter T helper cell metabolism during Th17/Treg differentiation. University of Michigan Department of Pathology Symposium.

Teaching Experience

Teaching Assistant, Biomolecular and Cellular Systems Laboratory (BME 20500), Purdue University, 2015.

Teaching Assistant, Biomechanics and Biomaterials Laboratory (BME 20600), Purdue University, 2015.

Teaching Assistant, Biomolecular and Cellular Systems Laboratory (BME 20500), Purdue University, 2014.

Teaching Assistant, Genetics and Molecular Biology Laboratory (BIO 214), Wake Forest University, 2010-2011.

Teaching Assistant, Comparative Physiology Laboratory (BIO 114), Wake Forest University, 2009-2010.

Professional Activities

2012 North Carolina Leadership Academy Graduate, NC Society of Clinical Laboratory Scientists

Awards and Honors

2006 Miami University Undergraduate Research Grant.

2016 Purdue University College of Engineering, Estus and Vashti Magoon Award for Excellence in Teaching

2016 Purdue Institute of Inflammation, Immunology, and Infectious Disease Poster Award Travel Grant

PUBLICATIONS

Peer-reviewed Publications

1. **Friesen LR**, Kuhn RE. Fluorescent microscopy of viable Batrachochytrium dendrobatidis. J Parasitol. 2012;98(3):509-12. doi:10.1645/GE-2973.1.
2. Zimmerman MK, **Friesen LR**, Nice A, Vollmer PA, Dockery EA, Rankin JD, Zmuda K, Wong SH. Multi-center evaluation of analytical performance of the Beckman Coulter AU5822 chemistry analyzer. Clin Biochem. 2015:4-8. doi:10.1016/j.clinbiochem.2015.06.010.
3. Hashimoto-Hill S, **Friesen L**, Kim M, Kim CH. Contraction of intestinal effector T cells by retinoic acid-induced purinergic receptor P2X7. Mucosal Immunol. 2016;(July):1-12. doi:10.1038/mi.2016.109.
4. Kim M, **Friesen L**, Park J, Kim HM, Kim CH. Microbial metabolites, short-chain fatty acids, restrain tissue bacterial load, chronic inflammation, and associated cancer in the colon of mice. Eur J Immunol. 2018:1235-1247. doi:10.1002/eji.201747122.
5. Hashimoto-Hill S*, **Friesen L***, Park S, Im S, Kaplan MH, Kim CH. RARα supports the development of Langerhans cells and langerin-expressing conventional dendritic cells. Nat Commun. 2018;9(1):3896. doi:10.1038/s41467-018-06341-8. ***equal contribution.**
6. Hashimoto-Hill S, Kim M, **Friesen L**, Ajuwon KM, Herman E, Schinckel A KC. Differential food protein-induced inflammatory responses in swine lines selected for reactivity to soy antigens. *Allergy*. 2019. doi:10.1111/all.13757.